Investigation of blunt injuries and the force associated with a skull fracture due to impact with a Hopkinson pressure bar: an animal model.

By

Lisa Jane Coetzé
BSc (Stell), BScMedScHons (Stell)
CTZLIS001

SUBMITTED TO THE UNIVERSITY OF CAPE TOWN
In partial fulfillment of the requirements for the degree
MPhil (Biomedical Forensic Science)

Faculty of Health Sciences
University of Cape Town

Date of submission: January 2015
Supervisor: Dr Marise Heyns
Department of Clinical Laboratory Sciences
Division of Toxicology and Forensic Medicine
University of Cape Town

UNIVERSITY OF CAPE TOWN
IYUNIVESITHI YASEKAPA • UNIVERSITEIT VAN KAAPSTAD

Declaration

I, Lisa Jane Coetzé, hereby declare the work on which this minor dissertation/thesis is based is my original work (except where acknowledgements indicate otherwise) and neither the whole work nor any part of it has been, is being, or is submitted for another degree in this or any other university.

I empower the university to reproduce for the purpose of research either the whole or any portion of the contents in any manner whatsoever.

Signature: Signed by candidate Date: 7/05/2015

Lisa Jane Coetzé
MPhil Biomedical Forensic Sciences
University of Cape Town
Faculty of Health Sciences

Abstract

Homicide is one of the leading causes of death in South Africa. Homicides as a result of a firearm, sharp instrument or blunt object, may all potentially inflict severe cranial trauma. Often the lateral aspect of the cranium is fractured in homicidal assaults, however, the focus of head injury biomechanics has been the frontal bone. This is due to automotive-related incidents. Thus it is important for researchers to broaden their knowledge on lateral head impacts. This data could ultimately act as a tool in making cranial bone trauma analysis less subjective in nature.

This minor dissertation discusses human cranial bones and explores different types of cranial fractures. It further provides an in depth discussion on the different types of experimental tests and specimens used in biomechanical testing. A current review on the literature surrounding head impacts is also provided. The research conducted for this minor dissertation uses the Cape (Chacma) Baboon as a model to attempt to simulate cranial blunt trauma observed in human bone.

Fifteen Cape (Chacma) Baboon head specimens were subjected to a single temporo-parietal impact. These specimens were impacted with an aluminium striker bar that resembles the dimensions of a hammer (length: 23cm, circumference: 40cm and weight: 200g). The aim of these hammer tests were to characterise soft and hard tissue wound morphology as a result of blunt cranial impacts. Resulting data was analysed to determine if a significant correlation existed between impact velocity or energy and the extent of trauma observed.

The remaining twelve Cape (Chacma) Baboon specimens were all subjected to a single impact in the temporo-parietal region. These specimens were impacted with a Hopkinson pressure bar, which is manufactured from the same material as the striker bar. The aim of the Hopkinson pressure bar tests was to attempt to determine the force of impact. The use of the Hopkinson pressure bar to determine fracture forces in baboon head specimens is novel.

The fracture forces obtained in the current study compare well with literature investigating lateral impacts. Furthermore, the fracture patterns obtained in the current study realistically simulate cranial trauma seen in humans. It would therefore be beneficial to advance research using the baboon model and Hopkinson pressure bar apparatus.

Table of contents

Chapter One

Foreword

1.1. List of figures

1.2. List of tables

1.3. List of abbreviations

FE – Finite element

BISRU – Blast Impact and Survivability Research Unit

3D – Three-dimensional

CT – Computed tomography

1D – One-dimensional

GAM – Gravity accelerated mass

HPB – Hopkinson pressure bar

SHPB – Split-Hopkinson pressure bar

DIHB – Direct impact Hopkinson bar

Notations used in literature

N – Force (Newton)

mm^2 – Contact area (millimeters square)

v – Velocity (m/s)

mm – Length (millimeters)

m – Length (meters)

N/mm – Bone stiffness (Newton millimeters)

J – Energy (Joules)

kg – Mass (kilograms)

g – Mass (grams)

Notations used in calculations

τ – Time for stress wave to travel the length of the bar

c – Constant speed of sound

L – Length

E_y – Young's modulus

ρ – density

t –time

σ – Stress

K_G – Gauge factor

V_{in} – Wheatstone bridge voltage

V_{out} – Output stress

ε – Strain

P – Pressure

A – area

W – Work

D – Displacement

KE – Kinetic energy

Chapter Two

The protocol

Title: Investigation of blunt injuries and the force associated with a skull fracture due to impact with a Hopkinson pressure bar: an animal model.

Supervisor: Dr Marise Heyns

marise.heyns@uct.ac.za

Keywords: Blunt force trauma, Laceration, Skull fracture, Applied force, Hopkinson pressure bar, Cape (Chacma) Baboon

---

2.1. Background

Fracture pattern identification and interpretation are core components of forensic science. As there is a great deal of paucity in skull fracture tolerance data, the examination of cranial fractures is one of the greatest challenges for a forensic pathologist [1]. Forensic pathologists conduct post-mortem examinations in a subjective manner to determine whether a questionable death is in fact natural, homicidal, suicidal or accidental. However, determining the manner of death is a very trying task by which the interpretation of the trauma inflicted cannot be determined by pathological examination alone [2].

During these examinations it is difficult to distinguish between accidental and abusive blunt trauma observed in humans. For this reason, in court the defense may ask questions such as: what was the most likely weapon and force that was used to inflict such an injury? As well as: was the force used intended to be fatal? These are questions pathologists often do not have the answer for, as there are no general guidelines for them to consult while writing up a medico-legal post-mortem report [1,3]. It is therefore imperative to try and develop guidelines, which could potentially assist in making post-mortem's more objective. This objectivity could be achieved by providing a means for identifying the site and force of impact, the sequence in

which blows occurred, as well as determining the object responsible for the trauma seen in humans [2].

Head trauma is defined as any injury that results in damage to the brain, cranium or scalp. Damage is usually as a result of either blunt or sharp force trauma also known as a penetrating or closed injury. A penetrating injury is as a result of an accelerated object, such as a bullet, fracturing the cranium, as well as causing damage to brain tissue and surrounding structures. In contrast, a closed injury is one that does not penetrate the skull and is as a result of blows to the head with any blunt object [4]. Blunt objects can result in varying degrees of injuries that depend on the force and angle at which the blow strikes the skull. The human skull is known to be more durable in cases where the force of impact is dispersed rather than localised. The localisation of a blunt impact to the skull results in fractures and skin lacerations [3]. Furthermore, it has been observed that skull fractures often occur at bone suture interfaces, away from the site of impact, taking the path of least resistance and eventually radiating back to the initial site of impact [1].

It was proposed by Gurdjian and colleagues [5] that during blunt impact the skull develops areas of in-bending and out-bending, due to compressive and tensile forces respectively. Compression of the skull results in radiating fractures that occur directly underneath the site of impact. On the other hand, the area under tensile stress, where fractures are thought to initiate, tends to be situated away from the site of impact. Under a compressive force, bone is two times stronger in contrast to a tensile force and hence the elastic and plastic components of bone will fail first under a tension before compression [2].

2.2. Literature review

The current understanding of head trauma biomechanics largely depends on case studies, as well as experimental work that has been conducted in the past. During the mid-1800's, (as cited in [10]), intact cadaver heads were compressed between perpendicular plates of wood. Through this experiment, alterations in the skull diameter were measured and tensile and compressive forces were observed in opposite directions of the skull. Unfortunately, a limitation of this study is that forces were not recorded. However, this study was improved on in 1876, whereby both intact and scalped cadaver heads were used. Again fracture forces were not recorded, however this particular study found that the scalp has no influence over the biomechanical properties of a skull during impact. In other words identical fracture patterns were observed in both the intact and scalped cadavers [10].

By 1880, Mersserer [6], who conducted tests in a lateral direction on 13 unembalmed cadaver heads, was one of the first researchers to report on fracture forces. Mersserer reported fracture forces ranging from 3923-5884 Newton (N) and 2942-7845 N in male and female specimens respectively. Furthermore, Mersserer also reported that the frontal region of the skull is more durable than the lateral region of the skull.

On the other hand, in a more recent study by Gurdjian and colleagues [5], it was found that the lateral region of the skull was able to withstand a greater force in contrast to the frontal region. Gurdjian reported energy forces ranging from 800-1223 N and 653-1230 N for the anterior-parietal and posterior-parietal region respectively. Gurdjian obtained these results through a free fall model, which involves an intact cadaver head treated with a stress coat lacquer, being dropped from a specific height to impact with a solid surface below. In addition to Gurdjian's [5] above-mentioned finding, he noted that linear fractures occur secondary to

fractures from tensile forces (in-bending) and that the fracture tolerance was lower in dry skulls when compared to fresh specimens. Gurdjian's last finding indicates the effect desiccation has on bone and the manner in which it fractures.

Following on from Gurdjian's work [5], Nahum and colleagues [7] set out to determine the effect contact area has on skull bone tolerance. Drop-tests were set up, whereby an object of a particular mass is dropped from a specified height in a modified tower and impacts with the cadaver skull below. They recorded a minimum tolerance level of 2450 N for males and 2000 N for females, with a standard contact area of 645 millimeters squared (mm^2) in the temporo-parietal region. The results reported by Nahum [7] exceed those of Gurdjian and colleagues [5] and this highlights Gurdjian's main limitation namely, the use of the stress coat lacquer.

Thali et al. [8] expanded on Nahum's work [7] by designing a skin-skull-brain model. Nahum's methodology was repeated and the force and angle at which the weapon struck the skin-skull-brain model was adjusted according to weight/drop height and the position of the body under the drop tube respectively. The outcome of this study was that the skin-skull-brain model is a suitable proxy for the human skull and it allows the realistic simulation of blunt trauma in order to reconstruct specific characteristics.

More recently and due to the expense of the skin-skull-brain model, Verschueren et al. [9], proposed a new cadaver impact test set-up. It involves two pendulum structures, which have one degree of freedom for rotational movement. The pendulum set up consists of an implement attached to one of the pendulum structures, which during testing impacts with the skull. Furthermore, the pendulum model allows the head to move after impact creating the most realistic simulation of blunt head trauma.

To date researchers are working on mathematical models, which can assess blunt force trauma. The advantage of such a model is that medical ethics, as well as the unavailability of specimens will be eliminated. However, the finite element (FE) model is known to over-estimate the fracture force and further validation of these models is required [10].

2.3. Justification

Although head injury simulations are not new to the medical scene, very few studies have been conducted on blunt trauma caused by a specific implement. In 2011, Sharkey and colleagues [3] devised an experimental model that was used to assess the trauma inflicted on the scalp of porcine specimens. This model consisted of a drop tower through which a single impact, with specific implements was delivered to the fronto-parietal region of the skull. The implements that were tested included a common fall to the ground, stamping with a shoe and blows with a hammer or broom handle. Other than this above-mentioned study, there is very little data available to assist one in investigating blunt force trauma due to a specific implement.

In addition to the paucity in data, it is assumed that the porcine model is the most appropriate model to simulate blunt head trauma in humans [3]. However, to date, no study simulating cranial fracture patterns has been conducted on various animal models, while comparing these findings to those of cadavers.

Therefore this proposed project is a continuation of a project currently being conducted by Calvin Mole, a fellow University of Cape Town student. Through his project it was observed that the porcine model was not replicating fractures seen in former studies on cadavers. This necessitates the need to conduct research in a different animal model and has led to the

proposal of this current project in order to investigate if there is a more suitable animal model available as a proxy for humans.

2.4. Objectives

2.4.1. Primary objective

- The primary objective of this research project is to determine the force and energy involved in inflicting blunt head trauma due to blows with a Hopkinson pressure bar (HPB).

2.4.2. Secondary objectives

- To characterise the fracture inflicted due to blunt impact with a HPB.
- To characterise the wounds inflicted to the soft tissue due to blunt impact with a HPB.
- Summarise and present the findings of this research project in the form of a publishable article in a suitable journal.

2.5. Research plan

2.5.1. Methods

For the purpose of this project, *Papio ursinus* more commonly known as the Cape (Chacma) Baboon is of particular interest. All head specimens will be obtained through Hano Smits and Schultz Marais, who have permission to cull baboons on farms in the Wellington and Stellenbosch regions. Half of the head specimens will be delivered to the Health Sciences Campus at the University of Cape Town in leak-proof body bags and upon delivery will be frozen. The other half of head specimens will be delivered fresh on the day of testing. The

collection, transportation and delivery of the specimens to the university will follow the protocol described in the SOP 2013/1/SOP/INC001.01 (Appendix A1).

One freezer will be used for this research project and will only be utilised for storing head specimens that are ready for testing and also those ready for disposal. The freezer is run independently on its own cooling system (-20°c) and will specifically only be utilised for the purpose of storing head specimens during this research project.

Once ready for testing, the head specimens will be transported to the department of engineering, Blast Impact and Survivability Research Unit (BISRU) lab, which is situated on Upper Campus at the University of Cape Town. All specimens will be transported to the engineering department on Upper Campus according to the SOP 2013/1/SOP/INC002.01 (Appendix A2). Prior to testing each head specimen will be examined for any outward signs of head trauma and those suitable will then be suspended upside down in netting by an adjustable suspension system, which is held in front of the gas gun. For the purpose of this research project, the adjustable suspension system will be used in order to generate a more realistic simulation of head movement during a blunt blow, as well as give a more accurate outcome of the trauma inflicted. This system will also ensure that the parietal region of the head specimens is impacted.

2.5.2. Gas gun

The gas gun is located in BISRU and makes use of compressed shop air in order to propel a striker bar into the head specimen. The velocity of the striker can be altered by adjusting the pressure of the compressed air in the gas gun.

2.5.3. Blunt object (Hopkinson pressure bar)

For the purpose of this research project a rigid cylindrical striker bar and HPB will be used. The dimensions of the striker bar include a mass of 200 grams (g) and diameter of 40 millimeters (mm), representing a hammer. The HPB has the same diameter as the striker bar and is 1.5 meters (m) in length. Upon testing, the striker bar will propel into the HPB, which will impact with the suspended head specimen. The purpose of the HPB is to monitor the one-dimensional (1D) stress wave theory. This can aid in generating data on the amount of pressure the head specimen experiences during impact, as well as the particular weapon used. Furthermore, the force, impact velocity, displacement and pressure can be calculated. This data could be useful for doctors examining those admitted to hospital with head trauma, as well as assisting pathologist's conducting post mortem examinations.

2.5.4. Area of Impact

The parietal region of the skull will be impacted during testing. This region has been chosen as the site of impact as it is of a uniform thickness. This allows one to better observe fractures compared to the frontal bone, which mainly results in skull depression in trauma cases [2]. Secondly, a noteworthy amount of experimental studies have mainly focused on the blunt impacts to the frontal region of the skull. In contrast very few laboratory studies have focused on the trauma associated with blunt impact to the lateral aspect of the skull. This highlights the significant importance of generating research for forensic pathologists' in court [10]. Lastly, according to Kroman and colleagues [2] it would be best to avoid sutures, as they are known to be energy absorbers, altering the fractures patterns observed elsewhere. The impact due to the HPB will all be inflicted on the right side of the skull and this is merely for consistency purposes.

2.5.5. Data analysis

Thirty-three Cape (Chacma) Baboon heads will be required for this research project. Fifteen of these specimens will be subjected to a single blow with the HPB alone. These fifteen head specimens will be scalped and divided into groups of five, whereby they will be impacted once at speed of 10 meters per second (m/s), 15 m/s and 20 m/s. The velocities with which the gas gun fires can be adjusted by either increasing or decreasing the pressure used to activate the gas gun. The velocity at which the gas gun strikes is monitored by a light based velocity trap. The other eighteen head specimens will be tested under two conditions. These conditions being intact and scalped heads. The head specimens will again be tested under the above-mentioned velocities, however instead of five heads being tested at each velocity, three specimens will be tested for both conditions.

Following impact, the specimen heads will be analysed in the Entomology lab in the Division of Toxicology and Forensic Medicine for outwards signs of skin trauma, such as abrasions or lacerations. Skin trauma will be documented in terms of anthropomorphic data such as length and breadth measurements and will be photographed. All trauma will be measured by use of flexible measuring tape in order to follow the contours of the skull. Head specimens will then be examined for any signs of skull fracturing. In order to visualise skull trauma the skin, as well as the periosteum will need to be removed. Specimen's positive for the visual inspection of skull fractures will be further dissected in order to document the trauma.

2.5.6. Disposal of specimen remains

Once testing and documentation of blunt head trauma and fractures has terminated, the specimen remains will be stored in a freezer at -20°C. The specimens will then be transported to the University of Cape Town's Medical waste unit, where the BCL medical waste company

collects the remains. The disposal of specimens will follow the guidelines of SOP 2013/1/SOP/OUT001.01 (Appendix A3).

2.6. Work plan

	December	January & February	March	April	May	June	July	August	September	October	November
Proposal											
Ethics											
Literature review											
Introduction and methods											
Testing											
Results and discussion											
Write-up article											
Publish article in suitable Journal											

2.7. Reference list

[1] Baumer TG, Passalacqua NV, Powell BJ, Newberry WN, Fenton TW, Haut RC. Age-Dependent Fracture Characteristics of Rigid and Compliant Surface Impacts on the Infant Skull-A Porcine Model. J Forensic Sci 2010;55:993-997.

[2] Kroman A, Kress T, Porta D. Fracture Propagation in the Human Cranium: A Re-Testing of Popular Theories. Clin Anat 2011;24:309-318.

[3] Sharkey E, Cassidy M, Brady J, Gilchrist M, NicDaeid N. Investigation of the force associated with the formation of lacerations and skull fractures. Int J Legal Med 2011;126:835-844.

[4] Asgharpour Z, Baumgartner D, Willinger R, Graw M, Peldschus S. The validation and application of a finite element human head model for frontal skull fracture analysis. J Mech Behav of Biomed Mater 2014;33:16-23.

[5] Gurdjian ES, Webster JE, Lissner HR. The mechanism of skull fracture. J Neurosurg 1950;7:106-114.

[6] Messerer O. über Elastizität and Festigkeit der menschlichen Knochen. J G Coltaschen Buchhandling 1880.

[7] Nahum AM, Gadd CW, Danforth J. Impact tolerance of the skull and face. Proc Stapp Car Crash Conf 1968;12:302-316.

[8] Thali MJ, Kneubuehl BP, Dirnhofer R. A “skin–skull–brain model” for the biomechanical reconstruction of blunt forces to the human head. Forensic Sci Int 2002;125:195-200.

[9] Verschueren P, Delye H, Depreitere B, Van Lierde C, Haex B, Berckmans D et al. A new test set-up for skull fracture characterisation. J Biomech 2007;40:3389-3396.

[10] Yoganandan N, Pintar FA. Biomechanics of temporo-parietal skull fracture. Clin Biomech 2004;19:225-239.

2.8. Amendments to protocol

Since the commencement of this study, certain aspects of the methodology have been adjusted and the paragraphs that follow highlight and justify these changes.

Initially head specimens were to be obtained from Hano Smits and Schultz Marais. However, this collection process was halted by the requirement of a research permit from Cape Nature. This put a considerable amount of stress on the available time period in which head specimens were to be collected. This drawback was circumvented through the donation of Cape (Chacma) Baboon specimens, by Esmé Beamish and Justin O'Riain from the Cape Peninsula Baboon Research Unit. The remaining specimens were obtained from Cape Nature once the research permit had been granted.

Furthermore, instead of testing fresh head specimens, all head specimens were frozen on delivery to the Health Sciences campus, University of Cape Town. This is again linked to the delay in obtaining baboon specimens, as well as the demand for the HPB apparatus.

During the progression of this current study, it was decided to take scalp and skull thickness measurements of all head specimens. These measurements were used to determine if a significant correlation existed between scalp thickness and observed trauma or between skull thickness and observed trauma.

The impact site was also adjusted and the reason for this being that the Cape (Chacma) Baboon has a very small parietal bone. Additionally this bone is situated extremely close to a thick orbital ridge. This makes it challenging to impact specimens in a perpendicular manner and therefore the temporo-parietal region was impacted instead.

Only twenty-seven head specimens were tested, this is largely due to specimen availability in the short collection period. Fifteen of these head specimens were thawed forty-eight hours prior to impact. Nine of these head specimens were scalped and the remaining six were intact. These head specimens were subjected to one of the three impact velocities described in the above protocol. Three scalped and two intact head specimens were tested per velocity. The second group of twelve head specimens was thawed forty-eight hours prior to testing and these specimens were scalped. The HPB didn't inflict any hard tissue trauma under condition A (~10 m/s). Therefore the velocity of impact was increased per impact. Each head specimen was impacted once only.

Chapter Three

A structured literature review

Insights into intrinsic and extrinsic factors which influence cranial fractures in blunt force trauma simulations

3.1. Introduction

Cranial blunt force trauma can be described as any incident that may lead to a brain, skull or scalp injury [1]. Moreover, it stands to be classified as a closed head injury produced by an object, with a low velocity measured in m/s striking a relatively large surface area [2,3]. A substantial amount of research has been conducted in the field of head injury biomechanics. These studies utilise various experimental test set ups, namely the free fall [4], drop tower/ guided falls [5-10] and pendulum tests [11,12], as well as the three-dimensional (3D) printing [13-16], electrohydraulic piston [1,17] and FE model [3,18-20]. The data generated from these biomechanical studies have enriched our understanding of the structural behavior of bone under an external load. However, the exact mechanism of a skull fracture to the lateral aspect of the cranium is yet to be fully clarified [21].

This is partly due to the fact that few studies have attempted to determine impact forces to the lateral region of the cranium. The main focus of biomechanical research has been automotive-related impacts to the frontal region of the cranium [3,21,22]. Nonetheless, in developing countries, such as South Africa, road-traffic accidents only account for 35.2% of all non-natural deaths. The predominant cause of non-natural death is homicide-related (45.7%) [23]. More specifically the main cause of head injury within this division is described as involving a firearm (50.7%), sharp instrument (33.0%) or blunt object (10.6%) respectively [23,24]. Even though homicide-related deaths, which generally involve lateral trauma, are commonplace, they are yet to be investigated appropriately in a laboratory setting [19].

In addition to the aforementioned varying experimental test set ups, there tends to exist some differences in the field of head injury biomechanics. More specifically, discrepancies have arisen in the site of fracture initiation, as well as the force associated with trauma observed and whether or not the implement responsible for trauma can be deciphered. Owing to these discrepancies, it is hardly surprising that it is a challenge for forensic pathologists to comprehend the exact mechanism behind cranial blunt force trauma to the lateral cranium, in relation to impact forces and the types of resulting trauma inflicted by specific implements [18,25]. It should be noted however, that blunt force trauma in general is perceived to be the most challenging type of skeletal trauma to interpret. This is partly due to the unpredictable response of bone to an external load [26]. It is therefore imperative to extensively study the factors that influence the response of bone to an external load [27].

The purpose of this literature review is to explore experimental set ups and specimens utilised in the investigation of skull fractures. These are discussed in detail to ensure a thorough understanding of the methodology utilised by researchers presented in this review. It further discusses known criteria of both intrinsic and extrinsic factors that influence skull fractures in relation to cranial blunt force trauma. The search strategy employed for this review involved an initial search in Google Scholar to scope the literature available on the subject. Subsequently, selected articles were obtained by searching the University of Cape Town's online Library Catalogue. Keywords that were utilised during the literature search include, blunt force trauma, applied force, skull fracture, laceration and head injury biomechanics. Furthermore, no restraint was placed on the year of publication, however the most recent articles were always searched for and, where applicable, were reviewed.

3.2. Anatomy of the cranium

The adult human cranium, which is symmetrical about the mid-sagittal plane, is both multifaceted and three-dimensional. Its main function is to house and protect the brain from damage due to external forces [21]. During the early stages of foetal growth, membranes surround the developing brain. Ossification centers develop within these membranes, which will form the individual cranial bones. The openings or gaps between these newly formed cranial bones are referred to as fontanelles. Fontanelles subsequently undergo interdigitation and ossification, which results in suture closure in addition to a 75% stiffness observed in an adult cranium in comparison to only 4% in that infants [21,28].

The regions of an ossified adult cranium are constitutionally identical and consist of three individual layers, namely two rigid layers and an inner cancellous layer [4,21]. The rigid outer and inner tables of the cranium lie parallel to one another. These tables comprise compact bone with the outer table being twice as thick as the inner table. The central layer of soft cancellous bone, also known as the diploë, separates these tables and it is this cancellous zone that is interposed by sutures [28]. These interchanging layers of compact and spongy bone form the structural basis of adult cranial bones. Cranial bones include the frontal, ethmoidal, sphenoidal, occipital as well as the paired temporal and parietal bones [4]. In the anatomical position, the frontal bone is the most anterior cranial bone, whereas the most posterior aspect of the cranium consists of the occipital bone. The paired parietal bones are partially posteriorly situated and, in conjunction with the temporal and sphenoidal bones, make up the lateral aspect of the cranium. Lastly, the ethmoidal bone forms the most anterior aspect of the base of the cranium (Figure 3.1) [4,21]. Of all the aforementioned cranial bones only the temporal bones are generally concave in nature [4,21,28]. In summary, the eight adult cranial bones are not merely robust structures, but more importantly possess ductility that enables

them, to a certain extent, to accommodate external forces. This mechanism will be further discussed below.

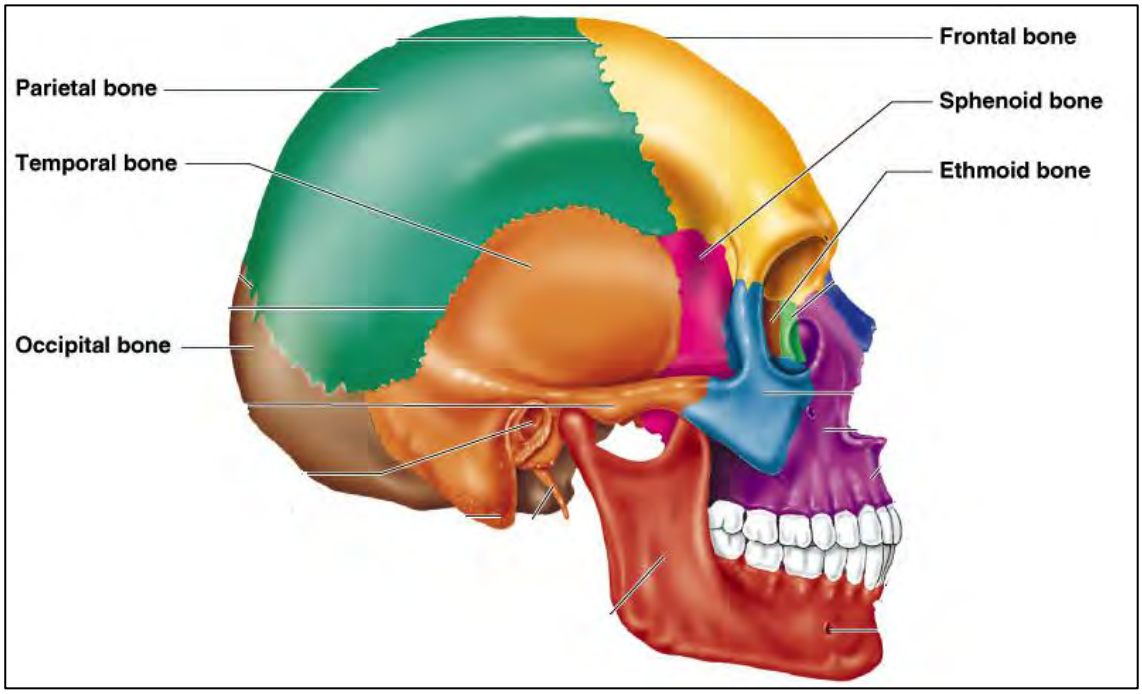

Figure 3.1: Anatomy of the human cranium. The eight cranial bones are highlighted above [47].

3.3. Cranial fractures

Bone is described as being viscoelastic in nature and its response to an external load involves the absorption of impact energy through bone deformation [21,24]. Deformation often involves the direct intrusion of the impact site and, according to Newton's Third Law of Motion, a compensatory area of extrusion remote to the impact site, can be expected [2,28]. However, when a load is ceased, bone will return to its original shape and size provided that the elasticity threshold is not exceeded. Nonetheless, if bone is placed under significant strain and the elasticity threshold is exceeded, definitive permanent distortion may result [27]. Under such circumstances the inner table, which is convexly displaced, will fracture under the tearing action of tension and a consequent fracture may result in the outer table due to compressive force (Figure 3.2) [27-29]. In addition to permanent distortion, there may be a

respective increase in tension and compression in the outer and inner tables surrounding the impact site [2,28].

Permanent distortion may afford to several types of cranial fractures as a result of blunt force trauma, which could arise from the aforementioned mechanism [28,30]. Cranial fractures include linear, depressed, diastatic and, in rare circumstances, basilar skull fractures [29]. These fractures will be discussed further below.

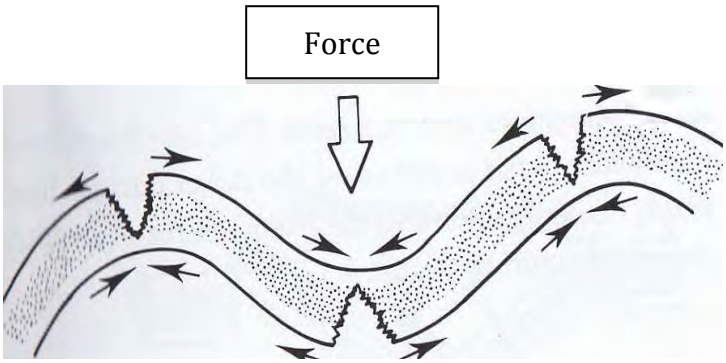

Figure 3.2: Illustration of bone deformation and the sites of fracture initiation. Inward pointing arrows are indicative of compressive forces, whereas the outward pointing arrows represent tensile forces [28].

3.3.1. Linear fracture

A common fracture resulting from a force being applied over a broad surface area is a linear fracture (Figure 3.3) [28,29]. A linear fracture is typically seen in low-velocity impacts and most likely propagates following the path of least resistance along the cranium [30]. Such fractures may transverse the inner and outer tables of the cranium presenting as either a straight or curved line of significant length. Linear fractures typically radiate outwards from a depressed area, however it is believed that they may also arise from a point distant to the impact site and in rare circumstances, may extend into a suture resulting in diastasis [28].

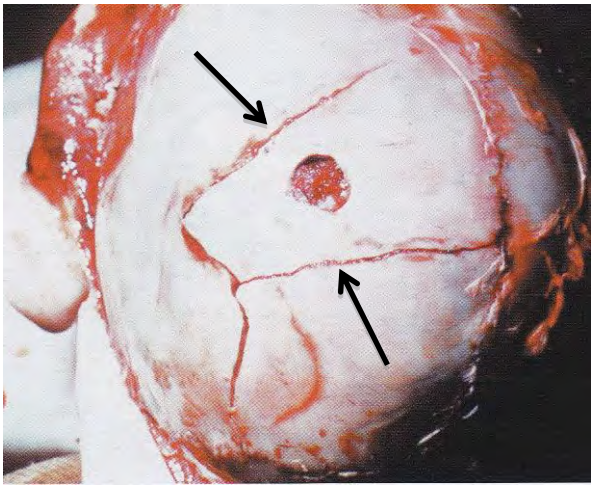

Figure 3.3: Image of linear fractures as a result of cranial blunt force trauma. The arrows indicate linear fractures on the lateral aspect of the cranium [28].

3.3.2. Depressed fracture

In contrast to linear fractures, a localised, high-velocity impact applied to a small surface area may result in a depressed fracture (Figure 3.4) [30]. For example, when a hammer strikes the cranium, there is often the inward displacement of bone representing the dimensions of the implement itself. However it should be noted that depressed fractures are less dependent on the actual dimensions of the implement and are more dependent on the velocity at which the implement strikes the cranium [6,29].

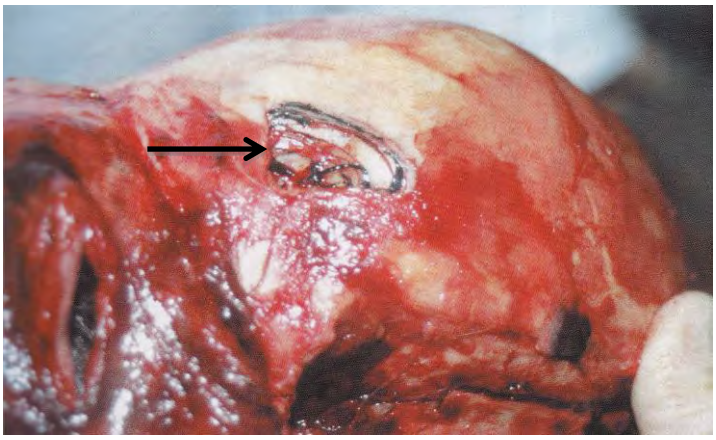

Figure 3.4: Image of a depressed skull fracture. The arrow indicates a depressed fracture, which is commonly as a result of focal objects such as a hammer [28].

3.3.3. Diastatic fracture

A diastatic fracture, which is commonly observed in infants and young children, involves the widening of a suture, as a result of a fall or a blow to the vertex (Figure 3.5) (24). This fracture is frequent in children due to incomplete suture fusion, which consequently assists in fracture propagation [30].

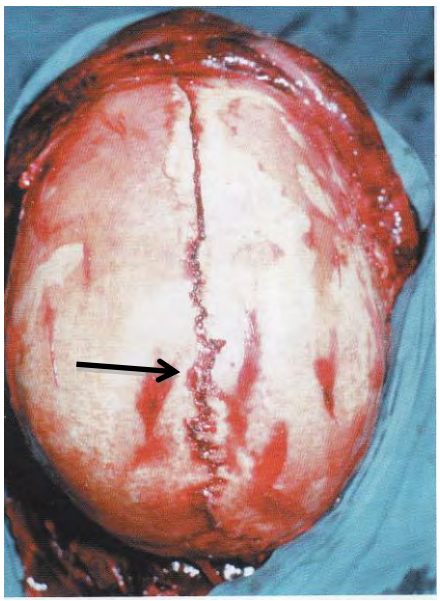

Figure 3.5: Image of a diastatic fracture. The arrow indicates diastasis of the sagittal suture [28].

3.3.4. Basilar fracture

Basilar fractures, such as hinge and ring fractures, rarely occur from implement-related cranial blunt force trauma [4,28]. However, they may arise as a result of blunt force impact of high energy or high-energy-ballistic trauma to the lateral part of the head [31]. Similarly if the chin or forehead regions of the cranium are subjected to a tremendous amount of force, a basilar fracture also known as the “motorcyclists fracture” may result (Figure 3.6) [6,29]. A basilar fracture presents at the cranial base, which by virtue is structurally weak due to the presence of multiple bone orifices and traverses from the lateral aspect of the cranium, across the middle cranial and pituitary fossae to the opposite, lateral aspect of the cranium [28,30].

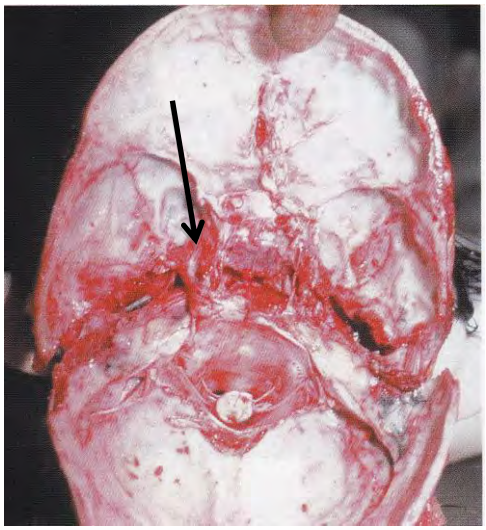

Figure 3.6: Image of a basilar fracture. The arrow indicates a basilar fracture anterior to the foramen magnum [28].

It is important to note however that the fracture types discussed above need not occur in isolation, but may present as a combination of two or more fracture types, for example a comminuted or spider's-web fracture (Figure 3.7) [28,31]. A probable mechanism of a comminuted fracture upon impact and in addition to the previously described depressed fracture, involves the development of secondary and tertiary fractures as a result of an intense kinetic energy [2,22]. It has been postulated by Delye and colleagues [11] that these subsequent fractures develop as a consequence of the primary fracture decreasing the load carrying capacity of bone. Secondary fractures include linear fractures that radiate outwards from the impact site, whilst tertiary fractures are concentric in nature, both initiating and terminating perpendicularly to radiating fractures [2]. It is this combination of radiating and concentric fractures that give rise to the characteristic spider's-web appearance [2,13]. Secondary and tertiary fractures terminate when crossing the path of a primary fracture, which dissipates their remaining impact energy [32].

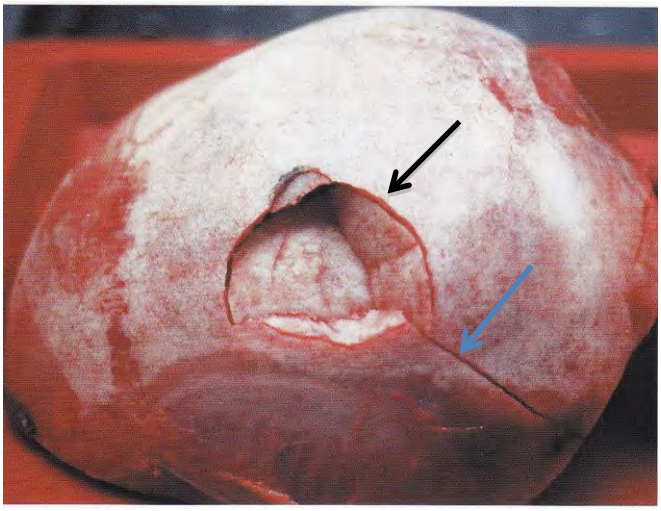

Figure 3.7: Image of a comminuted depressed fracture. The black arrow indicates a concentric (tertiary) fracture, whereas the blue arrow indicates a radiating (secondary) fracture [28].

In summary cranial bone is perceived capable of recovering from an external load, however if the elasticity threshold happens to be surpassed, the bones will undoubtedly fail [27]. Additionally, the assumption that cranial fractures present overall in a defined manner is too simplistic. For example individual fractures can present as linear, depressed, diastatic or basilar fractures, whereas a combination of fractures such as a comminuted fracture may also present. The varying dimensions of fractures as well as the unpredictable nature of bone, emphasise the importance for researchers to develop appropriate means through which cranial fractures can be investigated fully, especially in relation to the lateral aspect of the cranium.

3.4. Studying skull fractures

Head injury biomechanics have been studied extensively in animal and cadaver models in conjunction with biomechanical experimentation, to conceptualise fracture initiation and propagation patterns [22,28]. Various biomechanical impact set ups have previously been used to investigate skull fractures [33]. In addition to biomechanical set ups, numerous specimens have been investigated, some more extensively than others. These include human

volunteers, animal models, cadavers and anthropomorphic dummies [25]. These specimen types will be discussed in greater detail in the next section.

3.4.1. Specimen types

The ideal specimen would be a human volunteer as one can accurately monitor properties such as elasticity, compressibility, pressure and skull density. However, due to ethical constraints, human volunteers can only provide data on sub-injury biomechanics as they may only be subjected to non-injurious tests [21,25]. Alternative specimens that could be subjected to injurious impacts include animal models, such as the pig (porcine model) and cadavers. More specifically, animal models can investigate the skin's loading response by monitoring factors such as stretch, torsion, compression and shear forces [5]. Furthermore, both animal and cadaver models are known to simulate the skull's physiological response to injury [1,9,25]. Cadavers, despite characteristic post mortem changes, can circumstantially be extrapolated to real-world situations [19,21]. Conversely, an animal model is constrained in its applicability to *in vivo* humans due to discrepancies in skull shape and thickness. Animal research also has the potential to be expensive and time consuming [34]. Furthermore, ethical guidelines regarding the utilisation of animal tissue in research are necessary.

First and foremost, animals play a crucial role in understanding diseases and injuries in humans. This is undoubtedly important in making advancements in the fields of science and medicine. However, animals used in research should not be placed under unnecessary stress and if an alternative to an animal model is available, animal ethics will not be granted [35]. In contrast, the primary limitation of cadaveric material is its unavailability that may often result in a small sample size, which is non-representative of varied age, race and sex groups [1].

Medical ethics and difficulties in the acquisition of human tissue can be circumvented through synthetic models with an indefinite shelf life [25,34]. An example is the skin-skull-brain model, its components include the skull, scalp, periosteum and brain being represented by a polyurethane sphere, silicon cap, latex layer and 10% ordnance gelatin material respectively (Figure 3.8) [36].

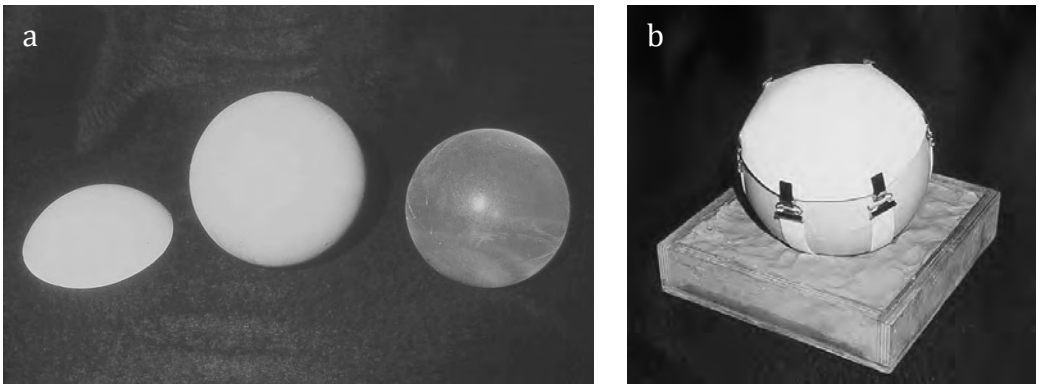

Figure 3.8: The skin-skull-brain model. In (a) from left to right are shown the components of the skin-skull-brain model. This includes the silicon cap, polyurethane sphere and the ordnance gelatin material (b) An example of the constructed skin-skull-brain model [34].

The 10% ordnance gelatin is heated and injected into the polyurethane sphere and this is followed by the attachment of the silicon cap to the sphere with modified suspender-straps [25]. Despite this specimen being able to simulate actual forensic case situations, it fails to accurately replicate human biological systems and can thus not be extrapolated to real-life situations [25,36]. For example the human head is held in position by ligaments, joints and muscles in the surrounding neck region. These structures reduce to some extent the energy of the impact and trauma inflicted. This deflection is not readily simulated in synthetic models. In addition, differences in fracture dimensions have been observed between the skin-skull-brain model and autopsy findings. These differences are justifiable by the absence of sutures in the synthetic models, which are known to act as energy sinkholes during fracture propagation [16].

Limitations such as medical ethics surrounding animal usage, as well as the unavailability of cadaveric material, are encountered all too often in research. However, it is unrealistic to exclude them as suitable models. Even though synthetic models offer a solution to these limitations, the expenses incurred in their production are often not feasible. This highlights the necessity for researchers to explore alternative models that are easily accessible, abundant and inexpensive. Most importantly, animal models apart from the porcine model need to be assessed in their applicability to experimental test set ups utilised in biomechanics. These experimental tests will be discussed in detail in the section to follow.

3.4.2. Types of experimental tests

It should be noted that animal models, cadavers as well as synthetic models, are possible specimens that may be utilised in conjunction with the following experimental tests.

3.4.2.1. Free fall test

The free fall test is described as involving an intact cadaver or cadaver head being dropped in an unconstrained manner from a specified height onto a solid surface below. During the 1950's this was the method of choice, as it was thought to accurately record the peak force at the time of fracture [4]. However, a constraint is that impact location cannot be well defined upon impact, as there is no control over the cadaver head during free fall [12].

3.4.2.2. Entrapped and free fall drop tower tests

The drawback of not being able define impact location has been approached through drop tower tests. This set up is referred to as a drop tube with a movable object of a predetermined mass being dropped from a specific height onto a skull below (Figure 3.9) [12,36]. The dropping distance of the tube as well as the weight of the impacting object influences the

striking force, whereas the adjustment of the skull's position allows the angle of impact to be altered [36]. Furthermore, specific implements can be attached to the impacting surface of the drop tower. This test set up has a three-fold improvement of the aforementioned free fall test. Firstly, during testing, head impact location can be controlled whilst secondly, there is a possibility of measuring local skull deformation, and lastly the force delivered to the skull can be determined [16]. A downfall however, is that the skull is often entrapped, lending to it being crushed between a rigid surface (backing material) and a movable object [12]. This restraint leads to a state of greater bone stress, which in turn results in a more extensive pattern of fracturing under the same magnitude of impact energy and contact force in comparison to other experimental tests. This limitation can be addressed with the use of the free fall drop tower, in which the skull is subjected to a single blow by the impacting surface, preventing the crushing phenomenon altogether [9].

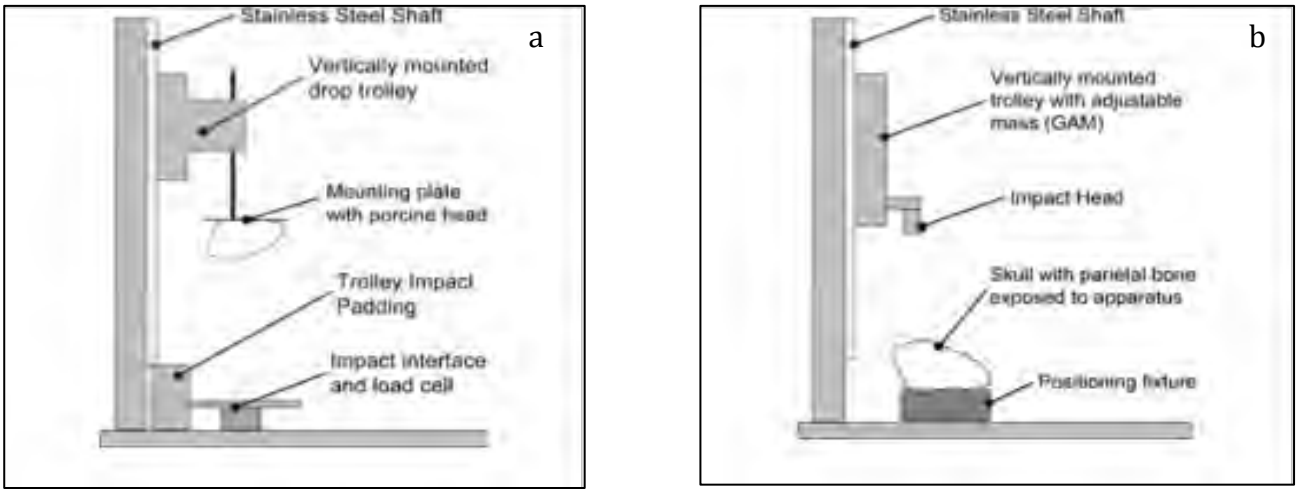

Figure 3.9: Entrapped vs. free fall drop tower. The entrapped drop tower is represented in (a) and the free fall drop tower is represented in (b). In image (a), the specimen is attached to the mounting plate and is dropped from a specific height to impact with the load cell that in turn records force. In image (b), the specimen is subjected to an additional weight, the gravity accelerated mass (GAM) [9].

3.4.2.3. Pendulum test

Although the free fall drop tower test is an improvement on the free fall method, it does not allow the specimen to move in an unconstrained manner as would be expected in a typical

cranial blunt trauma blow. This is however to a certain extent achievable through the pendulum test seen in Figure 3.10, which allows a specimen to move with one degree of freedom, more specifically in one direction only, in the plane of impact [12]. It should be noted however that this movement is not of the specimen itself, but rather of the pendulum to which a specimen is rigidly attached [3].

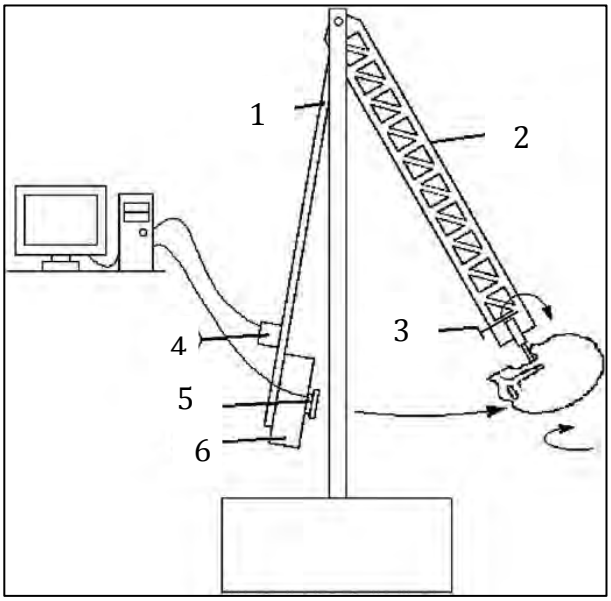

Figure 3.10: Schematic view of the pendulum model. (1) Steel pendulum, (2) aluminium pendulum, (3) specimen attachment site, (4) laser displacement sensor, (5) force sensor and (6) additional weights [12].

This set up is described as two pendulums attached to a steel structure mounted onto a wall. One pendulum, constructed from aluminium, is responsible for supporting the specimen, whereas the second pendulum, constructed from steel, impacts the supported specimen [12]. The latter pendulum has a cylindrical impactor attached to it that can measure contact area, force and specimen deformation [11].

Computer generated models, namely 3D printing and the FE model, are becoming increasingly popular in investigating head injury biomechanics. These experimental models are attractive due to eliminated medical ethics, as well as the fact that actual specimen material is not

required in experimental testing. However, these models are lacking in certain areas, more specifically the FE model. This model relies on the quantified biomechanical response parameters of the above-mentioned test set ups to develop and ultimately validate a model. For example force-displacement data that is generated from experimental tests is used in designing and assessing the validity of an FE model [1,3].

3.4.2.4. Three-dimensional printing model

3D printing is a means of compiling data and co-ordinates from a computed tomography (CT) scan in order to recreate a physical model of broken bones with a 3D printer (Figure 3.11). An apparent advantage is that there are no ethical considerations. Furthermore, the impact direction and suspected weapon could potentially be determined through comparisons with numerous implements [15,16].

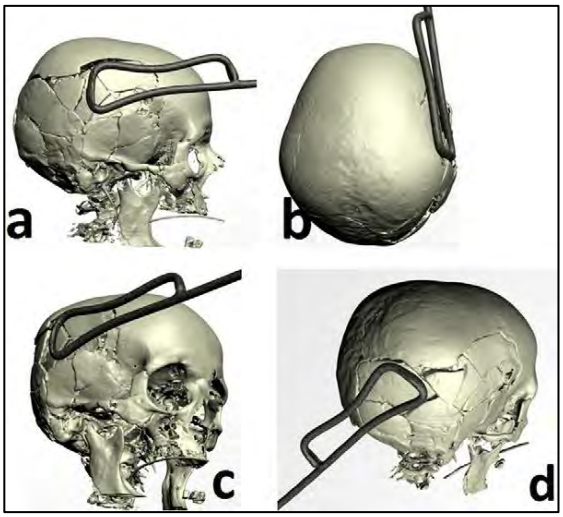

Figure 3.11: A computer-generated depiction of three-dimensional printing. The suspected weapon, a metal fire poker is superimposed onto different cranial regions and this gives insight as to how the trauma was inflicted [15].

3.4.2.5. Finite element model

The construction of an FE model consists of three stages. The first stage, known as pre-processing, involves the development of a geometric model in addition to determining biological material properties for model development [18]. These properties can be obtained

through medical images such as a CT scan and are converted into numerical codes in order to be compatible with the FE program code [3,18].

The second stage referred to as main processing involves the actual development of the specimen model [18]. For instance various components of the specimen, through numerical codes, are represented by shell and brick elements meshed together. An FE model representing an average-sized human head typically consists of the, skull, scalp and face as well as the falx of the brain, brain-skull interface and brain stem [3]. Once the model is developed it is filled with a solid material in order to approximate the weight of the brain, and head injuries can then be explored under different impact conditions [20].

The final stage, which is described as post-processing, involves the visualisation and interpretation of the results yielded by the FE model [18]. Even though the FE model provides reproducible results that circumvent exhaustive experimental procedures on human and animal specimens, the results should always be assessed in conjunction with replicated laboratory experiments (Figure 3.12) [33,37]. An advantage of this model is that it can realistically simulate dynamic loads, and at the same time provide valuable information in the prediction of head injuries. In addition to the FE model not being able to determine the exact impact location, it cannot determine injury tolerance due to a lack of data on the failure criteria of complex biological materials [3,21]. Further validation of this model as a forensic tool is necessary as the force required to fracture a skull is often overestimated by the FE method [3]. It is postulated that the overestimation observed in the FE model largely depends on numerous criteria.

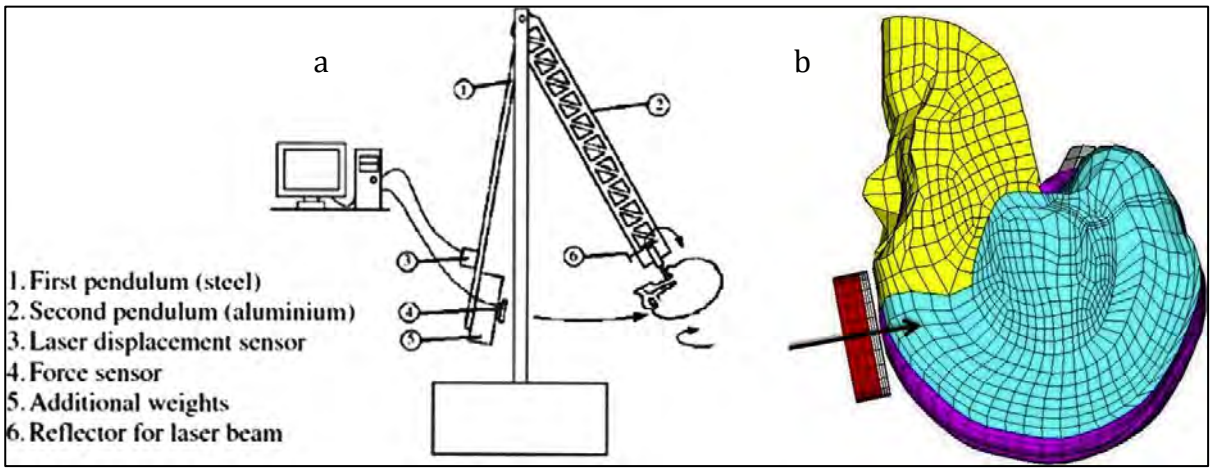

Figure 3.12: Illustration of the pendulum model and corresponding finite element (FE) model. The pendulum experimental set up represented by (a) is conducted first, followed by the FE model in (b). The data between the two methods is compared to assess the validity of the FE model [3].

These criteria include a known mismatch in bone stiffness between cadaver specimens and a simulated head in the FE model. To date, this optimisation technique has not been utilised, as it is believed to create an artificial representation of the human head. Furthermore, geometric differences between these two models tend to contribute towards overestimation, more specifically, the lack of regional variations such as variable bone thickness and detailed facial structures in the FE model. It is suggested that numerous future experimental tests should be conducted in conjunction with the numerical FE model [37]. This will not only allow researchers to grasp a satisfactory understanding of the FE model, but will advance the development of personalised FE models which contain the specific dimensions of the experimental specimen (cadaver) under investigation. It is emphasised that with these criteria in place overestimation can be keep to a minimum [3]. Once more, the issue of determining the exact impact location is raised and if this is a characteristic of interest, the piston model could be used as an alternative [6].

3.4.2.6. Piston model

This model consists of a hydraulic or pneumatic piston being operated by compressed air to impact a skull specimen. Together a piston controller, analog to digital converter and

computer are used to generate biomechanical data (Figure 3.13). An advantage of this model is that direct contact area can be measured, in addition to specimen deformation. Furthermore, it is possible to alter the impact area on the cranium as well as vary the impact velocity. Again specimens should not be restrained if altered stress distribution and skull deformation are to be avoided. Instead it is suggested that specimens be suspended in a manner that allows them to move in a free and realistic fashion [6,12].

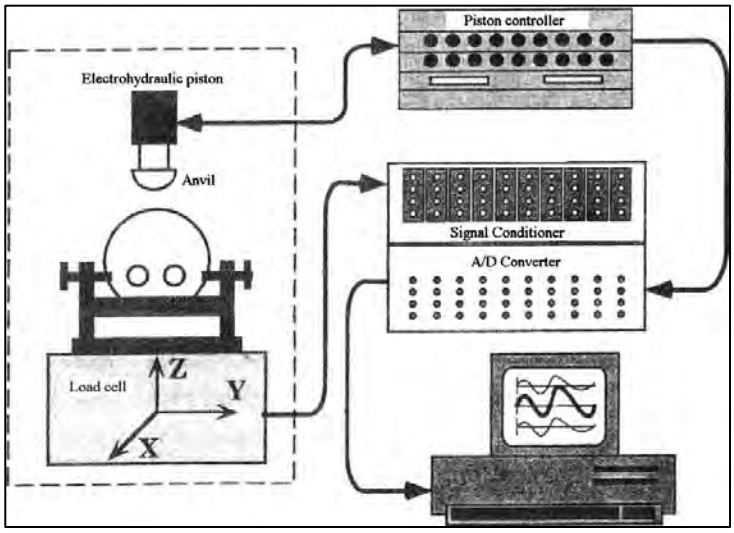

Figure 3.13: Schematic diagram of the piston model. The specimen can be orientated in any direction in the load cell. Upon impact the data is captured by the analog to digital converter and computer [1].

As described above, there are a variety of experimental tests available to investigate cranial fractures. All of these tests lack in certain aspects, however they can be suitable when chosen according to certain experimental measures of interest. For example, if impact location were under investigation, then all the abovementioned tests, except for the free fall test would be applicable. Even though it might be the case that the FE model and 3D printing are the most ideal tests, this technology is not widely available or thoroughly validated. This is an area of focus for future research as both tests eliminate the limitations of the above-described specimens and experimental test combinations. Additionally researchers could focus on eradicating the drawbacks of the non computer-generated tests mentioned above. In summary

it is proposed that the piston model, even though it has limitations, is the most applicable experimental test for this current study.

Before researchers develop and utilise the abovementioned experimental set ups, it is important for them to understand intrinsic as well as extrinsic factors that influence fracture patterns in cranial blunt force trauma [7,20,22]. These factors will be discussed in detail below.

3.5. Criteria that influence skull fractures

The two core topics of discussion in this section are intrinsic and extrinsic factors. Intrinsic factors that will be explored in detail include; the presence of hair and scalp thickness, followed by cranial bone thickness and stiffness and local skull geometry. Furthermore, skull geometry includes numerous anatomical landmarks, namely sutures, foramina, sinuses as well as buttresses, all of whose location affects bone integrity in response to an impact [27,30]. Additionally, the fracture initiation site and bone disease are also discussed under intrinsic factors. Extrinsic factors that are reviewed in this section include the force of an impact as well as the effect of the dimensions of a blunt implement on fracture patterns.

3.5.1. Intrinsic factors

3.5.1.1. Presence of hair and scalp thickness

The elastic properties of the scalp and attached hair markedly dampen the resultant blunt impact energy [11,28]. This energy can be absorbed by the skin's mechanical resistance mechanism, which entails collagen and elastin fiber matrices. In a relaxed state these matrices are unordered, however when a force is applied, skin dissipates the energy through the

rearrangement of elastin fibers into an ordered state. This enables them to bear the load while the collagen fibers remain unordered. As the energy of the load increases, collagen fibers align and assist the elastin fibers with load bearing. However, once the elasticity threshold of the scalp is exceeded it will fail and produce a laceration [11].

Sharkey and colleagues [5], whose study will be referred to in detail under the section "implement dimensions and impact force", have suggested that the minimum force required for laceration production is 4000 N. Subsequent to laceration production, the underlying cranium continues to absorb the impact energy [5,24]. More specifically, in a study by Raymond et al. [17] it was described that impacts to specimens (cadavers) with less than 7 mm of soft tissue resulted in a fracture, whilst no fractures were observed under the same impact conditions in specimens with soft tissue greater than 7 mm. In addition to the padding effect of an intact scalp, it is also thought to increase the diameter of a depressed fracture in comparison to a bare counterpart. Even though soft tissue is in part responsible for absorbing the energy of an impact, it is rather the nature of the underlying cranial bone that depicts the resulting trauma [28].

3.5.1.2. Cranial bone thickness and stiffness

The cranium is described as being non-uniform in composition and this ensues regional variations in cranial bone thickness, which in turn influences bone stiffness. Both of these variations affect the length and direction of fracture propagation [29]. For instance, Delannoy et al. [22], who utilised collaborated experimental data from 20 cadaver head specimens, reported the frontal bone to be the thickest (7.3 mm). However the parietal bone was described as having an average thickness of 6.4 mm and the temporal bone, the thinnest cranial bone, had a thickness of 4.8 mm. Moreover the midpoint of the occipital bone was referred to as being 15 mm thick.

In addition to cranial bone thickness, Delannoy and colleagues [22] also reported on cranial bone stiffness. Stiffness influences bone's reaction to external forces such as stress and strain by resisting deformation during an impact [2,22]. Delannoy et al. [22], through analysing collaborated data on bones subjected to three-point bending, described varying cranial bone stiffness. For example, the temporal region was perceived to be the least stiff, 350 Newton millimeters (N/mm), in contrast to the parietal and frontal bones that have an average stiffness of 490 N/mm and 630 N/mm respectively. Both bone thickness and stiffness play a discernible role in bone tolerance. Yoganandan et al. [1], whose study is described in detail under the section "force required to fracture a skull", have claimed that the fracture threshold of the human cranium is between 14.1 to 68.5 Joules (J).

Delannoy et al. [22] have stated that a thin bone, such as the temporal bone, will fracture first during a blunt impact in comparison to its frontal counterpart. However, the findings of Delannoy and colleagues contend the findings of older studies, such as those conducted by Gurdjian [4], Hodgson [38] and Hodgson and Thomas [39], which describe the occipital bone as being the weakest followed by the midfrontal, posterior parietal and anterior interparietal regions. The discrepancies observed between older studies and more recent studies are probable due to advancements in the technology utilised to measure cranial thickness and stiffness. A second concern involves Gurdjian's use of a stress coat lacquer, which is known to increase bone stiffness, altering its response to an impact [4]. Even though it is tempting to discredit Gurdjian's research [4], it cannot be excluded as it forms a fundamental step in the advancement of head injury biomechanics. In addition to describing the temporal bone as the least ductile of cranial bones, Delannoy et al. [22] further suggest that fractures in this region are often extensive and perforate both the inner and outer tables. Moreover, they describe fractures at an equal impact force in a bone with an increased thickness and stiffness, to be less extensive with little bony perforation and often resemble the shape of the implement. Not

all cranial bone stiffness and thickness will fall into the above-described ranges; more specifically diseased bone is referred to as being frailer in comparison to healthy bone [40].

3.5.1.3. Bone disease

Genetic disorders such as Paget disease, osteogenesis imperfecta and osteoporosis all involve aberrant bone turnover, which essentially results in a loss of bone mass, increased structural weakness and a decreased fracture tolerance threshold [40-42]. Even though Paget disease and osteoporosis are described as having a later age of onset in comparison to osteogenesis imperfecta, they all increase the risk of an individual obtaining a fracture during blunt contact with objects [40,42]. For example a characteristic marker of osteogenesis imperfecta, also known as brittle bone disease, is the presence of Wormian bones at sutures in the cranium. These bones, like sutures are described as acting as lines of structural weakness, offering the path of least resistance for fractures to propagate themselves along [41]. Consequently Wormian bones, along with fractures as a result of bone disease, are often mistaken in the clinical setting for a fracture as a result of child abuse in osteogenesis imperfecta, or elderly abuse in osteoporosis cases [41,42]. It should be noted that it is important for careful clinical examinations to be conducted in order to exclude bone disease as the primary cause of a fracture in suspected blunt trauma cases [41]. Furthermore, structural weakness is not solely dependent on bone disease, but rather geometric cranial structures that foster fracture propagation.

3.5.1.4. Overall skull geometry

Thinner regions of the cranium that are referred to above, are perceived to be less structurally stable and are reinforced by thickened areas know as buttresses [27,28]. Natural thickening of the cranium occurs in the midfrontal, anterior and posterior temporal regions, as well as the midoccipital region. As previously mentioned, a fracture is most likely to take the path of least

resistance through weaker structures, and thus run perpendicularly to buttresses or avoid buttressed areas altogether [2,32]. Buttressed areas are therefore described as guiding fractures as they enable bone to be more resilient under loading [2,4]. However, due to the varying fractures referred to in biomechanical research, one should approach the utilisation of buttressed areas in fracture pattern prediction with caution. This highlights the fact that the exact path of a fracture, regardless of what criteria are taken into account, is difficult to predict [32]. Additionally, the pathway of cranial fractures is described as encompassing sutures, sinuses and foramina, which are mainly located at the base of the cranium. It is these well-known areas of structural weakness that fractures extend towards, as they offer the path of least resistance and may also be involved in terminating fractures [4,32]. Although the above-mentioned structures aid in the propagation of fractures, it is ambiguous as to whether or not they are accountable for fracture initiation.

3.5.1.5. Impact site and fracture initiation

To date, there is still an ongoing debate in the forensic community as to whether or not a fracture initiates at the site of impact [7]. Historically, static and quasi-static tests were the focus of head injury research. More recently however biomechanical research has evolved to follow a more dynamic approach of testing [21]. This era of dynamic testing has led to numerous studies investigating the location of fracture initiation [4,7,9-11,43]. As previously mentioned, Gurdjian et al. [4] were described as the first researchers to make use of the stress coat lacquer technique, through which they hypothesised that linear fractures initiate in a region peripheral to the impact site. This hypothesis was investigated by treating embalmed cadaver heads with the stress coat lacquer and subsequently subjecting them to impacts with a free fall drop tower test.

In 2010 Baumer et al. [7] described their investigation of Gurdjian's methodology [4] through an entrapped drop tower test, however, unlike Gurdjian's research, the stress coat lacquer was not utilised and a porcine model was investigated instead of cadavers. Similarly in 2013, Powell et al. [9] used the porcine model with the same methodology as Gurdjian [4]. Despite the slight discrepancies between these studies, such as the specimen types and experimental set ups, all three studies described fractures occurring at a predictable site of out-bending, generally at bone-suture interfaces, remote to the impact site. Furthermore these fractures travel towards the impact site and then subsequently travel away from it in the opposite direction [4,7,9]. Nonetheless, it has been explained in Baumer et al. [7] and Powell et al. [9] studies that the immature nature of the cranial bone used or the anatomical discrepancies between animal and human models may have influenced their results. This further questions the validity of their results, which are in comparison to the already debatable findings of Gurdjian [4].

Both older and more recent literature [10,11,43] is at odds with the above-mentioned findings. It is the more recent research however that challenges Gurdjian's [4], Hodgson [38] and Hodgson and Thomas [39], as well as Baumer [7] and Powell's [9] findings. Again impact location was investigated through various techniques namely, the drop tower [10,43] and the pendulum technique [11] in combination with different impact locations. These include the temporo-parietal [43], frontal [11] and the parietal regions [10]. All three studies [10,11,43] assert that fractures initiate at the impact site and successively travel away from the impact site until all energy has been dissipated. Kroman et al. [10], through high-speed video analysis, further verified this. These studies are not entirely comparable with one another and this stresses the crucial difficulty in determining the site of fracture initiation in cranial blunt force trauma [8,10]. In addition, it questions the use of varying experimental test set ups and

specimen combinations between independent researchers who negate the consequences thereof [8].

In summary it would be naïve to assume that in all cases bone can withstand the same stresses of an external force. It is suggested by the above-reviewed literature that the presence of hair, as well as a scalp thickness greater than 7 mm renders cranial bone less compliant to the effects of an impact [11,17]. Furthermore, the temporal bone, which is situated in the lateral aspect of the cranium is perceived to be the least tolerant (decreased thickness and stiffness) to an impact and will undoubtedly fail first [22]. Similarly, certain geometric features of the cranium such as buttresses, sutures, sinuses and foramina are known regions of structural weakness and can all influence fractures by offering the path of least resistance [2].

Furthermore, diseased bone, which is known to have decreased bone stiffness, tends to fracture at a lessened fracture tolerance level. More importantly these fractures may not necessarily have arisen as a result of inflicted trauma. It is therefore imperative for clinicians to take bone disease into consideration before concluding inflicted injuries are as a result of trauma [41]. From this, it can be concluded that it is important for researchers to develop an understanding of the intrinsic factors that could potentially influence their experimental data [27]. This is particularly of importance in data comparison between independent research groups and offers an explanation for discrepancies observed. It is critical to note that whilst intrinsic factors influence fracture patterns, they are not solely responsible for the manner in which bone fractures [32]. Fracture patterns also depend on extrinsic factors such as the impact force, dimensions of the blunt implement utilised as well as the velocity of the impact [26].

3.5.2. Extrinsic factors

3.5.2.1. Force required to fracture a skull

Various studies have described the force required to fracture the skull [1,3,11]. However the majority of these studies have focused on the frontal bone. Biomechanical force-deflection results of these various studies suggest that the skull's response to a load is nonlinear resulting in the production of complex fracture patterns.

The work of Yoganandan et al. [1] involved the investigation of various anatomical sites of unembalmed cadaver heads, namely the vertex, parietal and occipital regions, for impact loading under both quasi-static and dynamic testing conditions. Similarly, Delye et al. [11], subjected unembalmed cadaver heads to dynamic impact loading. However, these tests were only conducted on the frontal region. Asgharpour and colleagues [3] set out to simulate Delye's [11] experimental study through a numerical FE model. Loading was achieved through different test set ups in Yoganandan [1] and Delye's [11] studies. More specifically, Yoganandan and colleagues made use of the piston model whilst Delye and colleagues made use of the pendulum test. The quasi-static and dynamic loading conditions in Yoganandan's study were 2.54 m/s and 7.1-8.0 m/s respectively whereas the specimens in Delye's study were subjected to three different impact velocities. These include low velocity (3.60 ± 0.23 m/s), intermediate velocity (5.21 ± 0.04 m/s) and high velocity (6.05 ± 0.04 m/s). Similarly Asgharpour and colleagues [3] FE model was able to replicate the exact velocities of Delye's study.

Subsequent to testing, the force results of Yoganandan's [1] quasi-static loading were 4500-11900 N and hard tissue damage presented as linear fractures. In both Yoganandan's [1] dynamic test and Delye's [11] high velocity dynamic test, multiple fractures at a force of 8800-

14100 N and 10239 ± 2562 N were observed respectively. Furthermore, in Delye's [11] low and intermediate velocity groups, at a force of 5938 N and 11070 ± 26868 N respectively, only single linear fractures were observed. When Asgharpour's [3] FE model results were compared to those of Delye's pendulum test [11], it was found that the force in the low velocity group was 8623 N in comparison to Delye's 5938 N. In addition Asgharpour et al. [3] also referred to both the intermediate and high velocity forces being over-estimated in comparison to Delye's findings. Delye et al. [11] further noted during fracture initiation, the inner table fails when the bone elasticity threshold is reached whereas initial damage in the outer table only occurs around 3400 N. Furthermore, fractures were also consistently wider at locations distant from the impact site.

As previously mentioned, additional impacts may affect the load carrying capacity of bone. In Delye's study [11] it was described that when no fracture was observed, specimens were subjected to additional blows at higher impact energies until a fracture occurred. It is thus suggested that Delye's findings be approached with caution. In addition to this, in studies conducted by Delye et al. [11] and Yoganandan et al. [1], specimens were to an extent restrained, misrepresenting the natural response of the cranium to blunt trauma. This could account for higher fracture forces observed to what may occur in reality. Although the FE model is not restricted in rotational and translational movements like the piston and pendulum tests, it does overestimate the force required to fracture a skull and this study too should be cautiously interpreted [3].

In summary, the most striking aspect of the above-reviewed studies investigating the force required to fracture a skull, is that they are not entirely comparable with one another. This includes debates on which cranial bone is more compliant to an external load, in addition to the force required to produce a fracture, as well as the site of fracture initiation. These

discrepancies exist, as there are numerous experimental tests and specimens available to study head injury biomechanics. Subsequently study results differ in terms of the impact force, fracture initiation site and the resultant fracture [8,9]. Consequently, these differences create a niche in which researchers need to establish a means of making biomechanical studies more comparable with one another across different research groups. For example the development of a method to scale data in order to compare it with data generated from an alternate experimental test.

3.5.2.2 Implement dimensions and impact force

To date very few studies have investigated fracture forces associated with specific implements [5,16,17,22,44]. In addition to force, shape and mass of the implement, the velocity at which it strikes the cranium can also influence a cranial fracture. The following studies are of particular interest as, like the current study, they have all explored cranial fractures in relation to a specific implement. Implements that have been of interest include the effect of an impacted rubber bullet on the human cranium by Raymond and colleagues [17], a hammer in independent studies by Sharkey et al. [5] and Mole et al. [44], in addition to a wooden handle, wooden floor and training shoe also investigated by Sharkey et al. [5]. Furthermore, Glasër et al. [16] has described the impact energy associated with a baseball bat. These studies will be further discussed in detail below. Mole's methodology [44] is of particular interest as the methods used in the current study are similar.

In 2009, Raymond and colleagues [17] subjected seven unembalmed cadaver heads to bilateral impacts in the temporal region at velocities of 20 m/s and 35 m/s, with a simulated rubber bullet fired with a pneumonic piston. Similarly in 2014, Mole et al. [44] employed the piston model through which thirty isolated porcine head specimens, each with a mass of 5

kilograms (kg) were subjected to a single fronto-parietal impact. Three separate velocity conditions ranging from 10 m/s to 25 m/s were utilised.

Fracture forces reported by Mole et al. [44] contend the findings of Raymond et al. [17]. For example, respective fracture forces reported by Raymond under condition A (~25 m/s) and B (~35 m/s) were 3659 N (± 1248 N) and 5809 N (± 1874 N). On the contrary Mole described a mean peak force of 3024 N under condition A (~10 m/s). Even though Mole's peak force is in close range to Raymond's peak force under condition A, the actual velocity of impact between the two studies differs by ~10 m/s. Furthermore, Mole's peak forces of 7234 N (± 1937.69 N) for condition B (~15 m/s) and 11730 N (± 2099.56 N) for condition C (~25 m/s) are both substantially larger than the peak force of 5809 N (± 1874 N) observed by Raymond and colleagues under their condition B (~35 m/s). It should also be noted that the velocity used in Raymond's study exceeds the velocities utilised by Mole lending to results that differ. Furthermore, it would be assumed that a greater velocity would be associated with an increased impact force, however this is not the case when comparing Mole and Raymond's studies.

In addition to reporting fracture forces, Mole [44] and Raymond [17] described resulting hard tissue trauma. More specifically, six out of the seven specimens in Raymond's study presented with depressed comminuted fractures under condition B, whereas only one minor linear fracture was observed under condition A [17]. Once more the work of Mole et al. [44] contends Raymond's findings. In Mole's study fourteen out of the thirty porcine specimens presented with depressed fractures, however only two of these observed fractures had associated comminuted fractures.

Even though Raymond et al. [17] and Mole et al. [44] both utilised the piston model and are the only two studies to investigate impacts above ~10 m/s, their results differ from one another. These differences make it challenging to compare results between studies and highlight limited standardisation in the field of head injury biomechanics. It is postulated that these discrepancies stem from the use of different specimens (cadavers vs. porcine specimens), in addition to different specimen numbers employed by each research group [17,44]. This advances the argument of approaching Raymond's [17] results with caution for several reasons.

The first reason is that Raymond only tested seven specimens in comparison to thirty specimens in Mole's study. Secondly, Raymond subjected these seven specimens to bilateral impacts in comparison to Mole's unilateral impacts. This is an area for concern, as an already weakened bone, as in also the case in the study conducted by Delye et al. [11], is known to be less tolerant to additional impacts. Thirdly, the simulated rubber bullet in Raymond's study was machined from aluminium, this raises another argument surrounding the validity of Raymond's work and it is highly likely that ammunition machined from aluminium would cause more damage than what would be expected from a rubber bullet [17]. Lastly, the different mean peak forces noted between these independent research groups [17,44] could solely be based on the fact that different cranial regions were impacted. For example, Mole et al. [44] targeted the fronto-parietal region, whereas Raymond et al. [17] impacted the temporal bone. As previously described by Delannoy et al. [22], the frontal and parietal regions are structurally the strongest of the cranial bones and it is therefore expected for them to withstand a greater threshold prior to fracturing in comparison to the temporal bone. More importantly, it should be kept in mind that porcine cranial bone differs geometrically from human cranial bone and this could be a probable cause for the discrepancies observed [44].

All of the above weaknesses highlighted in Raymond's study [17] limit the conclusions that can be drawn from this analysis. However, the porcine model utilised by Mole et al. [44] might not effectively simulate cranial blunt trauma seen in human bone, specifically in combination with the piston model. Furthermore, Mole and colleagues are the only research group to have utilised their chosen specimen and experimental test combination [44]. Additional studies have explored cranial fractures in relation to specific implements, however none of these studies have exceeded a velocity of 10 m/s. These studies will be described in detail below.

In 2011, Sharkey et al. [5] investigated, through an adapted drop tower, the force associated with various implements to the fronto-parietal region of porcine head specimens. Similar to Mole's study [44], Sharkey investigated a hammer, in addition to a wooden handle to simulate an intentional blow. Furthermore a wooden floor and training shoe were utilised to simulate an accidental fall and stomping action respectively [5]. In a study conducted by Glasër and colleagues [16] the energy associated with multiple blows to the cranium with a baseball bat was investigated through the drop tower test.

Glasër et al. [16] simulated impacts through the use of an anatomically correct skin-skull-brain model. A description of the drop tower set up involved a maple wood baseball bat being attached to a weight of 4.3 kg while being dropped from varying heights to impact with the skin-skull-brain model below. The experimental results were then compared to the observations made during the autopsy of a female who had received lethal blows to the cranium by what was suspected to be a maple wood baseball bat.

Subsequent to testing in all three studies [5,16,44], Sharkey [5] reported fracture forces ranging from 4149-8632 N, 6524-8676 N, 5757-10140 N and 3340-5524 N for the hammer, wooden handle, wooden flooring and training shoe impacts respectively. In order for damage

to occur all impacts, apart from those involving the training shoe, a force exceeding 4000 N was necessary. The most common fracture observed was suture separation due to impact with the hammer and wooden handle and, as would be expected of the focal implements, depressed fractures were second to suture separation. These results differ from Mole's [44] hammer impacts where the most common fracture observed was a depressed fracture. However, the forces associated with the hammer impacts in both Sharkey [5] and Mole's [44] studies are comparable with one another. This is most likely attributable to the fact that porcine head specimens were utilised in both studies and both research groups investigated the fronto-parietal region.

Similarly, the results of Glasërs study [16] also vary from Sharkey at al. [5]. Sharkey refers to the wooden handle as being accountable for the suture separation observed in porcine specimens. However in Glasërs [16] study, the maple wood baseball bat verifies that the autopsy case under investigation did in fact involve multiple blows with a baseball bat. These impacts were responsible for producing expanded, comminuted fractures with burst fractures to the base of the skull, as well as an extensive spider's-web like comminuted fracture to the right temporo-parietal bone. As previously mentioned in this review, the most likely cause of discrepancies observed is the varying experimental tests and specimens utilised by the independent research groups.

More specifically, the different experimental test set ups used in Sharkey [5] and Mole's [44] studies can be held accountable for the discrepancies in the fracture patterns observed in these studies. However, the discrepancies in fracture patterns observed between Sharkey [5] and Glasër's [16] studies could depend on the different test specimens that were utilised (porcine specimens vs. synthetic model).

Even though the fracture patterns observed in the above-reviewed studies all differ, they do imply that the shape of an implement as well as the velocity at which it impacts the cranium, influence fracture patterns. For example, a relatively broad blunt object at a high velocity may often result in linear or curvilinear fractures that are extensive with complete bony perforations. This type of fracture is often further associated with radiate and concentric fractures [5,22]. However, more focused impacts of a high impact velocity, such as the implement in the study by Mole et al. [44], as well as the projectile used in Raymond and colleagues study [17], tend to displace a small area of bone downwards resulting in a depressed fracture. This resulting fracture is not extended and is generally not associated with radiate or concentric fracture [17]. Mole's study [44] further illustrates that the impact force associated with specific implements can be determined through appropriate experimental set ups. This study also refers to the difficulty in identifying trends between the level of trauma and an applied velocity and impact force, as the resulting soft and hard tissue damage is often unpredictable and varies.

This unpredictability has led to some researchers, however, stating that care should be taken when determining the type of weapon involved with the production of a fracture. For example specific dimensions, such as the shape of the blunt implement can rarely be concluded from fracture morphology. This is in part due to the intrinsic criteria that are known to influence bone. Furthermore one should be aware of taphonomic factors and as such has to exclude these factors before an implement can be deemed responsible for the inflicted trauma [26].

3.6. Rationale

Many researchers, a few of whom have been discussed in this review, have attempted to determine the exact biomechanical mechanism of a lateral skull fracture through various

experimental set ups and a variety of specimens. However, to date this mechanism has not been entirely clarified by research conducted in the past, making it a challenge for current and future researchers to gain a true understanding on the theory behind head trauma biomechanics.

Firstly, there is currently a heavy reliance on older experimental work and case studies. Whilst these studies have advanced the field of head injury biomechanics, they are outdated and do not come without limitations. In particular, case studies are limited because they cannot determine the exact mechanism of trauma. Additionally, data from experimental work is limited as it is obtained in a controlled environment, through small samples sizes due to the unavailability and medical ethics that are associated with animal models and cadavers [1]. Secondly, as no validation studies have been conducted, it is inaccurate to assume that frontal biomechanical data is applicable to the lateral aspect of the skull [21]. Lastly, the studies that have explored the lateral aspect of the skull, have failed to adequately describe impact forces or the resulting soft and hard tissue trauma due to a blunt impact [21,24]. The two main reasons for this inadequacy will be discussed in detail in the paragraphs to follow.

The first shortfall develops from limited comparable studies in the field of head injury biomechanics. Consequently, through the standardisation of research, not necessarily worldwide, but rather within individual mortuaries, researchers could choose the most applicable specimen model and experimental set up combination in order to create an integrated system for conducting research in head impact biomechanics. Ultimately the data generated from a standardised experimental model would be invaluable in the examination of the force and fracture patterns of cranial blunt force trauma, as well as determining the weapon that may have inflicted the fatal injury. In addition it would allow separate groups of researchers to potentially compare validated results [9,22].

The second shortfall in lateral data arises mainly from the unpredictable manner in which bone fractures. For example, throughout this review various studies have been discussed in which none of them observed identical fracture patterns. This not only depends on the unpredictable nature of bone, but also on intrinsic and extrinsic factors, which are known to influence bone [26]. The primary reason for this challenge in interpreting fractures is that a significant amount of biomechanical studies are dedicated to investigating the impact tolerance of the skull's frontal region in terms of automotive-related impact conditions [3,21]. Even though road traffic accidents are the number one cause of head injuries in western countries, the same statistics do not apply for developing countries [3]. In addition to this, assailant-inflicted trauma often involves injuries to the lateral aspect of the skull. Nonetheless lateral loading is less frequently studied in a laboratory setting and this highlights the necessity for research in this particular domain [19,21,45].

In summary, this paucity in lateral impact data poses a significant challenge for forensic pathologists who often, with marginal scientific evidence, have to give an objective diagnosis of resultant cranial blunt force trauma fractures [1]. It is thus essential to reduce the subjectivity of expert witness testimonies through the generation of data in the lateral region of the skull. This knowledge will be invaluable in the interpretation of assailant-inflicted fractures, in addition to identifying specifics such as, the impact angle and location, the sequence of blows, as well as establishing the influence of implement dimensions and the impact force [10,16]. Furthermore, the impact force is especially important in terms of the legal system as the energy that an assailant delivered can be established and conclusions can be drawn to make an accurate analysis of the assailant's motive [25]. For example, was the force used indicative of self-defense or was it intended to do grievous bodily harm? [13,16,46].

3.7. Conclusion

In spite of all the past advancements that have been achieved in the head injury biomechanics field, additional research needs to be conducted before forensic pathologists can accurately interpret cranial facture patterns on a daily basis in post-mortem cases [22]. It can be concluded from this review that the intrinsic factors influencing a fracture in the lateral region of the cranium need to be taken into account prior to experimental testing [27]. Furthermore, it is suggested through standardised experimental tests and specimens that extrinsic factors are explored and understood to a greater extent [26]. This would aid in the amelioration of data paucity, as well as inconsistent studies. Moreover, future research could subsequently aid forensic scientists and pathologists in terms of homicide cases, by developing a means of assessing the trauma inflicted by a blunt impact in relation to the force of the impact due to a specific implement [18,22]. Therefore the aim of the current study is to employ similar methodology to that utilised by Mole et al. [44]. Contrary to Mole's study, a proxy animal model to the porcine model shall be investigated. This current study will entail the investigation of the force and energy associated with lateral impacts. In addition, it is hoped through this study to characterise soft and hard tissue trauma in relation to simulated hammer impacts. In conclusion this research could potentially contribute towards a guideline assisting in reducing the subjectivity of expert testimonies in court.

3.8. Reference list

[1] Yoganandan NA, Pintar FA, Sances A, Walsh PR, Ewing CL, Thomas DJ et al. Biomechanics of Skull Fracture. J Neurotrauma 1995;12:659-668.

[2] Hart GO. Fracture Pattern Interpretation in the Skull: Differentiating Blunt Force from Ballistics Trauma Using Concentric Fractures. J Forensic Sci 2005;50:1276-1281.

[3] Asgharpour Z, Baumgartner D, Willinger R, Graw M, Peldschus S. The validation and application of a finite element human head model for frontal skull fracture analysis. J Mech Behav Biomed Mater 2014;33:16-23.

[4] Gurdjian ES, Webster JE, Lissner HR. The mechanism of skull fracture. J Neurosurg 1950;2:106-114.

[5] Sharkey E, Cassidy M, Brady J, Gilchrist M, NicDaeid N. Investigation of the force associated with the formation of lacerations and skull fractures. Int J Legal Med 2011;126:835-844.

[6] McElhaney JH, Hopper RH, Nightingale RW, Myers BS. Mechanisms of Basilar Skull Fracture. J Neurotrauma 1995;12:669-678.

[7] Baumer TG, Passalacqua NV, Powell BJ, Newberry WN, Fenton TW, Haut RC. Age-Dependent Fracture Characteristics of Rigid and Compliant Surface Impacts on the Infant Skull-A Porcine Model. J Forensic Sci 2010;55:993-997.

[8] Jordana F, Colat-Parros J, Bénézech M. Diagnosis of Skull Fractures According to Postmortem Interval: An Experimental Approach in a Porcine Model. J Forensic Sci 2013;58:156-162.

[9] Powell BJ, Passalacqua NV, Fenton TW, Haut RC. Fracture Characteristics of Entrapped Head Impacts Versus Controlled Head Drops in Infant Porcine Specimens. J Forensic Sci 2013;58:678-683.

[10] Kroman A, Kress T, Porta D. Fracture Propagation in the Human Cranium: A Re-Testing of Popular Theories. Clin Anat 2011;24:309-318.

[11] Delye H, Verschueren P, Depreitere B, Verpoest I, Berckmans D, Vander Sloten J et al. Biomechanics of Frontal Skull Fracture. J Neurotrauma 2007;24:1576-1586.

[12] Verschueren P, Delye H, Depreitere B, Van Lierde C, Haex B, Berckmans D et al. A new test set-up for skull fracture characterisation. J Biomech 2007;40:3389-3396.

[13] Grassberger M, Gehl A, Püschel K, Turk, EE. 3D reconstruction of emergency cranial computed tomography scans as a tool in clinical forensic radiology after survived blunt head trauma—Report of two cases. Forensic Sci Int 2011;207:e19-e23.

[14] Thali MJ, Braun M, Brueschweiler W, Dirnhofer R. 'Morphological imprint': determination of the injury-causing weapon from the wound morphology using forensic 3D/CAD-supported photogrammetry. Forensic Sci Int 2003;132:177-181.

[15] Woźniak K, Rzepecka-Woźniak E, Moskała A, Pohl J, Latacz K, Dybała B. Weapon identification using antemortem computed tomography with virtual 3D and rapid prototype modeling—A report in a case of blunt force head injury. Forensic Sci Int 2012;222:29-32.

[16] Gläser N, Kneubuehl BP, Zuber S, Axmann S, Ketterer T, Thali MJ et al. Biomechanical Examination of Blunt Trauma due to Baseball Bat Blows to the Head. J Forensic Biomech 2011;2:1-5.

[17] Raymond D, Van Ee C, Crawford G, Bir C. Tolerance of the skull to blunt ballistic temporo-parietal impact. J Biomech 2009;42:2479-2485.

[18] Krabbel G, Appel H. Development of a Finite Element Model of the Human Skull. J Neurotrauma 1995;12:735-742.

[19] Sahoo D, Deck C, Yoganandan N, Willinger R. Anisotropic composite human skull model and skull fracture validation against temporo-parietal skull fracture. J Mech Behav Biomed Mater 2013;28:340-353.

[20] Bandak FA, Vorst MJV, Stuhmiller LM, Mlakar PF, Chilton WE, Stuhmiller JH. An Imaging-Based Computational and Experimental Study of Skull Fracture: Finite Element Model Development. J Neurotrauma 1995;12:679-688.

[21] Yoganandan NA, Pintar FA. Biomechanics of temporo-parietal skull fracture. Clin Biomech 2004;19:225-239.

[22] Delannoy Y, Becart A, Colard T, Delille R, Tournel G, Hedouin V et al. Skull wounds linked with blunt trauma (hammer example). A report of two depressed skull fractures – Elements of biomechanical explanation. Leg Med 2012;14:258-262.

[23] Butchart A, Peden M, Matzopoulos R, Phillips R, Burrows S, Bhagwandin N et al. The South African National Non-Natural Mortality Surveillance System–Rationale, Pilot Results and Evaluation. S Afr Med J 2001;91:408-417.

[24] Pierce MC, Bertocci GE, Berger R, Vogeley Ev. Injury biomechanics for aiding in the diagnosis of abusive head trauma. Neurosurg Clin N Am 2002;13:155-168.

[25] Cory CZ, Jones MD, James DS, Leadbeatter S, Nokes LDM. The potential and limitations of utilising head impact injury models to assess the likelihood of significant head injury in infants after a fall. Forensic Sci Int 2001;123:89-106.

[26] Dirkmaat DC, Cabo LL, Ousley SD, Symes SA. New Perspectives in Forensic Anthropology. Yearb Phys Anthr 2008;51:33-52.

[27] Berryman HE, Symes SA. Recognizing Gunshot And Blunt Cranial Trauma Through Fracture Intrepretation. In: K.J. Reichs, editor. Forensic Osteology: Advances in the Identification of Human Remains. 2nd ed. Springfield IL: Charles C Thomas; 1998. p. 333-352.

[28] Saukko P, Knight B. Head and Spinal Injuries. In: Bureau S, Ueberberg A, editors. Knight's Foensic Pathology. 3rd ed. London: Arnold Hodder headline group; 2004. p. 174-88.

[29] Ferrer E, de Notaris M. Contemporary Skull Fractures: Unusual Everted Fracture. World neurosurg 2011;76:417-418.

[30] DiMaio DJ, DiMaio VJM. Forensic Pathology. 2nd ed. London: CRC Press; 2001.

[31] DiMaio VJM, Dana SE. Blunt Force Injury. In: Froede RC, editor. Handbook of Forensic Pathology. 2nd ed. New York: CRC press Taylor and Francis Group; 2007. p. 73-104.

[32] Fenton TW, Stefan VH, Wood LA, Sauer NJ. Symmetrical Fracturing of the Skull from Midline Contact Gunshot Wounds: Reconstruction of Individual Death Histories from Skeletonized Human Remains. J Forensic Sci 2005;50:274-285.

[33] Sances AJ and Yoganandan N. Engineering Proceedings of a special symposium on maturing technologies and emerging horizons in IEEE. 1988:115-22.

[34] Thali MJ, Kneubuehl BP, Zollinger U, Dirnhofer R. The “Skin–skull–brain model”: a new instrument for the study of gunshot effects. Forensic Sci Int 2002;125:178-189.

[35] Muschler GF, Vivek PR, Patterson TE, Wenke JC, Hollinger DDS. The Design and Use of Animal Models for Translational Research in Bone Tissue Engineering and Regenerative Medicine. Tissue Eng PT B 2010;16:123-145.

[36] Thali MJ, Kneubuehl BP, Dirnhofer R. A “skin–skull–brain model” for the biomechanical reconstruction of blunt forces to the human head. Forensic Sci Int 2002;125:195-200.

[37] Yoganandan NA, Zhang J, Pintar FA. Force and Acceleration Corridors from Lateral Head Impact. Traffic Inj Prev 2004;5:368-373.

[38] Hodgson VR. Tolerance of the facial bones to impact. Am J Anat 1967;120:113-122.

[39] Hodgson VR, Thomas LM. Breaking strength of the human skull vs. impact surface cuvature. US Department of Transportation, HS-800-583, Springfield, VA .

[40] Rea SL, Walsh JP, Layfield R, Ratajczak T, Xu J. New Insights Into the Role of Sequestosome I/p62 Mutant Proteins in the Pathogenesis of Paget's Disease of Bone. Endocr Rev 2013;34:501-524.

[41] Rauch F, Glorieux FH. Osteogenesis imperfecta. The Lancet 2004;363:1377-1385.

[42] Rachner TD, Khosla S, Hofbauer LC. Osteoporosis: now and the future. The Lancet 2011;377:1276-1287.

[43] Nahum AM, Gatts JD, Gadd CW, Danforth J. Impact tolerance of the skull and face. Proc Stapp Car Crash Conf 1968;12:302-316.

[44] Mole CG, Heyns M, Cloete T. How hard is hard enough? An investigation of the force associated with lateral blunt force trauma to the porcine cranium. Leg Med 2015;17:1-8.

[45] Raymond D, Crawford G, Van Ee C, Bir C. Development of Biomechanical Response Corridors of the Head to Blunt Ballistic Temporo-Parietal Impact. J Biomech Eng 2009;131:094506-1-094506-7.

[46] Zugibe FT, Costello JT. Identification of a Murder Weapon by a Peculiar Blunt Force Injury Pattern and Histochemical Analysis. J Forensic Sci 1985;30:239-242.

[47] Marieb EN. Chapter 5: The Skeletal System. In: Larson S, Peyrefitte S., editors. Esstentials of Human Anatomy & Physiology. Ninth ed. San Francisco, CA: Pearson Benjamin Cummings; 2009. p. 146.

Chapter Four

A publication-ready manuscript

An analysis of the force associated with lateral cranial blunt force trauma in Cape (Chacma) Baboons

Lisa Jane Coetzé[a], Calvin Gerald Mole[a], Marise Heyns[a], Trevor Cloete[b]

a. **Division of Forensic Medicine and Toxicology, Department of Clinical Laboratory Sciences, Faculty of Health Sciences, University of Cape Town, Observatory, South Africa**
b. **Blast Impact and Survivability Research Unit (BISRU), Department of Mechanical Engineering, Faculty of Engineering and Built Environment, University of Cape Town, Rondebosch, South Africa**

***Correspondence to: Ms Lisa Jane Coetzé, Department of Clinical Laboratory Sciences, Faculty of Health Sciences, University of Cape Town, P.O. Box 13914, Mowbray, 7705, South Africa. E-mail: lisacoetze@gmail.com, Tel: +27 214066604, Fax: +27 214481249**

Abstract

Cranial blunt force trauma is a concern worldwide. However, despite the parietal bone frequently fracturing, the majority of studies have investigated frontal bone impacts. Additionally, few studies have determined the force involved in cranial blunt force trauma to the lateral side of skull. It is also important to consider the use of intrinsic factors as a tool in the biomechanical testing of bone. This could essentially contribute to a greater understanding of fracture patterns resulting from lateral cranial trauma. As such, the current study measures scalp and skull thickness and also attempts to determine the force at which the lateral region of the Cape (Chacma) Baboon skull fractures. Twenty-seven male Cape (Chacma) Baboon specimens were subjected to single impacts in the temporo-parietal region. Fifteen specimens were impacted with an aluminium projectile resembling the dimensions of a hammer head. The velocity of impact ranged from 10 m/s to 20 m/s. The remaining twelve specimens were subjected to impacts with an aluminium Hopkinson pressure bar (HPB). Each specimen was subjected to a single impact at an increased velocity. Only two specimens presented with superficial lacerations. The most common fracture observed was a circular penetrating fracture. These fractures often presented with associated radiating or concentric fractures. The mean peak fracture force was 6584.06 N (± 1815.22 N) and a mean displacement of 0.96 mm (± 0.16 mm) was observed. No clear trend existed between impact force and the extent of trauma. However, bone trauma observed in the baboon model resembles blunt trauma morphology observed in human bone.

Keywords: Blunt force trauma; Laceration; Skull fracture; Applied Force; Hopkinson pressure bar; Cape (Chacma) Baboon

4.1. Introduction

Globally 1.6 million people lose their lives each year due to violence. African men and woman are one of the demographics at greatest risk [1,2]. Specifically, in South Africa as a developing country with a turbulent past driven by constitutional racial segregation, a death rate of 157.8 per 100 000 exists due to violence [2,3]. This exceeds the death rate recorded for the African continent as a whole (139.5 per 100 000) [3]. Homicide is not only a concern in South Africa, but worldwide. However the crime statistics in South Africa are high, with 46% of deaths related to homicide. This rate is four times the recorded global rate [2,4]. Further, homicide-related deaths recorded in South Africa typically involve firearms (50.7%), sharp instruments (33.0%) and blunt objects (10.6%). All of these implements may potentially inflict a great amount of cranial trauma [4,5].

A number of extrinsic and intrinsic factors exist which may play a role in wound morphology associated with cranial trauma. Intrinsic factors, such as anatomical features, are important in assessing blunt force wound morphology of impacts to the head [6]. Intrinsic factors contribute towards the pattern of a fracture and as such could ultimately be used to predict fracture patterns and the cause of injury [7]. Intrinsic factors which may play a role in cranial fracture production and propagation include:

- Presence of hair and scalp thickness
- Cranial bone thickness and stiffness
- Overall skull geometry including buttresses, sutures, sinuses and foramina
- Impact site and fracture initiation

Even though these intrinsic factors are theoretically understood, they are currently not widely used as a tool to predict fracture patterns [7]. Bone responds differently to each impact. There

therefore exists a great amount of variation in the expression of fractures, even within cases involving the same mechanism [8]. Due to this unpredictability, it is a challenge to set up a guideline for predicting skull fractures [9-11]. It is therefore important for researchers to explore the use of intrinsic factors as a tool, which can contribute to an understanding of extrinsic factors (impact force) and bone trauma [9,12].

Numerous studies have however explored the mechanism associated with hard and soft tissue cranial trauma. These mainly include frontal bone impacts during automotive accidents [13]. Lateral head impacts, as well as those involving specific implements have been studied to a lesser extent. Furthermore these impacts often result in the parietal bone fracturing [7,13-15]. This lack of research could hamper experts in their ability to interpret observed trauma to the lateral portion of the head. This is especially true in identifying individual implements and the force associated with impact [10]. Furthermore, several studies rely largely on case studies and older experimental work. Varying methods used in these studies results in them not being entirely comparable with one another [16].

Specimens employed in these studies include human cadavers or cadaver head specimens, animal models and synthetic models [17]. These studies have also used various experimental set ups, including: free fall tests [13,18,19], drop tower tests [9,16,20-23], and pendulum tests [24], as well as three-dimensional (3D) printing [25-27], the finite element (FE) model [28] and piston model [29-32].

Mole and colleagues [32] recently used an adapted configuration of the piston model, the Hopkinson pressure bar (HPB). This is an apparatus commonly used to determine the properties of specimens during material testing [33]. Its use, however, in assessing fracture forces in whole specimens has not previously been described. Mole et al. [32] used whole

porcine head specimens in his study. These specimens were subjected to single impacts in the fronto-parietal region at velocities ranging from 10 m/s to 25 m/s. Half of the specimens were subjected to impacts with a projectile resembling a hammer, while the rest were impacted with the HPB. Fracture forces reported by Mole et al. [32] compare well with current literature, however differences in fracture morphology are present across studies.

It is important to expand on knowledge in head injury biomechanics. This includes further research on the biomechanics of lateral cranial impacts. The objectives of this study were threefold. The primary objective was to determine the fracture force associated with blunt impacts using the Cape (Chacma) Baboon skull as a model. The secondary objective was to describe soft and hard tissue wound morphology associated with impacts on the Cape (Chacma) Baboon skull. The aim was to discover if a trend existed between resultant trauma and impact force. The third objective was to measure scalp and skull thickness in Cape (Chacma) Baboon specimens. The aim was to determine if a significant correlation existed between these measurements and the extent of trauma.

4.2. Materials and Methods

The animal model of interest in this study is *Papio ursinus*, more commonly known as the Cape (Chacma) Baboon. Many cranial bones in primates are structurally comparable to human cranial bones [34,35]. For a detailed description of baboon cranial anatomy refer to “Appendix B”. Most studies [9,20,21,23,32,36,37] utilising animal models have focused on the porcine model. Although the porcine model is suggested to be a suitable surrogate for human bone [10,20], further research should be conducted on other animal models [32].

The current study utilises twenty-seven male Cape (Chacma) Baboon specimens for impact testing. Whole baboon heads of varying weights (1.32-3.64 Kg) were obtained from the Cape Peninsula Baboon Research Unit and Cape Nature. All specimens were frozen at -20°C upon delivery to the University of Cape Town, Faculty of Health Sciences. Specimens were thawed for forty-eight hours before testing and palpated to ensure that no pre-existing injuries were present. Any specimen with a head injury was removed from the study.

The current study employed the use of a suspension frame previously described by Mole et al. [32]. The rigid steel frame consists of an adjustable net suspended from hooks. Turnbuckles aid in adjustment of the net's position. This set up enables the specimen to move freely following impact, allowing a more realistic simulation of cranial blunt force trauma in contrast to restrained techniques [24]. Specimen restraint against a rigid backing material, such as in the entrapped drop tower tests, results in a specimen experiencing an added crushing force. This increases cranial bone stress and the likelihood of fractures occurring in response to a crushing force, rather than from impact alone [13,23,38].

Before testing, specimens were divided into groups of fifteen and twelve and referred to as the hammer and HPB tests respectively. The hammer tests described soft and hard tissue wound morphology and the HPB tests determined the force at which the Cape (Chacma) Baboon skulls fractured. After testing, a section of bone was removed from the right temporo-parietal region, which was measured with a digital calliper to get the average bone thickness measurements.

This study was granted ethical clearance by the Animal Research Ethics Committee of the University of Cape Town, Faculty of Health Sciences and Cape Nature of the Western Cape Conservation Board.

4.2.1. Hammer tests

The fifteen specimens within the hammer test group were divided into nine scalped and six intact specimens. The principal reason behind scalping was to find out if the baboon scalp and underlying muscle influences fracture morphology during impact. This involved removing pelage (fur) and the scalp, as well as the temporalis muscle overlying the right temporo-parietal region.

The projectile used was an aluminium striker bar and is similar to the projectile described by Mole et al. [32]. The dimensions of the striker bar were as follows: 20 mm diameter, 230 mm in length and a weight of 200 g. A gas gun, which uses compressed air, was utilised to subject each specimen to a single impact with the striker bar (Figure 4.1). Increasing or decreasing the pressure of the compressed air, adjusts the velocity at which the striker bar travels. A light-based velocity trap was used to measure the velocity of the striker bar. The hammer tests were performed under three different impact conditions; condition A, B and C were conducted at approximately 10 m/s, 15 m/s and 20 m/s respectively.

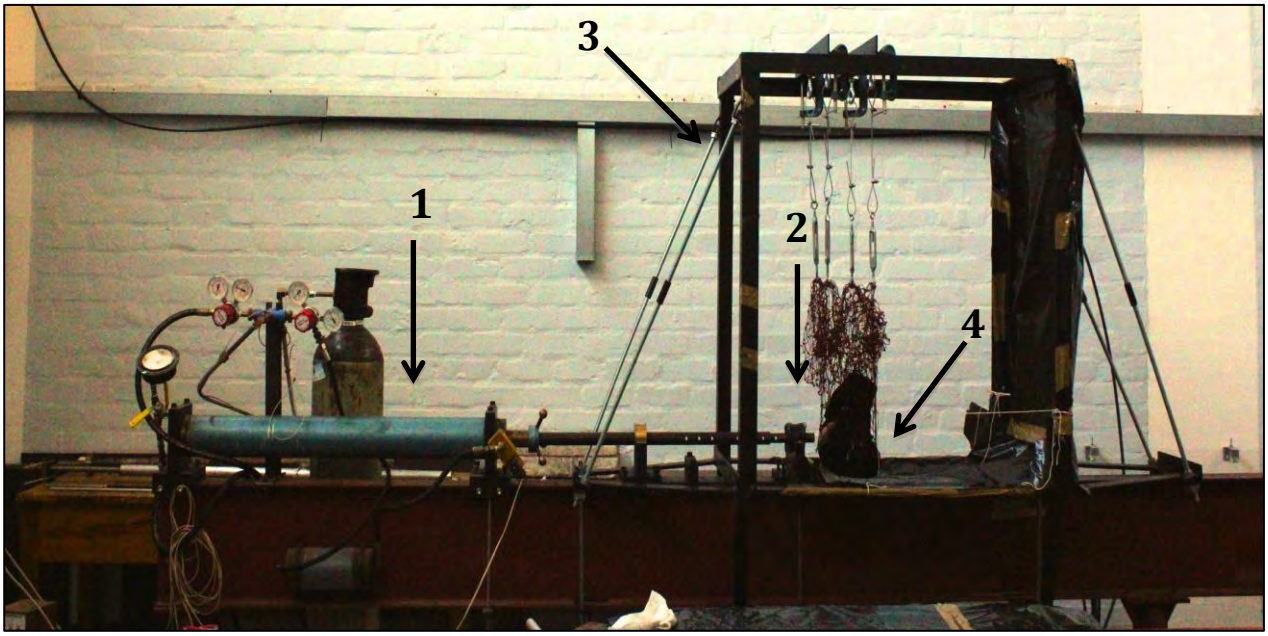

Figure 4.1: Hammer test configuration. 1 – Gas gun, 2 – Velocity trap, 3 – Suspension rig, 4 – Suspended baboon specimen

Following testing, all scalped specimens underwent a visual inspection for the presence of cranial fractures. This involved removing any remaining periosteum, followed by measurements and photography. Intact specimens were examined for the presence of lacerations and soft tissue was removed to allow underlying fractures to be exposed. Similar to scalped specimens, wound morphology was documented with measurements and photography.

4.2.2. Hopkinson pressure bar tests

All twelve specimens in the HPB test group were scalped. These specimens were subjected to a single right temporo-parietal impact with an aluminium HPB (Figure 4.2). For a detailed description of the HPB configuration refer to "Appendix C". The dimensions of the HPB are as follows, 20 mm in diameter and 1.5 m in length. Two sets of diametrically opposed strain gauges were placed a third of the way down from both ends of the HPB. The purpose of the strain gauges is to record the force of impact. Aligned teflon bushes, which act as built in clamps, were utilised to ensure near frictionless motion of the HPB during impact. Each successive test was performed at increased velocities until a fracture occurred.

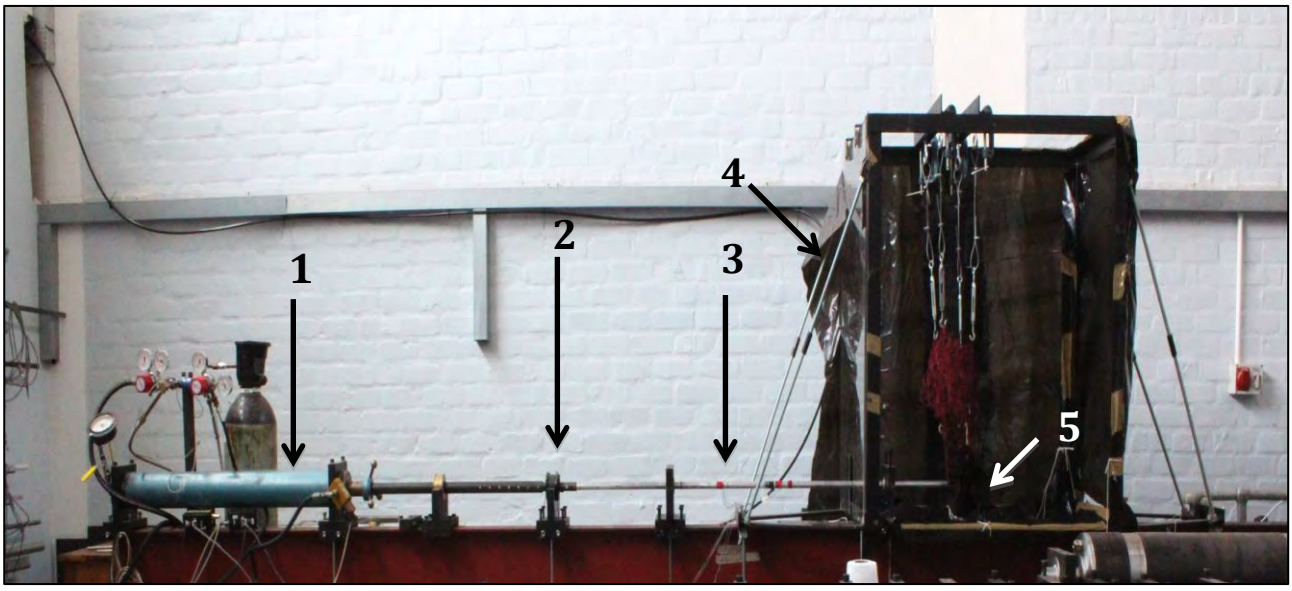

Figure 4.2: Hopkinson pressure bar configuration. 1 – Gas gun, 2 – Velocity trap, 3 – Hopkinson pressure bar, 4 – Suspension rig, 5 – Suspended baboon specimen.

During testing, the striker bar is propelled forward to impact with the HPB and this produces a compressive stress wave. This drives the HPB forward to impact perpendicular to the suspended Cape (Chacma) Baboon specimen. Two phenomena occur in response to an impedance mismatch between the HPB and specimen. Firstly, at the interface between the specimen and HPB, part of the compressive wave transfers into the specimen and remains a compressive wave, travelling back and forth within the specimen. Secondly, the remainder of the original compressive wave reflects back along the HPB as a tension wave. These compression and tension waves are recorded by the previously mentioned strain gauges. This one-dimensional stress wave theory draws inferences on the load the specimen is subjected to. It is further possible to determine the impact force, energy and velocity as well as displacement [39]. Following impact, specimens were examined for fractures, which were documented in a similar fashion to the hammer tests.

4.2.3. Statistical analysis

One Way Analysis of Variance (ANOVA) and the Kruskal-Wallis test were used to analyse parametric and non-parametric data respectively, to determine if a significant difference occurred between the three impact conditions. These conditions were also individually analysed, and the two sample t-test and Mann-Whitney test were used for parametric and non-parametric data respectively. A Spearman rank correlation test was conducted to find out whether a correlation existed between data and resultant hard tissue damage or not. All statistical calculations were performed using STATA 11 (StataCorp, Texas, USA).

4.3. Results

4.3.1. Hammer tests

All nine scalped specimens of the hammer test group presented with a fracture. Examples of these fracture types are shown in figure 4.3. Of the six intact specimens, two had soft tissue

damage and none showed any signs of a fracture. Overall, the striker velocity (P=0.003) and kinetic energy (P=0.003) were significantly different between the impact conditions. Also, the resulting velocity and kinetic energy between individual conditions were significantly different. No significant difference in scalp (P=0.380) and skull (P=0.591) thickness was noted between impact conditions. Also, no significant correlation existed between energy and hard tissue damage (r=0.51, P=0.16), or between skull thickness and hard tissue damage (r=-0.09, P=0.76). However, a trend is emerging between the velocity of impact and hard tissue damage (r=0.51, P=0.06).

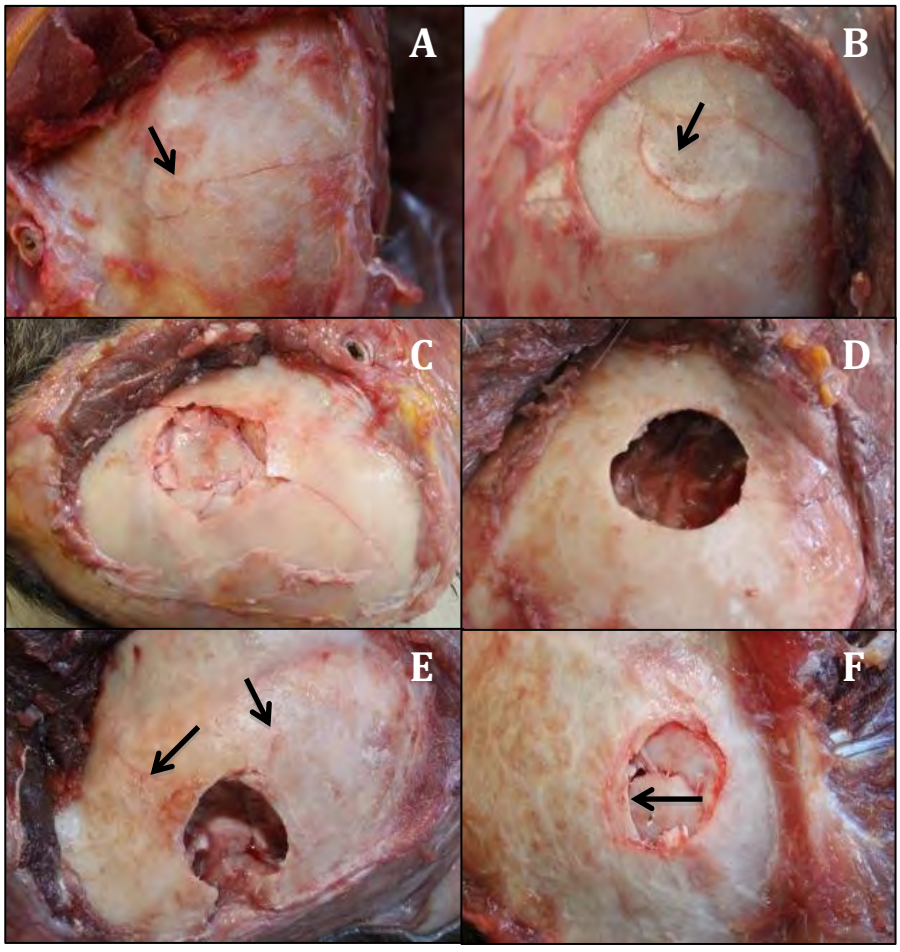

Figure 4.3: Types of fractures observed in hammer and Hopkinson pressure bar tests. A – Linear, B – Semi-circular linear, C - Depressed comminuted, D – Penetrating, E – Penetrating with radiating, F – Depressed with concentric.

As seen in Table 4.1, specimens under condition A were impacted with a mean striker velocity of 9.63 m/s (± 0.40 m/s). This resulted in a mean kinetic energy of 9.28 J (± 0.77 J). One specimen presented with a linear fracture measuring 31.10 mm in length and another specimen as a semi-circular, linear fracture measuring 13.65 mm in length. Furthermore a specimen presented with a semi-circular, slightly depressed fracture (20.38 mm), and an associated radiating fracture measuring 4.56 mm in length. Also, this specimen showed signs of localised deterioration of the inner bone table. Two specimens did not have any soft or hard tissue damage.

Specimens under condition B experienced a mean striker velocity of 15.87 m/s (± 1.84 m/s). This resulted in a mean kinetic energy of 25.46 J (± 5.42 J), resulting in three fractures. Hard tissue trauma was consistent with circular penetrating fractures. Specifically, the fracture noted in one of the specimens was 19.69 mm x 25.17 mm in diameter. The penetrating and associated concentric fracture in another specimen measured 22 mm x 25 mm in diameter. Also, this concentric fracture had two radiating fractures measuring 2.32 mm and 1.73 mm in length. Furthermore, one of the specimens presented with a penetrating fracture measuring 19.96 mm x 21.93 mm in diameter. Two intact specimens presented with superficial lacerations. These included circular (1 mm x 2 mm) and semi-circular (4 mm x 2 mm) lacerations. None of the intact specimens under condition B presented with fractures.

Specimens in condition C underwent impact at a mean striker velocity of 20.14 m/s (± 0.97 m/s). This led to a mean kinetic energy of 40.74 J (± 3.80 J) and resulted in three fractures. One specimen presented with a circular, penetrating fracture (19.80 mm x 23.22 mm) and a radiating fracture (12.25 mm). While another specimen had a penetrating and radiating fracture measuring 19.80 mm x 23.22 mm and 12.25 mm respectively. One of the specimens had a circular, penetrating fracture (21.47 mm x 44 mm) with four radiating fractures. The

radiating fractures measured 35.64 mm, 22.01 mm, 32.42 mm and 60 mm in length. None of the intact specimens under condition C presented with fractures or lacerations. All the penetrating fractures in condition B and C presented with internal beveling. One specimen was removed from the study because of advanced decomposition.

4.3.2. Hopkinson pressure bar tests

Eight fractures were present in the twelve specimens subjected to impacts with the HPB. Examples of these fracture types are shown in figure 4.3. Overall, no significant correlation existed between skull thickness and hard tissue damage ($r=-0.48$, $P=0.12$) or displacement and hard tissue damage ($r=0.10$, $P=0.75$). However, a significant correlation existed between impact energy and hard tissue damage ($r=0.71$, $P=0.009$). There was also a significant correlation between impact velocity and hard tissue damage ($r=0.71$, $P=0.009$). In Table 4.2, the overall mean striker velocity was 19.72 m/s (± 3.66 m/s), however the mean impact velocity was only 9.71 m/s (± 2.66 m/s). This resulted in a mean peak impact force of 5750.39 N (± 2057.63 N), a mean displacement of 0.96 mm (± 0.16 mm) and mean impact energy of 5.49 J (± 2.23 J).

Four specimens did not present with fractures at peak impact forces ranging from 1951.59-5228.72 N. However, one specimen presented with a depressed comminuted fracture measuring 17.67 mm x 21.24 mm at a peak force of 3981.04 N. Seven specimens fractured at an impact force above 5300 N and three of these specimens presented with linear fractures. Specifically, one specimen presented with a linear fracture at a peak force of 6170.41 N, measuring 12.87 mm in length. The other two specimens presented with semi-circular, linear fractures. Lengths were 15.15 mm and 13.26 mm at peak forces of 5319.18 N and 7233.33 N. Furthermore a specimen presented with a depressed comminuted fracture (26.66 mm x 21.15 mm) and four radiating fractures (39.11 mm, 13.54 mm, 9.2 mm and 6.43 mm), at a peak

impact force of 5882.35 N. However, another specimen presented with a semi-circular, slightly depressed fracture (20.13 mm) and radiating fracture (10.39 mm) at a peak force of 6446.10 N. Another specimen presented as a depressed comminuted fracture (18.93 mm x 13.83 mm), with an associated concentric fracture at a peak force of 7480.98 N. One specimen also presented as a depressed comminuted fracture (20.19 mm x 18.71 mm), at a peak force of 10159.12 N.

4.4. Discussion

The study of biomechanics of bone trauma explores how biological tissue responds to an applied mechanical force. Understanding the biomechanics of a skull fracture, as well as the influence of intrinsic factors are important tools for forensic scientists [8]. Also, the impact force and whether the assailant intended to do grievous bodily harm or not can be determined [16,25]. This knowledge could limit the subjectivity of evidence presented in court [16,21,32].

The use of the HPB apparatus in determining fracture forces in whole head specimens has only been described once previously [32]. However, the experimental combination of the HPB apparatus and Cape (Chacma) Baboon specimens is novel. The primary objective of the current study was to determine the force at which the temporo-parietal region of the Cape (Chacma) Baboon skull fractures. The second objective aimed to characterise resultant soft and hard tissue trauma. The scalp and skull thickness of specimens were also assessed.

The extent of soft and hard tissue damage was characterised through hammer tests similar to those employed by Mole et al. [32]. Despite using similar impact conditions, resultant fractures in the current study differ from those seen by Mole et al. [32]. For example, two linear fractures under condition A (~10 m/s) resulted in the current study, and this is consistent with low velocity impacts [8]. Mole et al. [32] however, noted a single depressed fracture

under similar conditions and this was the most common fracture in their study. Conversely, the most common facture in the current study presented as a penetrating fracture with a circular shape.

Depressed and penetrating fractures both result from high-energy loads impacting the skull [8]. The hammer tests in the current study resulted in two penetrating fractures, presenting with radiating fractures and one presenting with both concentric and radiating fractures. In contrast, the depressed fractures viewed in porcine specimens did not present with radiating fractures [32]. Similarly, Delannoy and colleagues [10] did not see radiating or concentric fractures in hammer impacts to the parietal bone of humans, however penetrating fractures were observed.

Despite differences between the current study and the study conducted by Delannoy et al. [10], the resultant fracture types were similar. Observed bone trauma was consistent with penetrating fractures. These lesions presented with sharp, regular edges on the outer table, while the inner table was beveled. Beveling of a similar nature was found in the current study.

Even though fractures were comparable between studies, the skull thickness of the impacted areas differs between the models used. In the current study, the temporo-parietal region had an average thickness of 3.52 mm (± 0.5 mm). This measurement is on the thinner side of human skull thickness, which can range from 4-7 mm [40]. Typically the temporal and parietal bone thickness in humans is on average 4.8 mm and 6.4 mm respectively [10]. Skull thickness is of interest as thinner regions of bone are more susceptible to fracture. These regions offer the path of least resistance and it is here that fractures often initiate and propagate [12,41].

Although Mole and colleagues did not measure skull thickness, the porcine skull is more angular in shape and often exceeds the overall thickness of humans [20,32]. The Cape (Chacma) Baboon skull is however, rounded like the human skull. Nonetheless, unlike the porcine skull, it is less robust. This is seen in the extensive fracture patterns of the Cape (Chacma) Baboon in contrast to the study by Mole et al. [32]. Despite a decrease in skull robustness and thickness, the Cape (Chacma) Baboon gives a more realistic simulation of fracture morphology, expected in humans in comparison with porcine specimens.

Unlike the scalped Cape (Chacma) Baboon specimens, the resultant soft and hard tissue damage of intact specimens, did not represent trauma expected from blunt impacts. Only two intact specimens had superficial lacerations and furthermore none of the specimens presented with fractures. However, under the same impact conditions as the current study, most of the porcine specimens in the Mole et al. study [32] had lacerations. Also, these porcine specimens presented with various types of fractures. The average scalp thickness of the porcine specimens was 6 mm, which is comparable to humans (5-7 mm) [32,40]. Thus lacerations would have been expected in the Cape (Chacma) Baboon specimens, as the average scalp thickness was only 1.33 mm.

This lack of soft and hard tissue damage may be attributable to the presence of a thick temporalis muscle overlying the temporo-parietal region. Muscle absorbs the energy of an impact and this reduces the stress that bone is exposed to. In a study by Delannoy [10], intact cadaver heads with soft tissue measurements exceeding 7 mm in thickness presented with no fractures after impact. However, specimens with less than 7 mm of soft tissue did fracture when subjected to an impact. In the current study, soft tissue thickness ranged from as little as 2 mm up to 11 mm. However, the Cape (Chacma) Baboon specimens with less than 7 mm of

soft tissue did not fracture. Also, scalped specimens in the HPB group only consistently fractured at impact forces above 5300 N.

Despite the fact the Cape (Chacma) Baboon scalp is thin it is tough. Environmental stimuli influence this, as well as the thick temporalis muscle and robust skull of wild baboons. These baboons consume a diet consisting of brittle foods. This includes fruits, roots, corms, leaves and tree gum [42,43]. The Cape (Chacma) Baboon spends a notable amount of time consuming corms and roots in comparison to other subspecies [43]. These food sources are mechanically resistant because of their textured and abrasive nature [43,44]. This increased mechanical resistance results in intensified biting and chewing forces. In response to increased tension in the masseter and temporalis muscles, the mandible and facial regions experience greater bone stress [45]. Frequent loading over an extended period of time results in masticatory muscle fibers, increasing in diameter and changing in composition [43,46]. Masticatory muscles, and in particular the masseter and temporalis muscle, become well developed and large [42,47]. Overtime these masticatory changes influence the osseous growth of the craniofacial skeleton [43,46,48]. This launches an osteoblastic response to increase bone apposition in both the neuro- and viscerocranium [43,45,46]. Wild baboons therefore have robust and heavily ridged skulls in comparison to their captive counterparts [42,45].

In response to extensive locomotion, wild primates achieve greater muscle use in contrast to captive primates. These active primates have thicker muscles. This influences the stress bone is subjected to, and results in increased apposition in the neck region [44]. Also, because of the selective pressures of sexual dimorphism, male Cape (Chacma) Baboons have enlarged and robust crania, and this leads to over-designed facial bones for fatigue loading during feeding in comparison to females [43,44].

The fracture forces obtained in the HPB tests compare well with current literature. The mean peak fracture force in the current study was 6584.06N (± 1815.22 N). Fracture forces ranged from 3981.04 N to 10159.12 N and gave rise to eight fractures. These fracture forces are similar to those reported by Mole et al. [32] and Sharkey et al. [21]. Sharkey and colleagues [21] subjected porcine head specimens to fronto-parietal impacts with a drop tower set up. Numerous implements were investigated. However, of importance were the hammer impacts. These impacts produced a mean fracture force of 6170 N (± 1654.78 N) and fracture forces ranged from 4149 N to 8632 N producing nine fractures. Through similar methodology to the current study, Mole et al. [32] subjected porcine head specimens to single fronto-parietal impacts. This resulted in a mean peak fracture force of 7760 N (± 4150 N) and fracture forces ranging from 1270 N to 12800 N producing nine fractures.

4.5. Limitations

In the current study, the authors noted the Cape (Chacma) Baboon specimens, unlike porcine specimens, failed to swing in an effective pendulum motion, during impact. Additionally, weights of baboon specimens were on average 2.68 kg, while the porcine specimens were 5 kg. This weight difference enables baboon specimens to swing quickly. This may have resulted in specimens not experiencing the full force of impact. Thus the second stress wave did not effectively interact with suspended specimens. Also, the impact velocity never exceeded 13 m/s in contrast to a striker velocity of 23.53 m/s. This resulted in less severe fracture patterns in the HPB test group in contrast to those of the hammer tests. Additionally, head specimens in the HPB test group had to be scalped, as the HPB needs to be in direct contact with bone in order to obtain reliable data.

The temporo-parietal region was the impact area of interest. It was however, challenging to orientate the specimen heads effectively. This is because of the robust brow ridges in wild baboons that act as attachment sites for masticatory muscles. The brow ridge acts as the center of gravity, allowing specimens, to roll sideways on impact, further limiting the force of impact.

It is problematic to get Cape (Chacma) Baboon specimens for biomedical research and this resulted in a small sample size. The authors therefore suggest interpreting the statistical analyses with caution.

4.6. Conclusion

Intrinsic factors, such as scalp and skull thickness, influence the production and propagation of fractures. However, attempting to determine the extent of this influence is challenging. In the current study scalp and skull thickness varied widely among baboon specimens. For this reason no significant correlation existed between scalp or skull thickness and the extent of trauma. Furthermore, no clear trend existed between impact force and observed trauma. However, an impact force above 5300 N was required to fracture the Cape (Chacma) Baboon skull.

This study does not give a definitive answer on whether baboons are an improvement on the porcine model in biomechanical investigations. Nonetheless, the current study realistically simulated fracture morphology seen in human bone. It would therefore be helpful to continue with research with the HPB and baboon specimen combination. This research should focus on finding an effective way to suspend baboon specimens in the piston configuration used in the

current study. It is also suggested that cranial differences between male and female Cape (Chacma) Baboons, as well as wild and captive baboons be investigated in future.

4.7. Acknowledgements

The authors would like to thank Esmé Beamish and Justin O'Riain from the Cape Peninsula Baboon Research Unit, as well as Cape Nature for their donation of baboon specimens. The authors thank the National Research Foundation (NRF) for financial support.

4.7.1. Conflict of interest

The authors declare no conflict of interest.

4.7.2. Role of funding

No funding agency was involved in the study design or collection, analysis and interpretation of data, writing or deciding to submit the paper for publication.

4.8. Reference list

[1] Meel BL. Homicide trends in the Mthatha area between 1993 and 2005. S Afr Med J 2008;98:477-480.

[2] Norman R, Matzopoulos R, Groenewald P, Bradshaw D. The high burden of injuries in South Africa. Bull World Health Organ 2007;85:695-702.

[3] Seedat M, Van Niekerk A, Jewkes R, Suffla S, Ratele K. Violence and injuries in South Africa: prioritising an agenda for prevention. The Lancet 2009;374:1011-1122.

[4] Butchart A, Peden M, Matzopoulos R, Phillips R, Burrows S, Bhagwandin N et al. The South African National Non-Natural Mortality Surveillance System–Rationale, Pilot Results and Evaluation. S Afr Med J 2001;91:408-417.

[5] Ambade VN, Godbole HV. Comparison of wound patterns in homicide by sharp and blunt force. Forensic Sci Int 2006;156:166-170.

[6] Hart GO. Fracture Pattern Interpretation in the Skull: Differentiating Blunt Force from Ballistics Trauma Using Concentric Fractures. J Forensic Sci 2005;50:1276-1281.

[7] Guyomarc'h P, Campagna-Vaillancourt M, Kremer C, Sauvageau A. Discrimination of Falls and Blows in Blunt Head Trauma: A Multi-Criteria Approach. J Forensic Sci 2010;55:423-427.

[8] Wescott DJ. Biomechanics of Bone Trauma. In: Siegel JA, Saukko PJ, editors. Encyclopedia of Forensic Sciences. 2nd ed. Oxford: Academic Press; 2013. p. 1-6.

[9] Baumer TG, Passalacqua NV, Powell BJ, Newberry WN, Fenton TW, Haut RC. Age-Dependent Fracture Characteristics of Rigid and Compliant Surface Impacts on the Infant Skull-A Porcine Model. J Forensic Sci 2010;55:993-997.

[10] Delannoy Y, Becart A, Colard T, Delille R, Tournel G, Hedouin V et al. Skull wounds linked with blunt trauma (hammer example). A report of two depressed skull fractures – Elements of biomechanical explanation. Leg Med 2012;14:258-262.

[11] Bandak FA, Vorst MJV, Stuhmiller LM, Mlakar PF, Chilton WE, Stuhmiller JH. An Imaging-Based Computational and Experimental Study of Skull Fracture: Finite Element Model Development. J Neurotrauma 1995;12:679-688.

[12] Fenton TW, Stefan VH, Wood LA, Sauer NJ. Symmetrical Fracturing of the Skull from Midline Contact Gunshot Wounds: Reconstruction of Individual Death Histories from Skeletonized Human Remains. J Forensic Sci 2005;50:274-285.

[13] Yoganandan NA, Pintar FA. Biomechanics of temporo-parietal skull fracture. Clin Biomech 2004;19:225-239.

[14] Kremer C, Sauvageau A. Discrimination of Falls and Blows in Blunt Head Trauma: Assessment of Predictability through Combined Criteria. J Forensic Sci 2009;54:923-926.

[15] Kremer C, Racette S, Dionne CA, Sauvageau A. Discrimination of Falls and Blows in Blunt Head Trauma: Systematic Study of the Hat Brim Line Rule in Relation to Skull Fractures. J Forensic Sci 2008;53:716-719.

[16] Kroman A, Kress T, Porta D. Fracture Propagation in the Human Cranium: A Re-Testing of Popular Theories. Clin Anat 2011;24:309-318.

[17] Cory CZ, Jones MD, James DS, Leadbeatter S, Nokes LDM. The potential and limitations of utilising head impact injury models to assess the likelihood of significant head injury in infants after a fall. Forensic Sci Int 2001;123:89-106.

[18] Hodgson VR, Thomas LM. Breaking strength of the human skull vs. impact surface cuvature. US Department of Transportation, HS-800-583, Springfield, VA .

[19] Gurdjian ES, Webster JE, Lissner HR. The mechanism of skull fracture. J Neurosurg 1950;2:106-114.

[20] Jordana F, Colat-Parros J, Bénézech M. Diagnosis of Skull Fractures According to Postmortem Interval: An Experimental Approach in a Porcine Model. J Forensic Sci 2013;58:156-162.

[21] Sharkey E, Cassidy M, Brady J, Gilchrist M, NicDaeid N. Investigation of the force associated with the formation of lacerations and skull fractures. Int J Legal Med 2011;126:835-844.

[22] Nahum AM, Gatts JD, Gadd CW, Danforth J. Impact tolerance of the skull and face. Proc Stapp Car Crash Conf 1968;12:302-316.

[23] Powell BJ, Passalacqua NV, Fenton TW, Haut RC. Fracture Characteristics of Entrapped Head Impacts Versus Controlled Head Drops in Infant Porcine Specimens. J Forensic Sci 2013;58:678-683.

[24] Verschueren P, Delye H, Depreitere B, Van Lierde C, Haex B, Berckmans D et al. A new test set-up for skull fracture characterisation. J Biomech 2007;40:3389-3396.

[25] Woźniak K, Rzepecka-Woźniak E, Moskała A, Pohl J, Latacz K, Dybała B. Weapon identification using antemortem computed tomography with virtual 3D and rapid prototype modeling—A report in a case of blunt force head injury. Forensic Sci Int 2012;222:29-32.

[26] Gläser N, Kneubuehl BP, Zuber S, Axmann S, Ketterer T, Thali MJ et al. Biomechanical Examination of Blunt Trauma due to Baseball Bat Blows to the Head. J Forensic Biomech 2011;2:1-5.

[27] Grassberger M, Gehl A, Püschel K, Turk, EE. 3D reconstruction of emergency cranial computed tomography scans as a tool in clinical forensic radiology after survived blunt head trauma—Report of two cases. Forensic Sci Int 2011;207:e19-e23.

[28] Sahoo D, Deck C, Yoganandan N, Willinger R. Anisotropic composite human skull model and skull fracture validation against temporo-parietal skull fracture. J Mech Behav Biomed Mater 2013;28:340-353.

[29] Yoganandan NA, Pintar FA, Sances A, Walsh PR, Ewing CL, Thomas DJ et al. Biomechanics of Skull Fracture. J Neurotrauma 1995;12:659-668.

[30] Raymond D, Crawford G, Van Ee C, Bir C. Development of Biomechanical Response Corridors of the Head to Blunt Ballistic Temporo-Parietal Impact. J Biomech Eng 2009;131:094506-1-094506-7.

[31] Raymond D, Van Ee C, Crawford G, Bir C. Tolerance of the skull to blunt ballistic temporo-parietal impact. J Biomech 2009;42:2479-2485.

[32] Mole CG, Heyns M, Cloete T. How hard is hard enough? An investigation of the force associated with lateral blunt force trauma to the porcine cranium. Leg Med 2015;17:1-8.

[33] Hopkinson B. A Method of Measuring the Pressure Produced in the Detonation of High Explosives or by the Impact of Bullets. Proc R Soc Lond A 1914;213:437-456.

[34] Fleagle JG. Primate adaptation and evolution. 3rd ed. San Diego: Academic Press; 2013.

[35] Ankel-Simons F. An introduction to primate anatomy. 3rd ed. San Diego: Academic Press; 2000.

[36] Calce SE, Rogers TL. Taphonomic changes to blunt force trauma: A preliminary study. J Forensic Sci 2007;52:519-527.

[37] Powell BJ, Passalacqua NV, Baumer TG, Fenton TW, Haut RC. Fracture Patterns on the Infant Porcine Skull Following Severe Blunt Impact. J Forensic Sci 2012;57:312-317.

[38] Delye H, Verschueren P, Depreitere B, Verpoest I, Berckmans D, Vander Sloten J et al. Biomechanics of Frontal Skull Fracture. J Neurotrauma 2007;24:1576-1586.

[39] Gray GT. Classic Split Hopkinson Pressure Bar Technique. In: Khun H, Medlin D, editors. ASM Handbook, vol. 8, Mechanical Testing and Evaluation, Ohio: ASM International; 2000. p. 462-476.

[40] Ruan JS, Prasad P. Biomechanical study of Head Injury. In: Yoganandan N, Pintar FA, Larson SJ, Sances A, editors. Frontiers in Head and Neck Trauma: Clinical and Biomechanical, Amsterdam: IOS Press; 1998. p. 378-379.

[41] Ferrer E, de Notaris M. Contemporary Skull Fractures: Unusual Everted Fracture. World neurosurg 2011;76:417-418.

[42] Off EC. Craniofacial Variation, Integration, and Evolutionary Diversification in Baboons [PhD Thesis]. South Africa: University of Cape Town; 2009.

[43] Leigh SR. Cranial Ontogeny of *Papio* Baboons (Papio hamadryas). Am J Phys Anthropol 2006;130:71-84.

[44] Ross CF, Metzger KA. Bone Strain Gradients and Optimization in Vertebrate Skulls. Ann Anat 2004;186:387-396.

[45] Lieberman DE. How and Why Humans Grow Thin Skulls: Experimental Evidence for Systemic Cortical Robusticity. Am J Phys Anthropol 1996;101:217-236.

[46] Kiliaridis S. The Importance of Masticatory Muscle Function in Dentofacial Growth. Semin Orthod 2006;12:110-119.

[47] Clement A, Hillson S. Do larger molars and robust jaws in early hominins represent dietry adaptation? A New Study in Tooth Wear. Archaeology Int 2013;16:59-71.

[48] Daegling DJ. Relationship of Strain Magnitude to Morphological Variation in the Primate Skull. Am J Phys Anthropol 2004;124:346-352.

4.9. Tables

Table 4.1: Hammer test results

Condition A ~ 10 m/s

Specimen ID	Scalp thickness (mm)	Skull thickness (mm)	Striker velocity (m/s)	Kinetic energy (J)	Laceration observed	Laceration size (mm)	Fracture observed	Fracture size (mm)
B28-14 (Scalped)	2	3.32	9.09	8.26	___	___	Linear	31.10
B2-14 (Scalped)	1	4.22	9.52	9.06	___	___	Semi-circular linear	13.65
B33-14 (Scalped)	1	3.45	9.63	9.27	___	___	Semi-circular depressed and radiating	20.38, 4.56
B1-14 (Intact)	2	3.88	10.20	10.40	None	___	None	___
B27-14 (Intact)	1	3.69	9.71	9.43	None	___	None	___
Mean	1.40	3.71	9.63	9.28				
Standard deviation	0.55	0.36	0.40	0.77				

Condition B ~ 15m/s

Specimen ID	Scalp thickness (mm)	Skull thickness (mm)	Striker velocity (m/s)	Kinetic energy (J)	Laceration observed	Laceration size (mm)	Fracture observed	Fracture size (mm)
B3-14 (Scalped)	3	3.78	16.67	27.79	___	___	Penetrating	19.69 x 25.17
B34-14 (Scalped)	3.5	4.15	16.54	27.36	___	___	Penetrating, concentric and two radiating	22 x 25, 2.32, 1.73
B17-14 (Scalped)	1	2.38	17.24	29.72	___	___	Penetrating	19.96 x 21.93
B16-14 (Intact)	3	3.42	16.26	26.44	Superficial circular	1 x 2	None	___
B24-14 (Intact)	0.55	3.56	12.65	16.0	Superficial semi-circular	4 x 2	None	___
Mean	2.21	3.46	15.87	25.46				
Standard deviation	1.34	0.66	1.84	5.42				

Condition C ~ 20m/s

Specimen ID	Scalp thickness (mm)	Skull thickness (mm)	Striker velocity (m/s)	Kinetic energy (J)	Laceration observed	Laceration size (mm)	Fracture observed	Fracture size (mm)
B26-14 (Scalped)	2	3.01	20.62	42.52	___	___	Penetrating and radiating	19.80 x 23.22, 12.25
B11-14 (Scalped)	1.5	4.07	19.26	37.48	___	___	Penetrating and radiating	19.80 x 23.22, 12.25
B12-14 (Scalped)	1	3.26	21.27	45.24	___	___	Penetrating and four radiating	21.47 x 44 35.64 22.01, 32.42, 60.0
B19-14 (Intact)	2	3.13	19.4	37.71	None	___	None	___
Mean	1.62	3.37	20.14	40.74				
Standard deviation	0.48	0.48	0.97	3.80				

Table 4.2: Hopkinson pressure bar test results

Specimen ID	Scalp thickness (mm)	Skull thickness (mm)	Striker velocity (m/s)	Impactor velocity (m/s)	Peak impact force (N)	Displacement at peak force (mm)	Impact energy (J)	Fracture observed	Fracture size (mm)
B21-14	1	3.48	13.98	5.29	1951.59	1.17	2.29	None	___
B4-14	2	3.12	20.41	9.88	3981.04	0.92	3.65	Depressed comminuted	17.67 x 21.24
B10-14	0.2	3.90	16.67	7.87	4083.34	0.78	3.17	None	___
B20-14	0.5	3.03	11.76	5.13	5068.55	0.55	2.78	None	___
B30-14	0.5	3.42	22.22	10.93	5228.72	1.06	5.54	None	___
B6-14	1	4.21	20.83	10.66	5319.18	1.03	5.46	Semi-circular linear	15.15
B18-14	1	2.67	21.98	11.68	5882.35	1.02	5.98	Depressed comminuted and four radiating	26.66 x 21.15 39.11, 13.54, 9.2, 6.43

B14-14	1	2.91	19.61	7.10	6170.41	0.92	5.69	Linear	12.87
B9-14	0.5	3.15	21.74	12.15	6446.10	1.00	6.47	Semi-circular slightly depressed and radiating	20.13 10.39
B15-14	1	3.78	21.74	11.78	7233.33	1.00	7.27	Semi-circular linear	13.26
B8-14	0.2	3.09	23.53	12.24	7480.98	1.04	7.79	Depressed comminuted and concentric	18.93 x 13.83
B35-14	1	3.35	22.22	11.78	10159.12	0.97	9.81	Depressed comminuted	20.19 x 18.71
Mean	0.83	3.34	19.72	9.71	5750.39	0.96	5.49		
Standard deviation	0.49	0.44	3.66	2.66	2057.63	0.16	2.23		

4.10. Highlights

- A fracture force above 5300 N is required for the temporo-parietal region in the Cape (Chacma) Baboon specimen
- Radiating and concentric fractures were produced on impact
- Fracture morphology is similar to those seen in human bone

Appendices

Appendix A

Standard operating procedures

Standard Operating Procedure

A1. Collection of Specimens

SOP Reference: **2013/1/SOP/INC001.01**
Version Number: **Version 1.0**
Effective date: **5 April 2013**

	Signature	Name (print)	Date
Authors		Dr Marise Heyns	
Reviewer			
Approved by			

"Our Mission is to be an outstanding teaching and research university, educating for life and addressing the challenges facing our society

Revision Log

Previous Version Number	Reason for Change	Details of Revision	Sign/Date (Author of SOP)	Sign/Date (PI)	Up-dated SOP Version Number

1. Introduction

This SOP documents procedures to be followed for the correct collection of animal tissue specimens.

2. Responsibility

It will be the responsibility of the Project Supervisor, student/s and all involved to adhere to this procedure.

3. Health and Safety

Appropriate personal protective equipment (PPE) should be used at all times. This includes the use of gloves, aprons, boots, and masks.

4. Procedure

4.1 On initial contact by the supplier, the following information is to be entered into the Research logbook/electronic system as standard:

- Name of project member
- Description of collection
- Location, date and time of collection
- Contact person at time of collection
- Contact person at time of delivery to UCT
- Additional comments, if applicable
- Contact telephone numbers of all persons involved in collection

4.2 Upon collection of the specimen, the research participant shall obtain written proof of such a collection by ensuring that Form 1 is accurately completed, signed and dated.

4.3 A copy of Form 1 is to be retained by the individual from whom the specimen is collected.

4.4 The specimen(s) is transported to UCT.

4.5 Upon delivery of the specimen to UCT, the research participant shall obtain written proof of such a delivery by ensuring that Form 1 is accurately completed, signed and dated.

5.0 Additional notes

5.1 The logbook for Collection described in 4.1 above will be provided and maintained by UCT.

LOGBOOK for Collection

To be completed for each contact made by research participant:

NAME of research participant: _____

DESCRIPTION of Collection: _____

_____

LOCATION: _____

DATE: _____ TIME: _____

ADDITIONAL COMMENTS: *(eg. Access issues, condition, route to premises, Veterinary certification/approval))*

_**_____**

_____

_____

_____

CONTACT PERSON at Collection: _____

Contact Number: _____

CONTACT PERSON at Delivery: _____

Contact Number: _____

Standard Operating Procedure

A2. Collection and delivery of Specimens

SOP Reference: **2013/1/SOP/INC002.01**
Version Number: **Version 1.0**
Effective date: **5 April 2013**

	Signature	Name (print)	Date
Authors		Dr Marise Heyns	
Reviewer			
Approved by			

Revision Log

Previous Version Number	Reason for Change	Details of Revision	Sign/Date (Author of SOP)	Sign/Date (PI)	Up-dated SOP Version Number

1. Introduction

This SOP documents procedures to be followed for the correct collection and delivery of animal tissue specimens.

2. Responsibility

It will be the responsibility of the Project Supervisor, student/s and all involved to adhere to this procedure.

3. Health and Safety

Appropriate personal protective equipment (PPE) should be used at all times. This includes the use of gloves, aprons, boots, and masks.

4. Procedure

4.1. On initial contact with the supplier, CSI Forensics Pty Ltd, the following information is to be entered into the Research logbook/electronic system as standard:

- Name of project member
- Description of collection
- Location, date and time of delivery
- Contact person from supplier at time of delivery
- Contact person from research project at time of delivery to project site
- Additional comments, if applicable
- Contact telephone numbers of all persons involved in collection

4.2. Upon delivery of the specimen to the research site, the research participant shall obtain written proof of such a delivery by ensuring that Form 1 is accurately completed, signed and dated.

4.3. A copy of Form 1 is to be retained by the individual from whom the specimen is collected.

5. Additional notes

5.1 The logbook for Delivery described in 4.1 above will be provided and maintained by UCT.

LOGBOOK for Delivery

To be completed for each contact made by research participant:

NAME of research participant: _____

DESCRIPTION of Collection: _____

_____

LOCATION: _____

DATE: _____ TIME: _____

ADDITIONAL COMMENTS: *(eg. Access issues, condition, route to premises, Veterinary certification/approval)*

_____

_____

_____

_____

CONTACT PERSON at Collection: _____

Contact Number: _____

CONTACT PERSON at Delivery: _____

Contact Number: _____

Standard Operating Procedure

A3. Disposal of Animal Tissue Waste

SOP Reference: **2013/1/SOP/OUT001.01**
Version Number: **Version 1.0**
Effective date: **5 April 2013**

	Signature	Name (print)	Date
Authors		Dr Marise Heyns	
Reviewer			
Approved by			

Revision Log

Previous Version Number	Reason for Change	Details of Revision	Sign/Date (Author of SOP)	Sign/Date (PI)	Up-dated SOP Version Number

1. Introduction

This SOP documents procedures to be followed for the correct disposal of animal tissue waste.

2. Responsibility

It will be the responsibility of the Project Supervisor, student and all involved to adhere to this procedure.

3. Health and Safety

Appropriate personal protective equipment (PPE) should be used at all times. This includes the use of gloves, aprons, boots, and masks. All tissue which has not been tested for contagions should be handled with care.

4. Procedure

4.1. Animal tissue waste **MUST NOT** come in contact with or be disposed of with human tissue waste.

4.2. All animal tissue will be disposed of by BCL Medical Waste Management, Delft.

4.3. Any small amount of animal tissue waste should be placed in disposable bags for biological content.

4.4. These bags must be frozen and stored at -20 ºC until incineration to prevent putrefaction of animal tissue.

4.5. Whole carcasses will be transported for incineration in appropriate animal waste bags, within body bags.

4.6. Carcasses too large for incineration must be sectioned appropriately prior to placement in an animal waste bag and body bag for transport.

4.7. Upon delivery of the specimen to the disposal service provider, the research participant shall obtain written proof of such a delivery by ensuring that Form 1 is accurately completed, signed and dated.

4.8. A copy of Form 1 is to be retained by the individual receiving the animal waste.

5. Additional notes

5.1 The logbook for Disposal described in 4.7 above will be provided and maintained by UCT.

LOGBOOK for Disposal of animal waste

To be completed for each delivery made by research participant:

NAME of research participant: _____

DESCRIPTION of Delivery: _____

_____

LOCATION: _____

DATE: _____ TIME: _____

ADDITIONAL COMMENTS: (eg. Access issues, condition, route to premises, etc.)
_____

_____

_____

_____

Supplier CONTACT PERSON at Delivery: _____

Contact Number: _____

Research CONTACT PERSON at Delivery: _____

Contact Number: _____

Appendix B

Primate cranial anatomy

B1. Primates in biomedical research

The chief focus of head injury biomechanics studies has been on cadavers. More recently however, there has been a shift towards the usage of animal and synthetic models [1]. In particular, the domestic pig (porcine model) has been of specific interest, and a handful of studies [1-4] have explored the porcine model in terms of head impacts. This shift from cadaveric material stems largely from its limited availability in addition to the medical ethics surrounding its usage [5].

A study conducted by Jordana et al. [1] has described the porcine model as being a suitable human surrogate due to numerous criteria. These criteria are as follows:

- A similar composition is described between porcine and human cranial bone.
- The human and porcine cranium possesses the same three layers of bone (outer and inner compact layer and the middle cancellous layer).

However, a recent study by Mole et al. [6] state that the fracture forces observed in the porcine model were comparable to those of cadaver and animal studies. However fracture patterns differed to the literature available. Mole et al. [6] suggest that further research should explore additional animal models.

An explanation for Mole and colleagues [6] suggestion is based on the following observations:

- In the porcine cranium, the outer and inner tables of compact bone are thinner, whilst the middle cancellous layer is thicker in comparison to a human cranium.
- The overall bone thickness in the porcine model exceeds bone thickness observed in humans.

- The porcine cranium is angulated in comparison to the human cranium, which is rounded.

For years animal models have been at the center of research and the most significant of these is nonhuman primates. This animal model is essential to biomedical research, and this stems from its close phylogenetic relatedness to humans [7,8]. Even though primates are not newcomers to the repertoire of biomedical research, the baboon is [7]. As such, the current study explores baboons in terms of lateral cranial blunt force trauma. More specifically, the Cape (Chacma) Baboon is of particular interest and will therefore be discussed in detail in terms of physical description and cranial anatomy.

B2. Cape (Chacma) Baboon

Baboons are endemic to Sub-Saharan Africa, which is populated mainly by five species. These namely include, *Papio hamadryas, Papio anubis, Papio cynocephalus, Papio papio and Papio ursinus.* Furthermore, it is thought that all species of baboons today have evolved from an urisnus-like ancestor [8].

Papio ursinus more commonly known as the Cape (Chacma) Baboon is widespread across South Africa and Botswana and may even extend as far as Northern Angola in the west (Figure B1). The Cape (Chacma) Baboon (Figure B2) is described as a large, robust baboon whose pelage (fur) is coarse ranging from black to a dark brown. An adult male can reach between 23-31 kg and females 14-16 kg [9].

Figure B1: Illustration of the African continent. The shaded area indicates the extent of the habitat of the Cape (Chacma) Baboon.

Figure B2: Photograph of the Cape (Chacma) Baboon [12].

All exposed skin in the Cape (Chacma) Baboon is generally black. This includes their muzzle, which is long, robust and more downwardly flexed, as observed in Figure B3, in comparison to other baboon species. Furthermore, this species populates an array of habitats ranging from desert, savanna, grasslands, woodlands and Cape Fynbos [9].

Figure B3: A photograph of one of the Cape (Chacma) Baboon head specimens utilised in the current study.

B3. Primate skull anatomy

Bones that comprise a primate skull are comparable to other mammals including *Homo sapiens* [10]. Only a few bones, namely the mandible and the three bones of the middle ear exist as separate entities. The remaining cranial bones fuse resulting in the formation of a hollow cranium (Figure B4) [8,11]. A primate cranium can further be divided into two regions. The first region is known as the posterior braincase or neurocranium and the second as the anterior facial region or splanchnocranium [11].

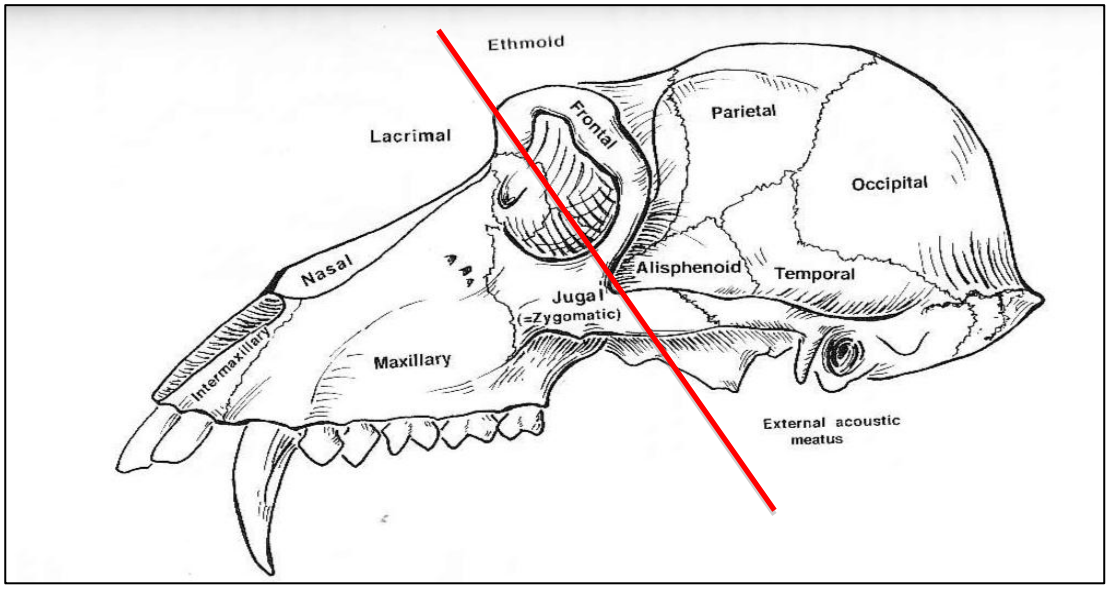

Figure B4: Sketch of baboon cranial anatomy. The red line indicates where the cranium is divided into the neurocranium and the splanchnocranium. The neurocranium lies on the right of the red line and the splanchnocranium lies on the left hand side [8].

B3.1. Neurocranium

The neurocranium houses and protects the brain and auditory system. Additionally, it acts as an attachment site for the muscles of mastication. The neurocranium is divided into three paired flat bones, more specifically the frontal, temporal and parietal bones [11]. These bones comprise the lateral and superior regions of the cranium. The occipital bone, which fuses inferiorly with the paired parietal bones, forms the posterior and inferior surfaces of the cranium [8,11]. The temporal bone of primates is quite a complicated bone, which is formed by a combination of the mastoid process, tympanic bone as well as the petrosal region, which surrounds the external acoustic meatus [8].

It is important to note that some literature refers to the primate sphenoid bone as a neurocranial bone whereas others describe it as splanchnocranial bone [8,10]. Whilst neither interpretation is deemed incorrect, it should be specified that the sphenoid bone fuses the neurocranium and splanchnocranium together. For the purpose of this current study, the sphenoid bone will be described under the next section, entitled “Splanchnocranium”.

B3.2. Splanchnocranium

The sphenoid bone, which is located at the interface of the neurocranium and splanchnocranium, comprises the lateral wall of the cranium. It also fuses posteriorly to the temporal bone of the neurocranium [10]. In addition to the sphenoid bone, the splanchnocranium houses the nose, orbits, the zygomatic (jugal) bone, as well as the pre-maxillary and maxillary regions that support the upper dentition [8,11].

B3.2.1. Anatomy of the orbital region

The external margin of the bony ring surrounding the orbits comprises superiorly the frontal bone, laterally of the zygomatic bone, medially of the lacrimal bone and inferiorly of the

maxillary bone. Furthermore, the hind walls of both orbits are formed by the sphenoid bone [8].

B3.2.2. Anatomy of the nasal region

Anterior and inferior to the orbital region lies the nasal region that points directly forward. The snout of a baboon, which includes the rostral and nasal bones, is generally longer and narrower in comparison to other primates [8]. Furthermore, nasal bones that comprise the nasal bridge cover the nasal cavity superiorly and the nasal septum is located in the center of this cavity. This septum further fuses superiorly with the ethmoid bone, which is located in the ethmoid notch and inferiorly with sphenoid bone. Both maxillary bones extend to articulate laterally with the zygomatic (jugal) bones [10].

B3.2.3. Measurements

Table B1: Scalp and skull thickness measurements of specimens in hammer tests

Specimen ID	Weight (kg)	Scalp thickness (mm)	Skull thickness (mm)
B26-14	3.50	2	3.01
B3-14	3.52	3	3.78
B11-14	3.10	1.5	4.07
B34-14	3.05	3.5	4.15
B17-14	3.14	1	2.38
B28-14	2.72	2	3.32
B12-14	2.59	1	3.26
B2-14	2.42	1	4.22
B33-14	2.02	1	3.45
B16-14	3.28	3	3.42

B1-14	2.94	2	3.88
B13-14	2.88	2	*
B19-14	2.88	2	3.13
B24-14	2.69	0.55	3.56
B27-14	1.89	1	3.69

* No measurements taken due to state of advanced decomposition

Table B2: Scalp, muscle and skull measurements of specimens in Hopkinson pressure tests

Specimen ID	Weight (kg)	Scalp thickness (mm)	Temporal muscle thickness (mm)	Skull thickness (mm)
B21-14	1.38	1	3	3.48
B20-14	1.43	0.5	2	3.03
B15-14	2.74	1	4	3.78
B30-14	3.08	0.5	9	3.42
B8-14	2.44	0.2	3	3.09
B4-14	3.14	2	10	3.12
B10-14	1.91	0.2	4	3.90
B6-14	2.69	1	1	4.21
B14-14	3.40	1	5	2.91
B9-14	2.62	0.5	4	3.15
B18-14	3.64	1	7	2.67
B35-14	1.32	1	9	3.35

B4. Reference list

[1] Jordana F, Colat-Parros J, Bénézech M. Diagnosis of Skull Fractures According to Postmortem Interval: An Experimental Approach in a Porcine Model. J Forensic Sci 2013;58:156-162.

[2] Baumer TG, Passalacqua NV, Powell BJ, Newberry WN, Fenton TW, Haut RC. Age-Dependent Fracture Characteristics of Rigid and Compliant Surface Impacts on the Infant Skull-A Porcine Model. J Forensic Sci 2010;55:993-997.

[3] Powell BJ, Passalacqua NV, Fenton TW, Haut RC. Fracture Characteristics of Entrapped Head Impacts Versus Controlled Head Drops in Infant Porcine Specimens. J Forensic Sci 2013;58:678-683.

[4] Sharkey E, Cassidy M, Brady J, Gilchrist M, NicDaeid N. Investigation of the force associated with the formation of lacerations and skull fractures. Int J Legal Med 2011;126:835-844.

[5] Yoganandan NA, Pintar FA, Sances A, Walsh PR, Ewing CL, Thomas DJ et al. Biomechanics of Skull Fracture. J Neurotrauma 1995;12:659-668.

[6] Mole CG, Heyns M, Cloete T. How hard is hard enough? An investigation of the force associated with lateral blunt force trauma to the porcine cranium. Leg Med 2015;17:1-8.

[7] VandeBerg JL, Williams-Blangero S, Tardiff SD. The baboon in biomedical research. 1st ed. New York: Springer; 2009.

[8] Ankel-Simons F. An introduction to primate anatomy. 3rd ed. San Diego: Academic Press; 2000.

[9] Kingdon J. Class Mammalia. In: Kingdon J, Happold D, Butynsk H, Hoffmann M, Happold M, Kalina J, editor. Mammals of Africa volumes 1-6. 1st ed. London: Bloomsbury; 2013. p. 225.

[10] Gebo D. Heads-Bones of the skull. In: Burke V, editor. Primate comparative anatomy. 1st ed. Baltimore: John Hopkins University Press; 2014. p. 63-64.

[11] Fleagle JG. Primate adaptation and evolution. 3rd ed. San Diego: Academic Press; 2013.

[12] Chacma Baboons - Kruger's Troops [Image on the Internet]. 2014 Oct 10; Available at: www.tydonsafaris.com. Accessed Nov 9, 2014.

Appendix C

Hopkinson pressure bar theory

C1. History

The concept behind the 1D stress wave theory has been evolving since 1872 from the meticulous research of Bertram Hopkinson [1]. Hopkinson's interest lay with the dynamic characterisation of materials. What were initially stress wave experiments in iron wires has today transpired into stress wave propagation in uniform cylindrical bars. However, with the turn of the 20th century, modifications to the HPB technique have allowed, in addition to compressive forces, cases of tension, torsion, shear forces, bending, as well as indentation to be investigated [2,3].

Today, the classic design of the HPB apparatus is commonly used in dynamic loading of materials including bone [3]. The configuration typically involves two to three bars that consist of a uniform material. All bars have an equal diameter to prevent the striker bar from rebounding following impact [2]. The shorter striker bar is propelled by a gas gun and impacts with the longer input pressure bar. Furthermore, a third bar known as the output pressure bar may also be used in conjunction with the striker bar and input pressure bar during testing. Input and output pressure bars are supported by teflon bushes to ensure frictionless motion during impact. This also assists in the accurate measurement of force and velocity associated with a single impact [3,4]. Strain gauges and a light-based velocity trap record these aforementioned measurements [3].

C2. One dimensional stress wave theory

When a force is applied to a deformable material over a short period of time, a 1D stress wave is produced and propagates parallel to the bar. As described earlier, the bars used during testing are generally equal in diameter. This, along with the assumption that the bars are

linear and dispersion free forms the fundamental basis of the 1D stress wave propagation theory. All of these criteria ensure that the system of bars remain in a state of linear-elastic stress and stress-distribution [2].

C3. Split-Hopkinson pressure bar

Although numerous HPB set ups have been described since 1872, it was Kolsky et al. [5] who in 1949 introduced the revolutionary design of the split-Hopkinson pressure bar (SHPB). This configuration is capable of measuring strain rates between $10^2 s^{-1}$ and $10^4 s^{-1}$. This classic design is still widely used today by engineers and scientists for high-strain testing of materials. However, subtle differences do exist between Kolsky's [5] original design and the currently used SHPB configuration. These differences lie mainly in the manner in which a stress wave is recorded. For example, Kolsky et al. [5], in addition Davies et al. [6] previously utilised parallel plates and cylindrical condensers to measure axial and radial bar displacements. However, current designs make use of strain gauges.

Furthermore, the modern SHPB configuration (Figure C1) includes a striker bar as well as an input and output pressure bar. The specimen, which is the material being tested, is inserted between these two pressure bars [2,3]. The mechanism by which the SHPB set up operates will be discussed in the section to follow.

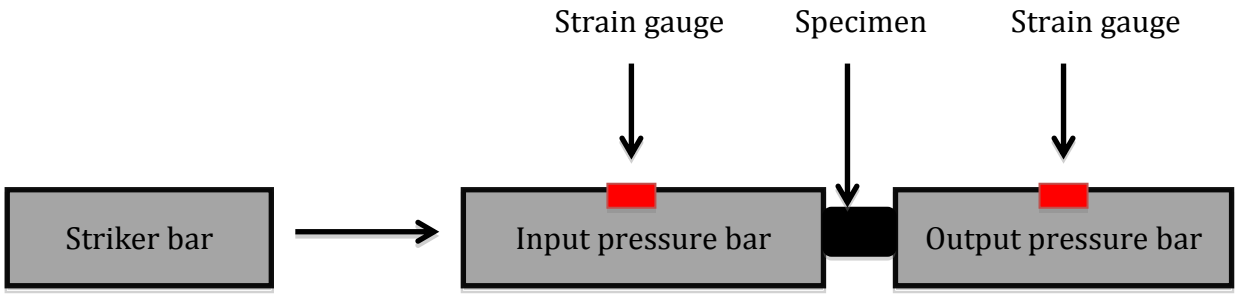

Figure C1: Schematic illustration of the split-Hopkinson pressure bar apparatus. Strain gauges are placed on the input and output pressure bars to record strain waves.

During testing, the striker bar is propelled forward by an air gun impacting with the input pressure bar. This consequently produces an incident, compressive stress wave (Figure C2).

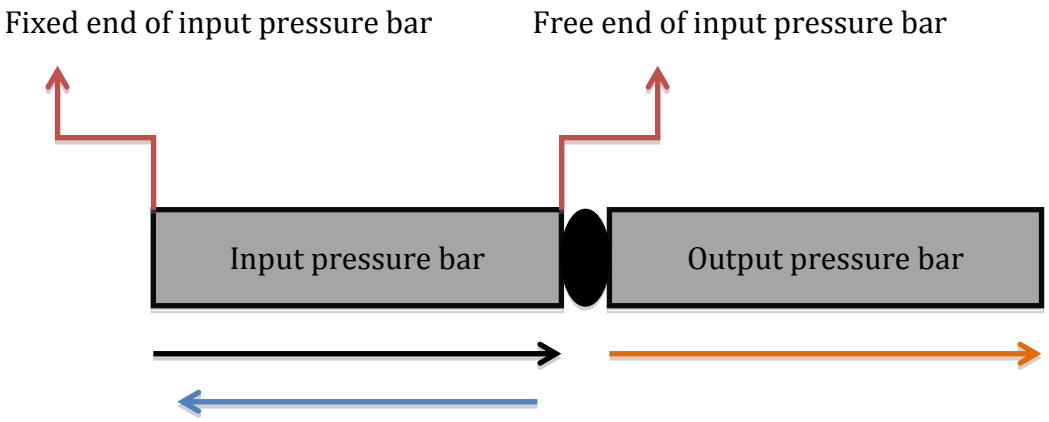

Figure C2: A detailed illustration of the impedance mismatch. In the diagram the red arrows indicate the fixed and free surface of the input pressure bar, whilst the black arrow indicate the compressive stress wave originating at the fixed end of the input pressure bar. It should be noted that this wave is partly transmitted into the output pressure bar (orange arrow) due to an impedance mismatch between the specimen and input pressure bar while the rest in reflected back down the input pressure bar (blue arrow).

This initial impact compresses a thin layer of the input pressure bar and consequently the compressive stress wave is passed onto an adjacent section of the bar. This transfer however only occurs if the stress of the striker bar on the input pressure bar is maintained [7]. While travelling the length of the input pressure bar, the compressive stress wave is measured by two diametrically opposed strain gauges [5]. Once the generated stress wave arrives at the specimen interface (free end), an impedance mismatch may result. This is a consequence of the specimen and input pressure bar materials not being identical. Thus, part of the stress wave is reflected along the input pressure bar as tension wave. This wave is again measured by the strain gauges. In contrast, the remaining compressive stress wave and resulting momentum are carried over to the output pressure bar [3,7]. Furthermore, several of these reflections will occur within the specimen, allowing the system to rapidly reach a state of equilibrium [3]. Once testing is complete, stress and velocity histories can be derived and used to infer the dynamic stress/strain curve of the specimen under investigation [5,8].

C4. Direct impact Hopkinson bar

In 1970, Dharan and Hauser [9] proposed a modified SHPB configuration called the direct impact Hopkinson bar (DIHB). This configuration measures strain rates of $10^3 s^{-1}$ to $10^5 s^{-1}$. The foremost discrepancy between the SHPB and DIHB configurations is that no input pressure bar is utilised in the DIHB configuration (Figure C3). Instead, the specimen is attached to the impact surface of the output pressure bar and is impacted directly by the striker bar.

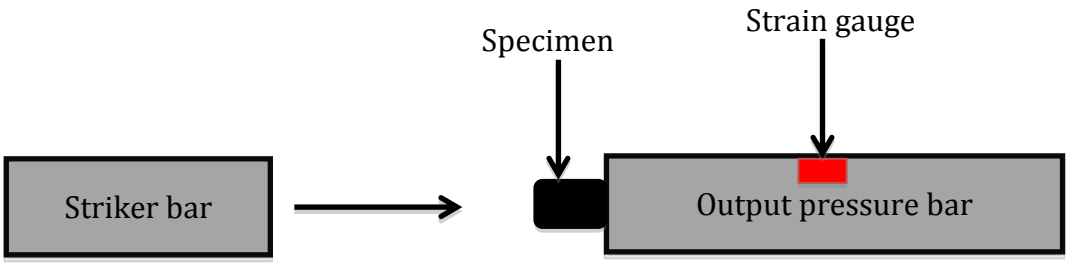

Figure C3: Schematic illustration of the direct impact Hopkinson bar. A strain gauge is only placed on the output pressure bar.

Consequently the lack of an input pressure bar has lead to the DIHB approach not being the method of choice for researchers aspiring towards describing the strain properties of a material under blast loading. This limitation impedes the establishment of a strain rate for the material under consideration [8]. It is therefore imperative that a direct strain measurement of the sample is recorded through additional sensors or high-speed photography. Another limitation is that this configuration cannot accommodate a long output bar. In summary it is suggested that the DIHB configuration be tailored to suit the variables of interest in the research being conducted [2].

C5. Experimental set up of direct impact Hopkinson bar

For the purpose of the intended research a modified version of the DIHB will be utilised, however the aforementioned 1D stress wave theory will still hold true. This configuration,

represented in figure C4, differs from the previously described DIHB set up in that no output pressure bar is utilised. Instead the striker bar impacts directly with the input pressure bar (HPB). This in turn impacts the specimen that is suspended in an adjustable net at the free end of the input pressure bar. The specimen of interest is *Papio ursinus* also known as the Cape (Chacma) Baboon and the temporo-parietal region shall specifically be impacted. Furthermore, strain gauges (Wheatstone bridge) and a velocity trap will be used to record the stress wave produced upon impact and the velocity of the striker bar respectively.

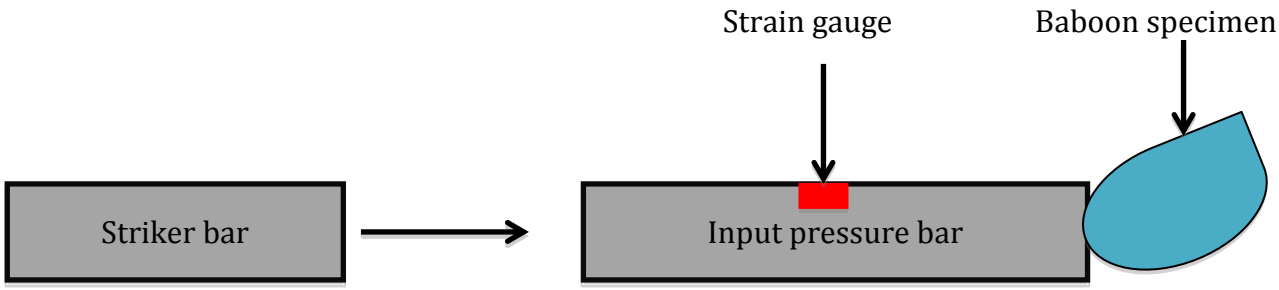

Figure C4: Illustration representing the experimental set up of the current study.

C6. Calculations

The calculations discussed below were derived from research conducted by Gama et al. [2], Gray [8], Spotts [7] and personal communication with Cloete (2014).

$$\boldsymbol{\tau = \frac{L}{c}} \tag{1}$$

From the above equation, tau (τ) is described as the time it takes for the stress wave to propagate, at a constant speed of sound (c), the length (L) of the input bar. In the current study, both the striker bar and input pressure bar are machined from aluminium and will

therefore possess a constant speed of sound of 5300 m/s. In addition to the above equation, the constant speed of sound can be calculated from the following formula:

$$\boldsymbol{c} = \sqrt{\frac{\boldsymbol{E_y}}{\boldsymbol{\rho}}} \tag{2}$$

This formula is based on Young's modulus (E_y), which is defined as a measure of elasticity. More specifically, it is the ratio of the stress acting on a material to the strain produced in that material, whilst ρ is a measure of density in the input pressure bar. Measuring the mass of the input pressure bar and dividing it by its volume is used to calculate ρ.

In the current study, the impact of the striker bar with the input pressure bar will give rise to a right running compressive stress wave (σ_R) at the fixed end (X=0) of the input pressure bar. This stress wave will be treated as a positive quantity. As previously mentioned this compressive stress wave will travel the length of the input pressure bar. On reaching the free end of the input pressure bar, the compressive stress wave shall interact with the baboon specimen. Due to an impedance mismatch, part of the compressive stress wave is reflected along its initial path as a tension wave with a negative quantity. This wave originates at the free end (X=L) of the input pressure bar and is further referred to as the left running wave (σ_L). The remainder of the right running compressive wave is transferred into the baboon specimen.

As σ_R initiates at the fixed end of the input pressure bar it will be equal in magnitude to the stress wave produced at σ_i:

$$\boldsymbol{\sigma_i = \sigma_R}\,, \quad \mathbf{0} < t < \tau \tag{3}$$

Following impact and a time period of τ, σ_L will arrive at the interface of the striker bar and input pressure bar (fixed end). It is at this interface that the positive σ_L and negative σ_R stress

waves interact (superposition) producing σ_i. Equation (4) further describes that if σ_R reaches a particular point on the input bar in a time of τ, then the opposite σ_L wave will reach the same point in a time of (t-τ).

$$\boldsymbol{\sigma_i(t) = \sigma_R(t) + \sigma_L(t - \tau)} \tag{4}$$

Equations (5) and (6) illustrate that in addition to σ_i, the strain gauge signal (σ_G) and the signal at the specimen end (σ_S) of the input bar can be measured at any time point:

$$\boldsymbol{\sigma_G(t) = \sigma_R\left(t - \frac{2}{3}\tau\right) + \sigma_L\left(t - \frac{1}{3}\tau\right)} \tag{5}$$

$$\boldsymbol{\sigma_S(t) = \sigma_R(t - \tau) + \sigma_L(t - \tau)} \tag{6}$$

More specifically σ_G represents the stress wave signal measured by diametrically opposed strain gauges a third of the way down of the input pressure bar. However, σ_S is the stress wave produced at the specimen interface as a result of the input pressure bar interacting with the specimen at its free end.

From equation (7), σ_i is described as possessing a stress wave equal in magnitude, if the time period is less than τ, to the stress wave at σ_G. However, if the time period is greater than τ, then σ_i is equal to zero, which is the magnitude of the stress wave at the free end of the input pressure bar.

$$\boldsymbol{\sigma_i(t) = \begin{cases} \sigma_G\left(t + \frac{1}{3}\tau\right), & t < \tau \\ 0\ , & t > \tau \end{cases}} \tag{7}$$

From equation (5), σ_G may be deduced at a third of the way down of the input pressure bar:

$$\boldsymbol{\sigma_G(t - \frac{2}{3}\tau) = \sigma_R(t - \tau) + \sigma_L(t - \tau)} \tag{8}$$

Furthermore, the subtraction of equation (8) from equation (4) and subsequent rearrangement results in the calculation of σ_R (t):

$$\boldsymbol{\sigma_i(t) - \sigma_G(t - \frac{2}{3}\tau) = \sigma_R(t) - \sigma_R(t - \tau)}$$

$$\boldsymbol{\therefore \sigma_R(t) = \sigma_i(t) - \sigma_G(t - \frac{2}{3}\tau) + \sigma_R(t - \tau)} \quad (9)$$

Additionally the reoccurrence formula, that allows σ_R to be calculated at any given point in time can be determined by substituting equation (7) into equation (9):

$$\boldsymbol{\sigma_R(t) = \begin{cases} \sigma_G\left(t + \frac{1}{3}\tau\right) - \sigma_G\left(t - \frac{2}{3}\tau\right) + \sigma_R(t - \tau), & t < \tau \\ -\sigma_G\left(t - \frac{2}{3}\tau\right) + \sigma_R(t - \tau), & t > \tau \end{cases}} \quad (10)$$

Equation (4) can be used to calculate σ_L at any given point in time:

$$\boldsymbol{\sigma_L(t) = \sigma_i(t + \tau) - \sigma_R(t + \tau)} \quad (11)$$

With reference to the strain gauge theory, the output stress wave recorded by the strain gauge is described as:

$$\boldsymbol{V_{out} = \frac{K_G N \varepsilon V_{in}}{4}} \quad (12)$$

Where K_G represents the gauge factor, N is the number of active arms present in the Wheatstone bridge, ε represents the strain experienced in the input bar and V_{in} is the Wheatstone bridge voltage. However, it is important to note that:

$$\boldsymbol{V_{out} = \frac{V_{read}}{G_{amp}}} \quad (13)$$

Where G_{amp} represents the gain

And

$$\boldsymbol{\varepsilon = \frac{\sigma}{E_y}} \quad (14)$$

Making the following substitution of equations (13) and (14) into equation (12) with appropriate rearrangement results in:

$$\boldsymbol{\sigma = \frac{4E_y}{G_{amp}K_G NV_{in}} V_{read}} \tag{15}$$

Furthermore, the wave signal can be represented as:

$$\boldsymbol{\sigma = K_C V_{read}}$$

$$\boldsymbol{\therefore K_C = \frac{4E_y}{G_{amp}K_g NV_{in}}} \tag{16}$$

Where K_c represents the calibration factor.

The pressure exerted on the specimen during impact with the input pressure bar can be calculated by multiplying σ_S (equation 6) with K_c (equation 16). From this, pressure (Pascal) is multiplied by the cross-sectional area (millimeter squared) of the input pressure bar and the force (N) of the impact at any given time is calculated:

$$\boldsymbol{Force = Pressure\ X\ Area} \tag{17}$$

In addition to force, the velocity of the impact at the free end of the input pressure bar may also be calculated.

Furthermore each of the stress waves (right and left running) has an associated velocity change (ΔV). More specifically:

$$\boldsymbol{\Delta V_R = \frac{\sigma_R}{\rho c}} \tag{18}$$

And

$$\boldsymbol{\Delta V_L = -\frac{\sigma_L}{\rho c}} \tag{19}$$

These abovementioned velocities when summed together can calculate the velocity at any point in the input bar:

$$\boldsymbol{V(t) = \Delta V_R(t) + \Delta V_L(t-\tau)} \quad (20)$$

Furthermore, the substitution of equation (18) and (19) into equation (20) produces the following:

$$\boldsymbol{V(t) = \frac{\sigma_R(t)}{\rho c} - \frac{\sigma_L(t-\tau)}{\rho c}} \quad (21)$$

And therefore the impact velocity experienced at specimen (free end of input pressure bar) is described as:

$$\boldsymbol{V_S = \begin{cases} 0, & t < \tau \\ \frac{\sigma_R(t-\tau)}{\rho c} - \frac{\sigma_L(t-\tau)}{\rho c}, & t > \tau \end{cases}} \quad (22)$$

The resulting displacement of the impact at any point in time is described below:

$$\boldsymbol{V_S = \frac{\Delta S}{\Delta t}} \quad (23)$$

$$\boldsymbol{\therefore \Delta S = V_S \times \Delta t} \quad (24)$$

$$\boldsymbol{\therefore S(t) = S(t-1) + \left(\frac{V_S(t-1)+V_S(t)}{2} \times \Delta t\right)} \quad (25)$$

In the aforementioned equations (23-25), S represents displacement, whilst V_s represents the impact velocity and Δt represents the change in time during the impact.

The resultant energy of the input pressure bar impacting with the specimen is derived from the work-energy principle:

$$\boldsymbol{W = FD = \frac{1}{2}MV^2} \quad (26)$$

Where W represents the work done (J), F refers to force (N), D is the displacement (meter), M is the mass of the striker measured in grams, and V is the impact velocity measured in m/s^{-1}.

C7. Reference List

[1] Hopkinson B. A Method of Measuring the Pressure Produced in the Detonation of High Explosives or by the Impact of Bullets. Proc R Soc Lond A 1914;213:437-456.

[2] Gama BA, Lopatnikov SL, Gillespie JWJ. Hopkinson bar experimental technique: A critical review. Appl Mech Rev 2004;57:223-250.

[3] Al-Mousawi MM, Reid SR, Deans WF. The use of the split Hopkinson pressure bar techniques in high strain rate material testing. Proc Instn Mech Engrs Part C 1997;211:273-292.

[4] Landon JW QH. Experiments with the Hopkinson Pressure Bar. Proc R Soc Lond A 1923;103:622-643.

[5] Kolsky H. An Investigation of the Mechanical Properties of Materials at very High Rates of Loading. Proc Phys Soc B 1949;62:676-700.

[6] Davies RM. A critical study of the Hopkinson pressure bar. Philos Trans R Soc Lond Ser A 1948;240:375-457.

[7] Spotts MF. Mechanical Design Analysis. Prentice-Hall INC, New Jersey 1964.

[8] Gray GT. Classic Split Hopkinson Pressure Bar Technique. In: Khun H, Medlin D, editors. ASM Handbook, vol. 8, Mechanical Testing and Evaluation, Ohio: ASM International; 2000. p. 462-476.

[9] Dharan CKH, Hauser FE. Determination of stress-strain chracteristics at very high strain rates. Exp Mech ;10:370-376.

Appendix D:
Design calculations

D1. Pressure calculations

The projectile (striker bar) utilised in this study is fired through a gas gun that expends compressed air. Increasing or decreasing the pressure at which the gas gun is fired adjusts the velocity of the projectile. The desired velocities in the current study were 10 m/s, 15 m/s and 20 m/s and these were acquired as follows:

$$\boldsymbol{KE = \frac{1}{2}MV^2 = PAL}$$

$$\boldsymbol{\therefore P = \frac{M \times V^2}{2AL}}$$

$$\boldsymbol{For\ example: \frac{0.2 \times (10)^2}{2 \times (3.14 \times 10^{-4}) \times 1}}$$

$$\boldsymbol{= 31847.13\ Pascal}$$

Table D1: Pressure calculation results

Mass (kg)	Velocity (m/s)	Area (m^2)	Length (m)	Pressure (Pa)	(KPa)	(Bar)
0.2	10	3.14 x 10^{-4}	1	31847.13	31.85	0.32
0.2	15	3.14 x 10^{-4}	1	71656.05	71.66	0.72
0.2	20	3.14 x 10^{-4}	1	127388.54	127.39	1.27

Appendix E:
Test results

Table E1: Hammer test results

Specimen ID	Gas gun pressure (KPa)	Striker velocity (m/s)	Kinetic energy (J)	Soft tissue damage	Hard tissue damage
B26-14 (scalped)	260	20.62	42.52	Scalped	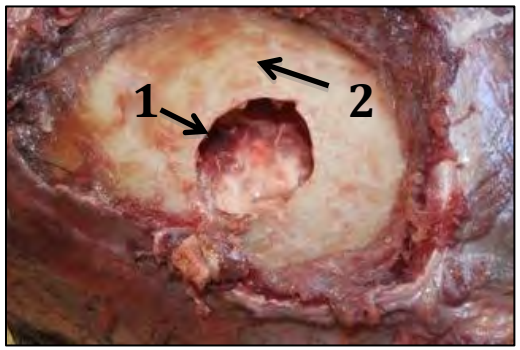 1-Full penetrating fracture (19.80 mm x 23.22 mm and 2-radiating fracture (12.25 mm)
B3-14 (Scalped)	180	16.67	27.79	Scalped	 Full penetrating fracture (19.69 mm x 25.17 mm)

Specimen ID	Gas gun pressure (KPa)	Striker velocity (m/s)	Kinetic energy (J)	Soft tissue damage	Hard tissue damage
B11-14 (scalped)	260	19.26	37.48	Scalped	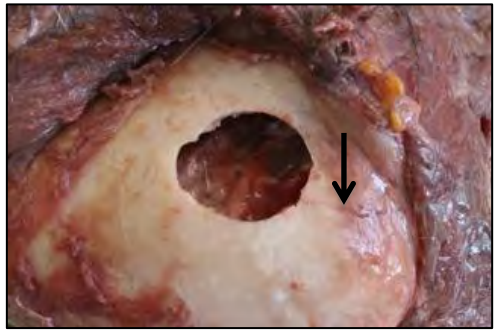 Full penetrating fracture (19.80 mm x 23.22 mm) with an associated radiating fracture (12.25 mm)
B34-14 (scalped)	180	16.54	27.36	Scalped	

					 Full penetrating fracture (22 mm x 25 mm), with a concentric fracture and two associated radiating fractures 2.31 mm and 1.73 mm

Specimen ID	Gas gun pressure (KPa)	Striker velocity (m/s)	Kinetic energy (J)	Soft tissue damage	Hard tissue damage
B17-14 (scalped)	180	17.24	29.72	Scalped	 Full penetrating fracture (19.96 mm x 21.93 mm)
B28-14 (scalped)	80	9.09	8.26	Scalped	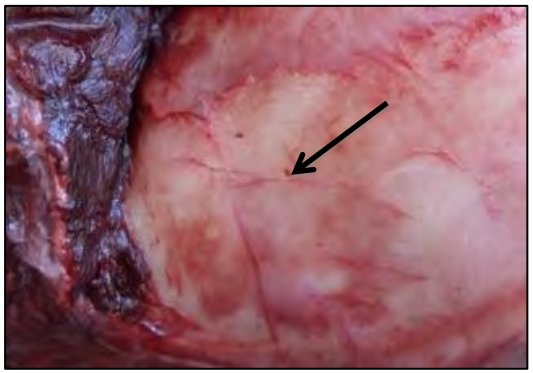 Linear fracture (31.10 mm)

Specimen ID	Gas gun pressure (KPa)	Striker velocity (m/s)	Kinetic energy (J)	Soft tissue damage	Hard tissue damage
B12-14 (scalped)	260	21.27	45.24	Scalped	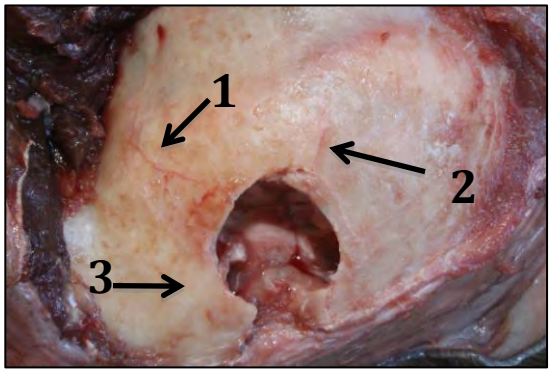 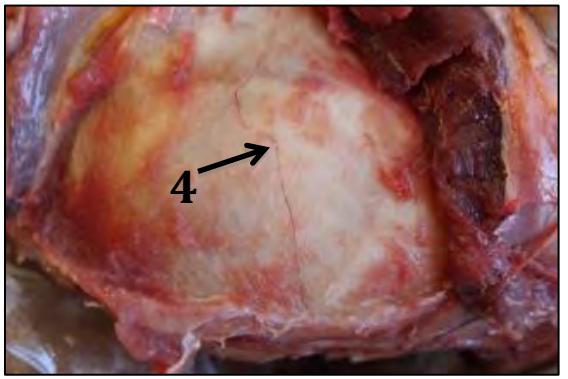 Full penetrating fracture (21.47 mm x 44 mm) with four associated radiating fractures. 1 – 35.64 mm, 2 – 22.01 mm, 3-32.42 mm and 4 – 60 mm.

Specimen ID	Gas gun pressure (KPa)	Striker velocity (m/s)	Kinetic energy (J)	Soft tissue damage	Hard tissue damage
B2-14 (scalped)	80	9.52	9.06	Scalped	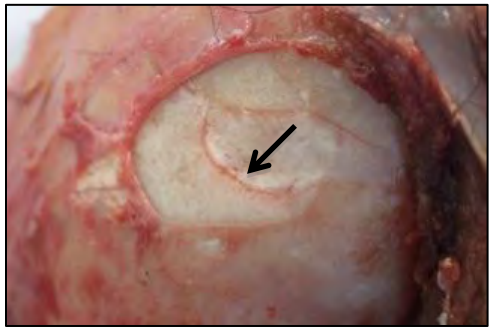 Semi-circular linear fracture (13.65 mm)
B33-14 (scalped)	80	9.63	9.27	Scalped	 1- Semi-circular depressed fracture (20.38 mm) with deterioration of the inner table and 2- associated radiating fracture (4.56 mm) which ends in the depressed fracture

Specimen ID	Gas gun pressure (KPa)	Striker velocity (m/s)	Kinetic energy (J)	Soft tissue damage	Hard tissue damage
B16-14 (intact)	180	16.26	26.44	 Superficial circular laceration (1 mm x 2 mm)	 No damage
B1-14 (intact)	80	10.20	10.40	 No damage	 No damage

Specimen ID	Gas gun pressure (KPa)	Striker velocity (m/s)	Kinetic energy (J)	Soft tissue damage	Hard tissue damage
B13-14 (intact)	260	21.27	45.24	 No damage	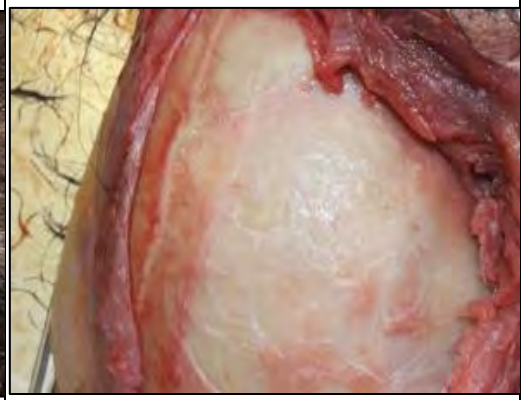 No damage
B19-14 (intact)	240	19.42	37.71	 No damage	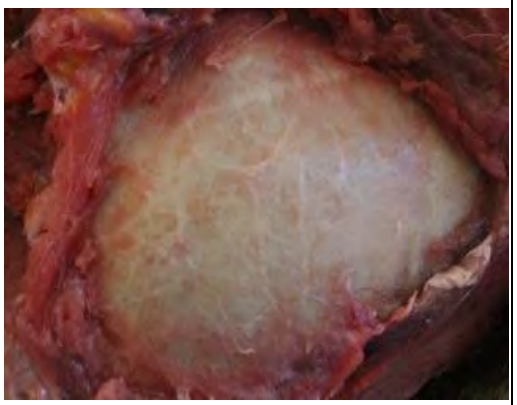 No damage

Specimen ID	Gas gun pressure (KPa)	Striker velocity (m/s)	Kinetic energy (J)	Soft tissue damage	Hard tissue damage
B24-14 (intact)	90	12.65	16.0	 Superficial circular laceration (4 mm x 2 mm)	 No damage
B27-14 (intact)	80	9.71	9.43	 No damage	 No damage

Table E2: Hopkinson pressure bar test results

Specimen ID	Gas gun pressure (KPa)	Impact velocity (m/s)	Impact energy (J)	Peak impact force (N)	Hard tissue damage
B4-14 (scalped)	260	9.88	3.65	3981.04	 Depressed comminuted fracture (17.67 mm x 21.24 mm)

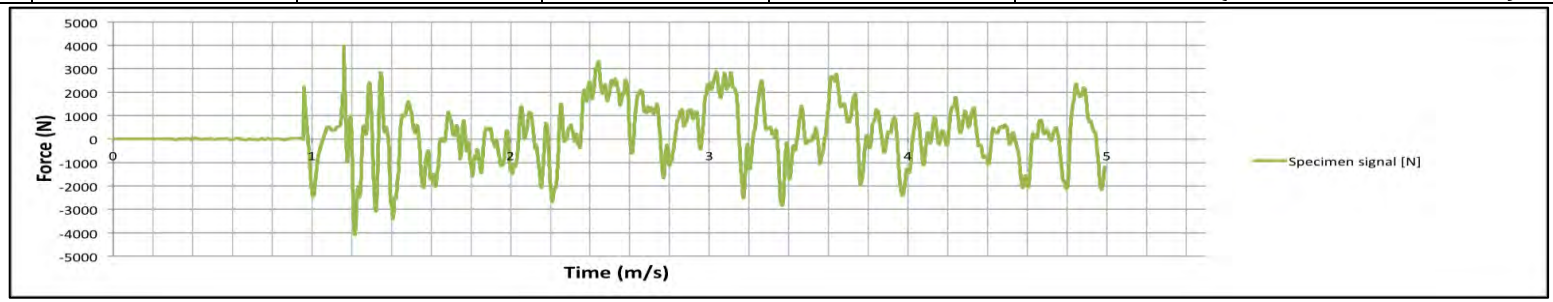

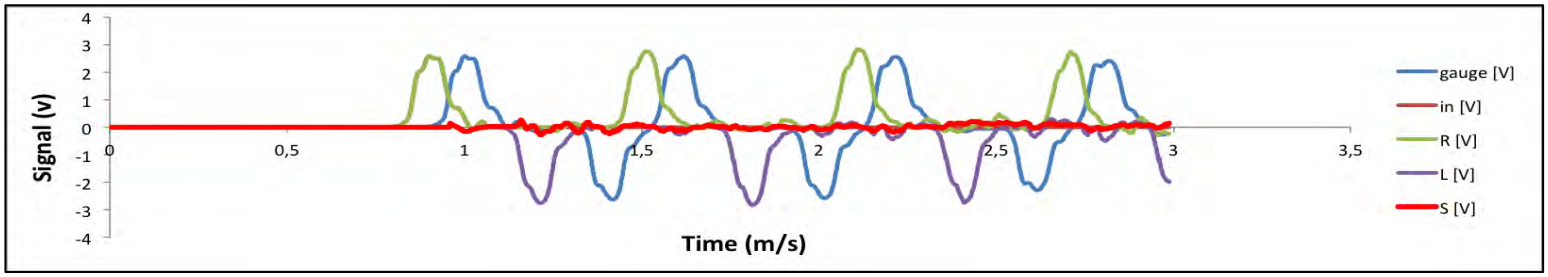

Specimen ID	Gas gun pressure (KPa)	Impact velocity (m/s)	Impact energy (J)	Peak impact force (N)	Hard tissue damage
B21-14 (scalped)	80	5.29	2.29	1951,59	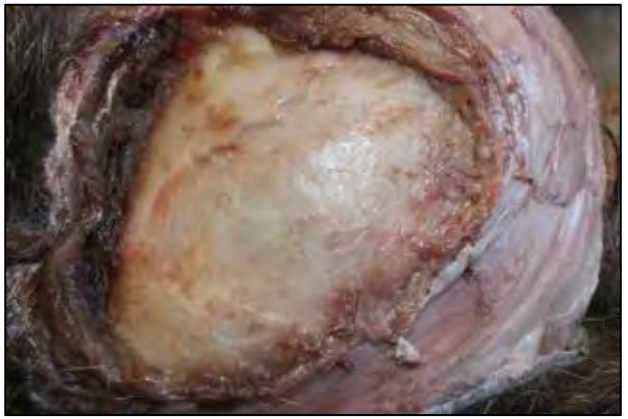 No damage

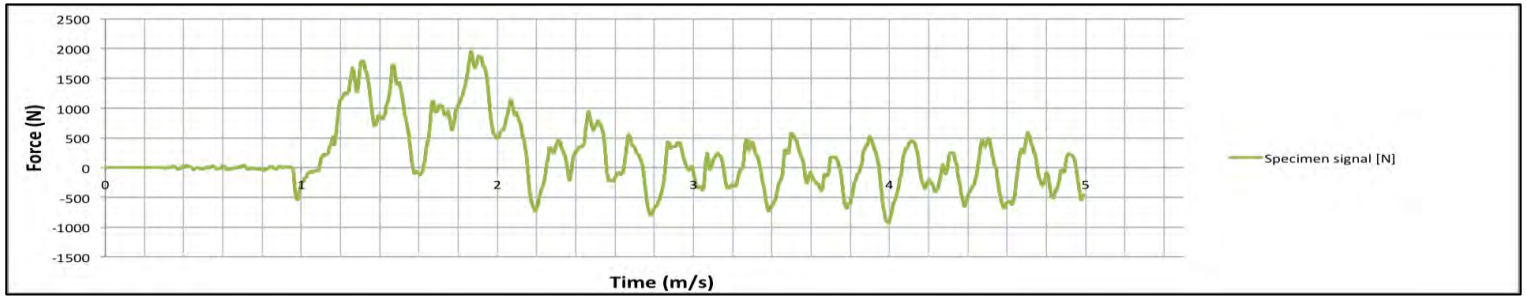

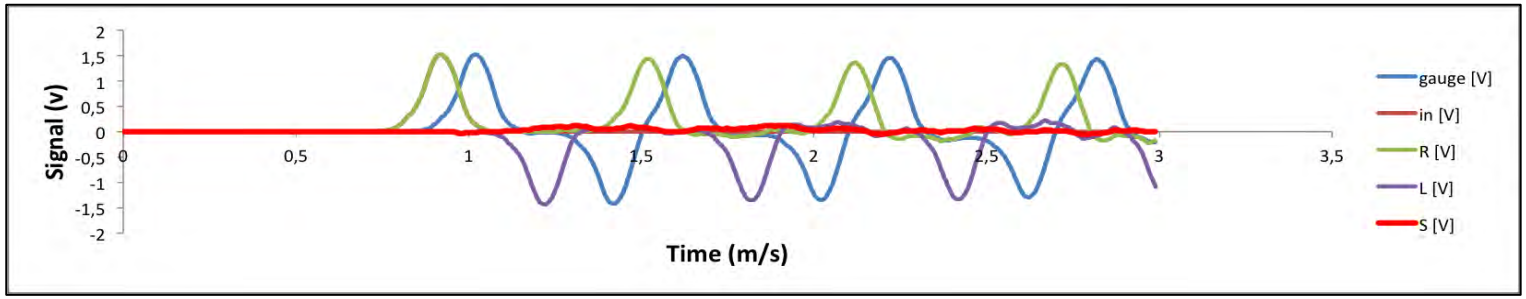

Specimen ID	Gas gun pressure (KPa)	Impact velocity (m/s)	Impact energy (J)	Peak Impact force (N)	Hard tissue damage
B10-14 (scalped)	80	7.87	3.17	4083.34	 No damage

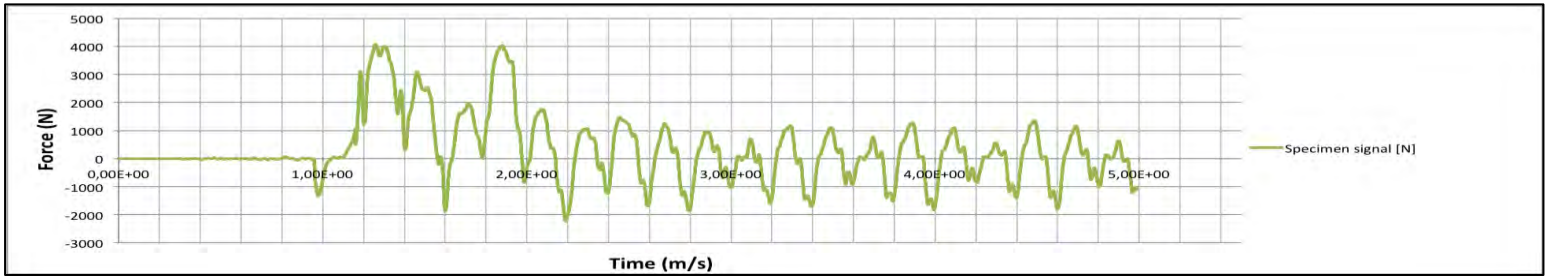

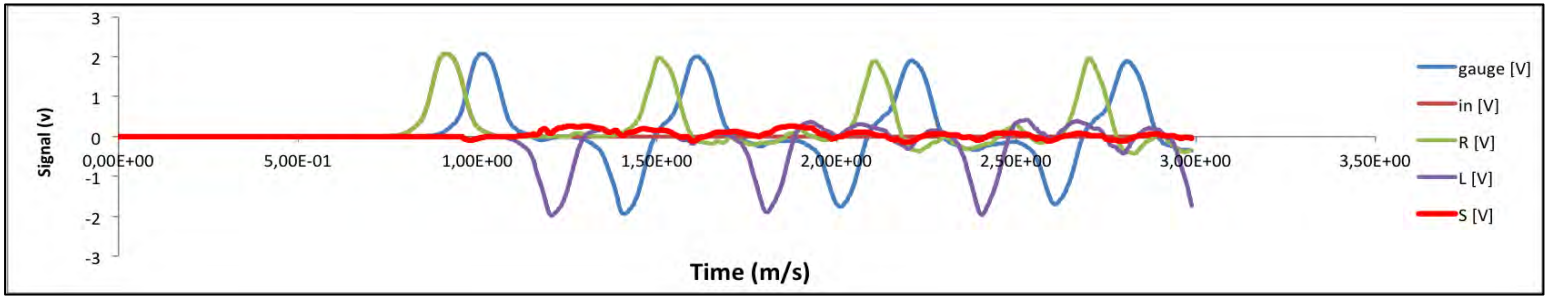

Specimen ID	Gas gun pressure (KPa)	Impact velocity (m/s)	Impact energy (J)	Peak impact force (N)	Hard tissue damage
B20-14 (scalped)	80	5.13	2.78	5068.55	 No damage

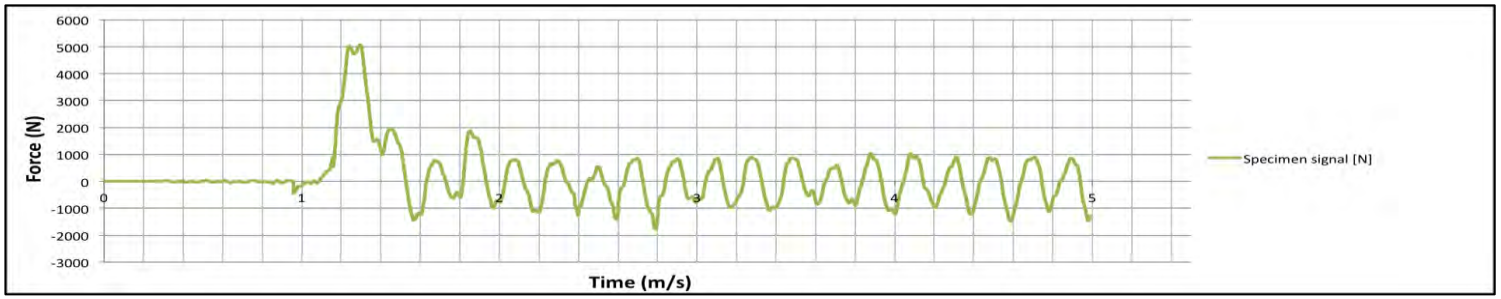

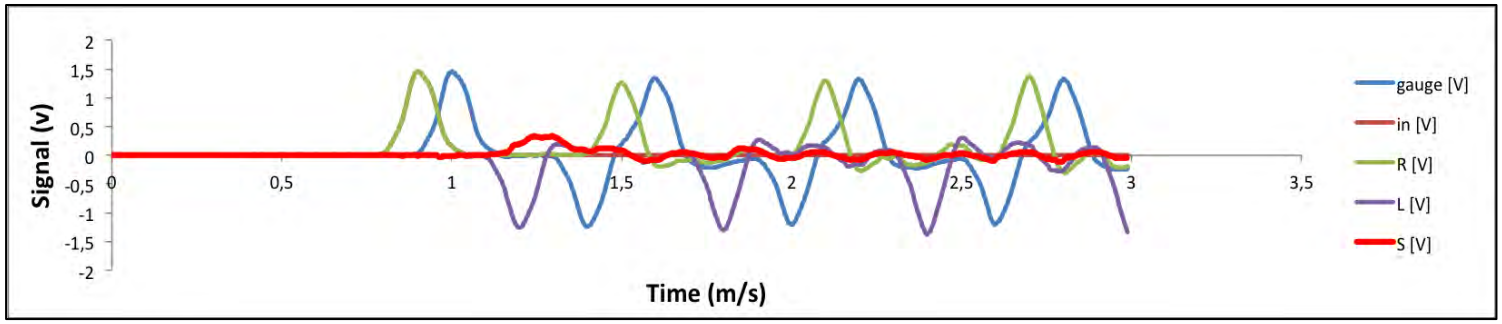

Specimen ID	Gas gun pressure (KPa)	Impact velocity (m/s)	Impact energy (J)	Peak impact force (N)	Hard tissue damage
B30-14 (scalped)	260	10.93	5.54	5228.72	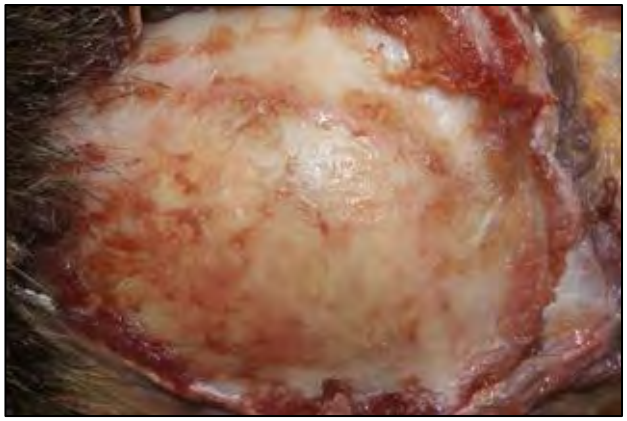 No damage

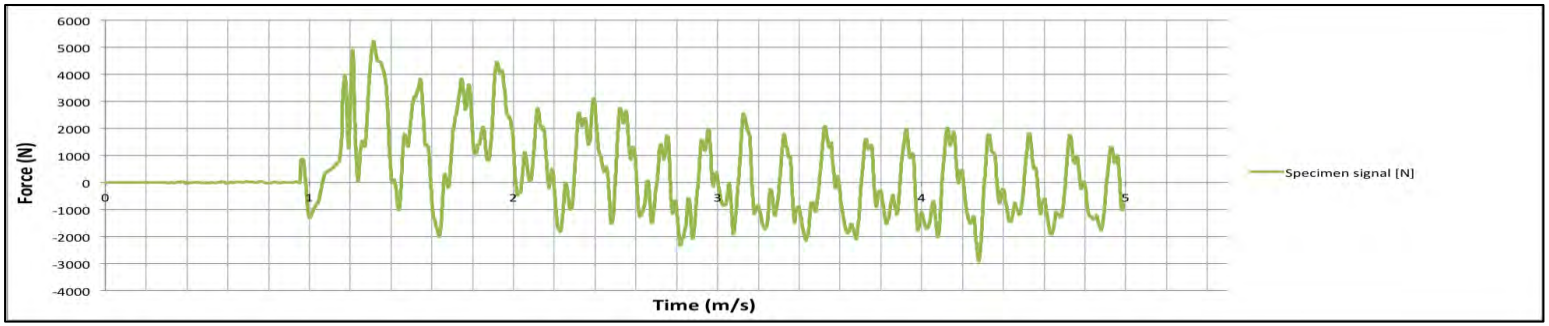

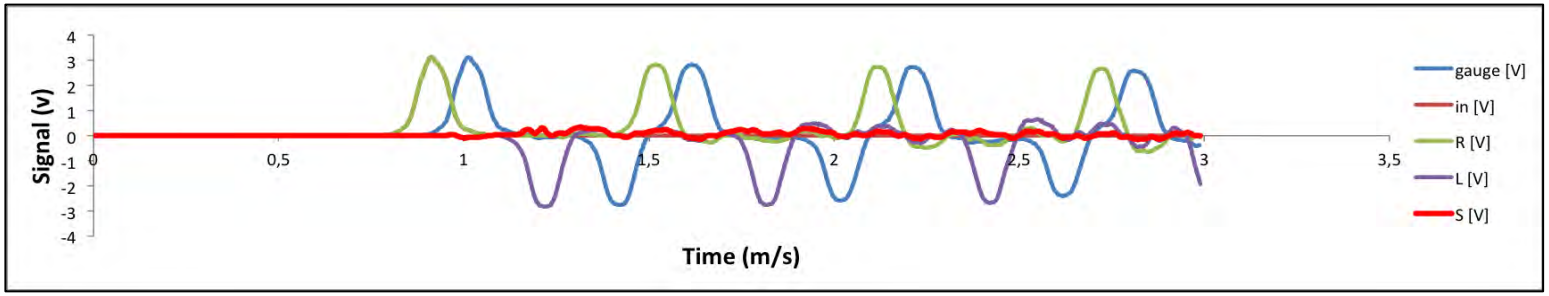

Specimen ID	Gas gun pressure (KPa)	Impact velocity (m/s)	Impact energy (J)	Peak impact force (N)	Hard tissue damage
B6-14 (scalped)	300	10.66	5.46	5319.18	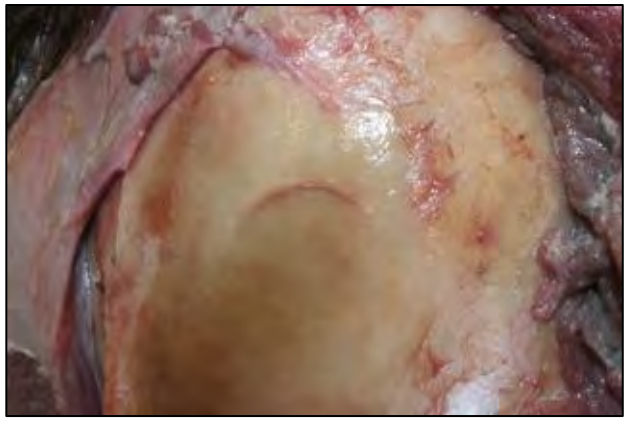 Semi-circular linear fracture (15.15 mm)

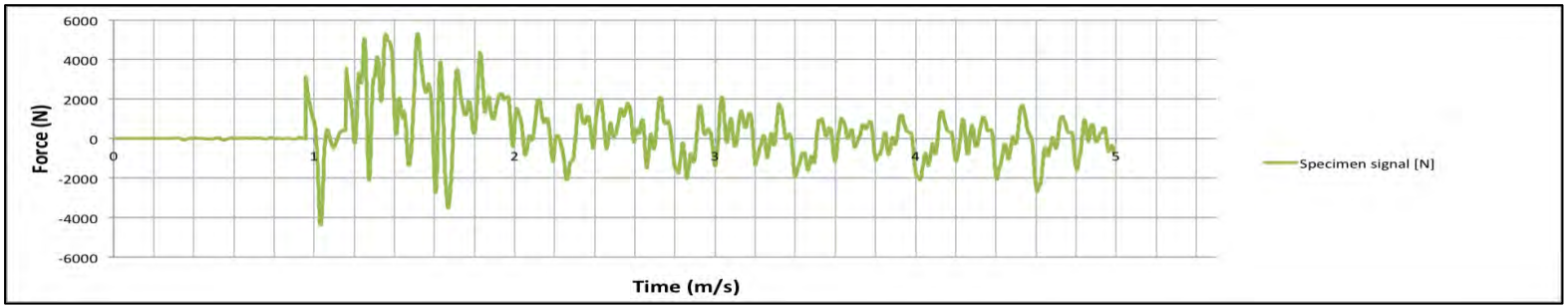

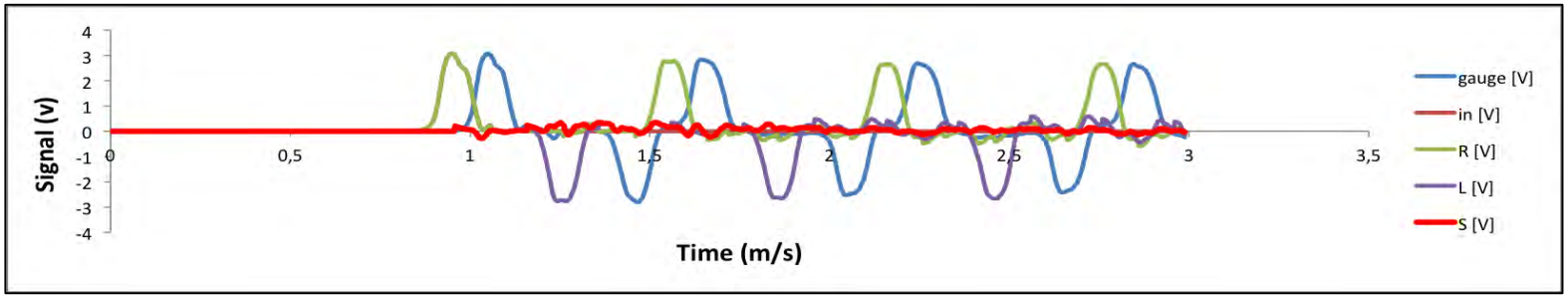

Specimen ID	Gas gun pressure (KPa)	Impact velocity (m/s)	Impact energy (J)	Peak impact force (N)	Hard tissue damage
B18-14 (scalped)	340	11.68	5.98	5882.35	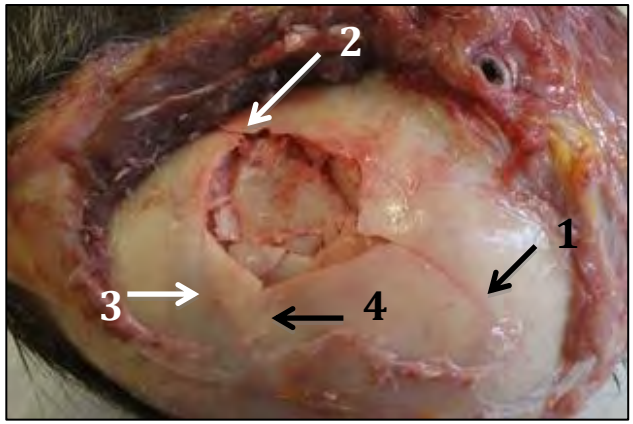 depressed comminuted fracture (26.66 mm x 21.15 mm) and four radiating fractures (1 – 39.11 mm, 2 – 13.54 mm and 3 – 9.2 mm and 4- 6.43 mm)

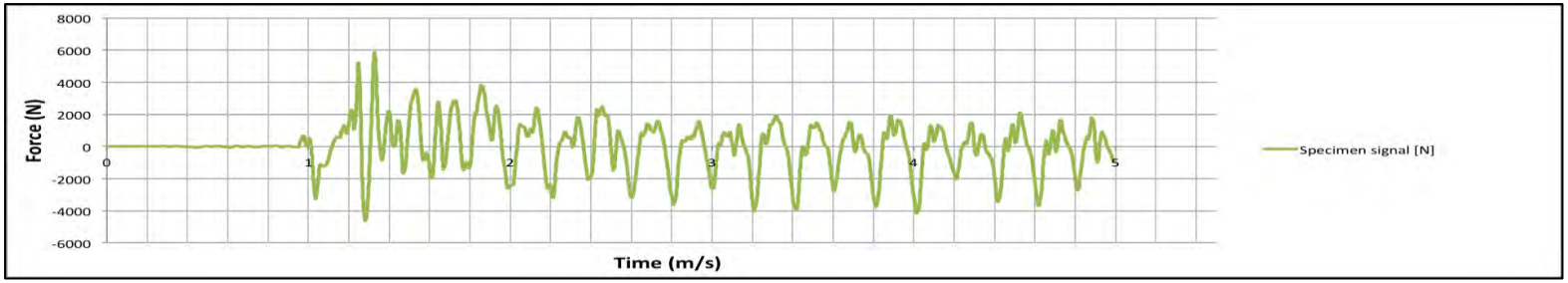

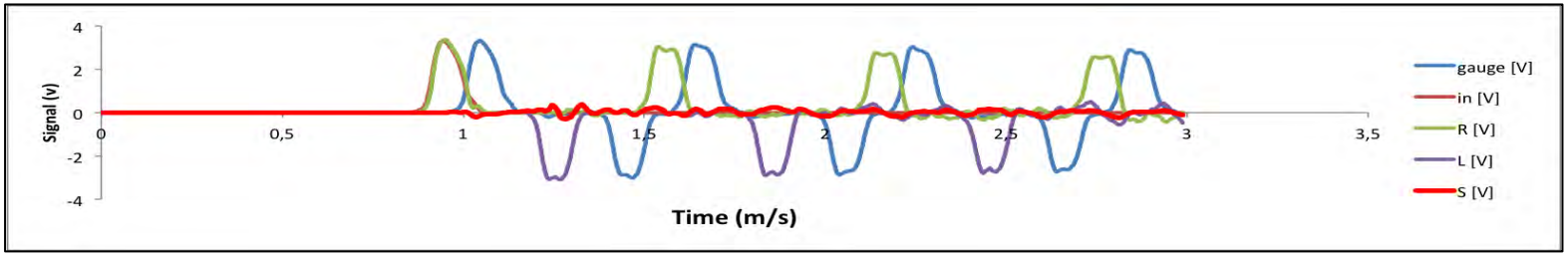

Specimen ID	Gas gun pressure (KPa)	Impact velocity (m/s)	Impact energy (J)	Peak impact force (N)	Hard tissue damage
B14-14 (scalped)	340	7.10	5.69	6170.41	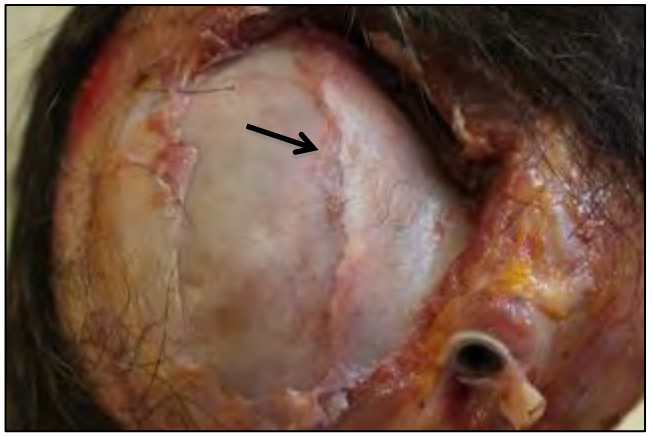 Linear fracture (12.87 mm)

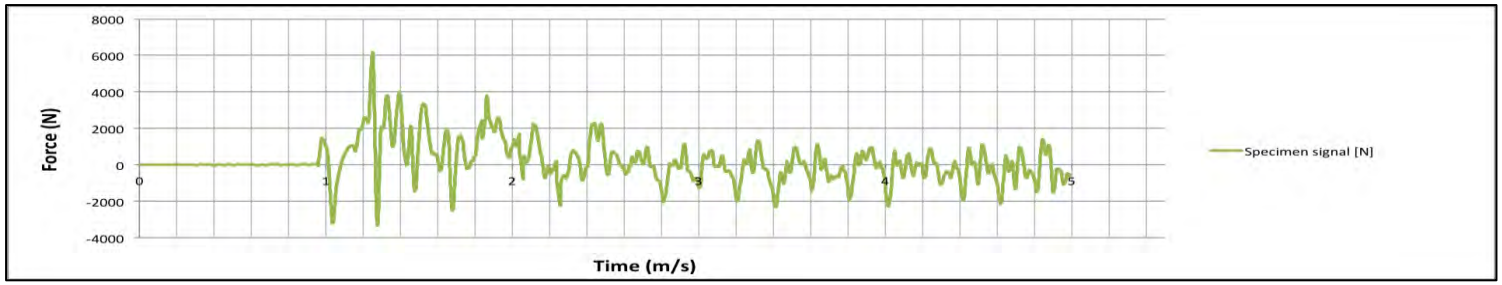

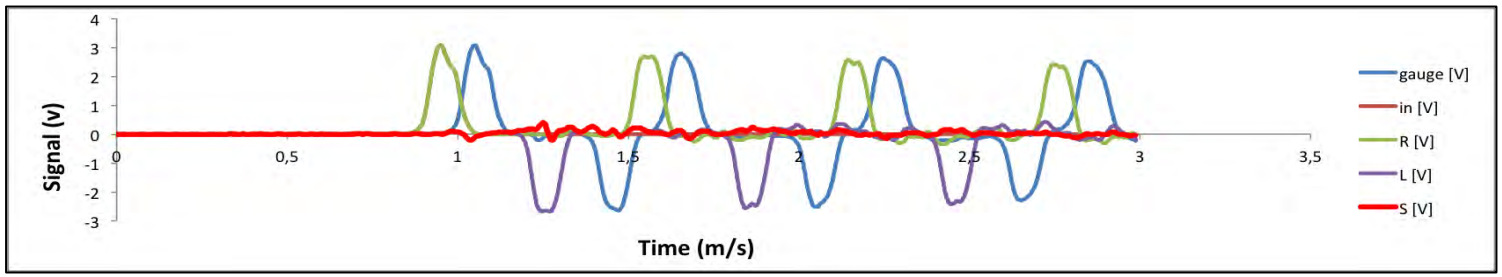

Specimen ID	Gas gun pressure (KPa)	Impact velocity (m/s)	Impact energy (J)	Peak impact force (N)	Hard tissue damage
B9-14 (scalped)	380	12.15	6.47	6446.10	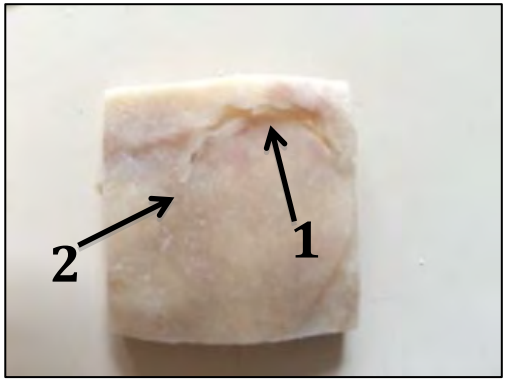 1- Semi-circular depressed fracture (20.13 mm), 2- radiating fracture (10.39 mm)

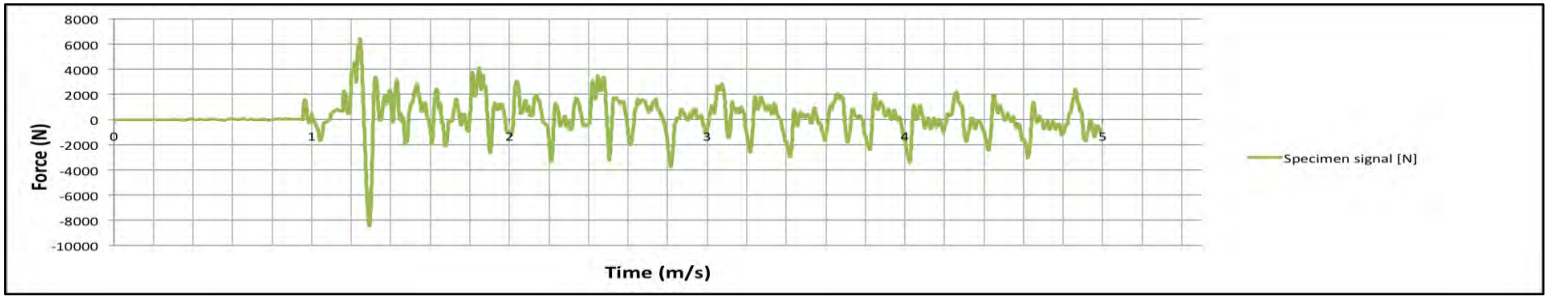

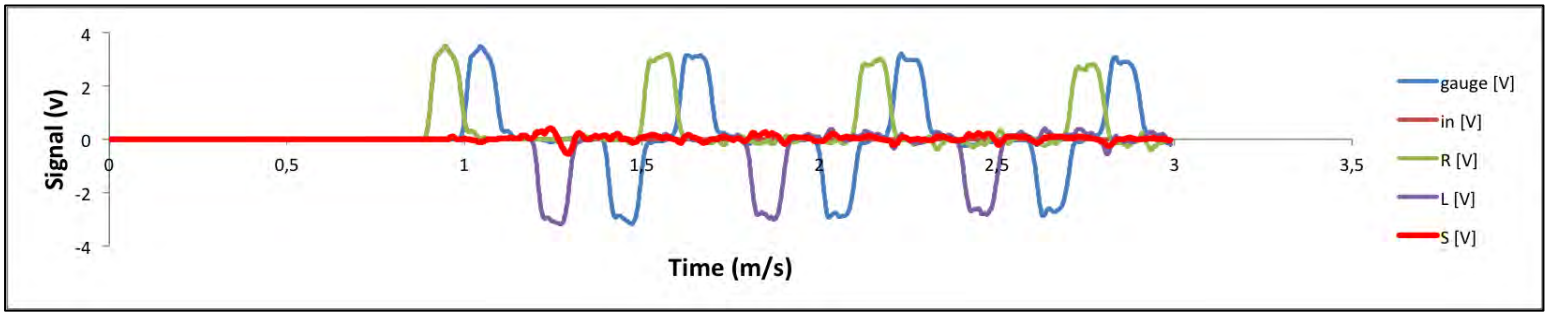

Specimen ID	Gas gun pressure (KPa)	Impact velocity (m/s)	Impact energy (J)	Peak impact force (N)	Hard tissue damage
B15-14 (scalped)	360	11.78	7.27	7233.33	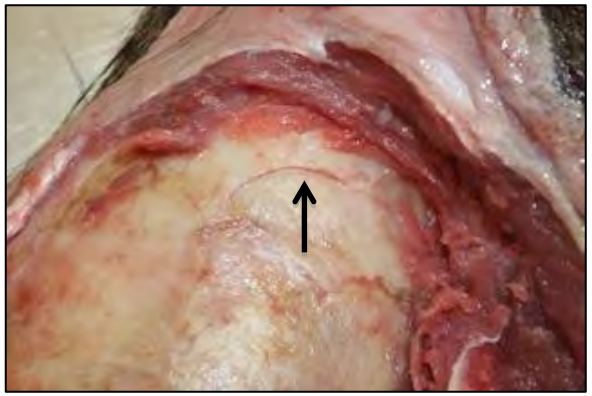 Semi-circular linear fracture (13.26 mm)

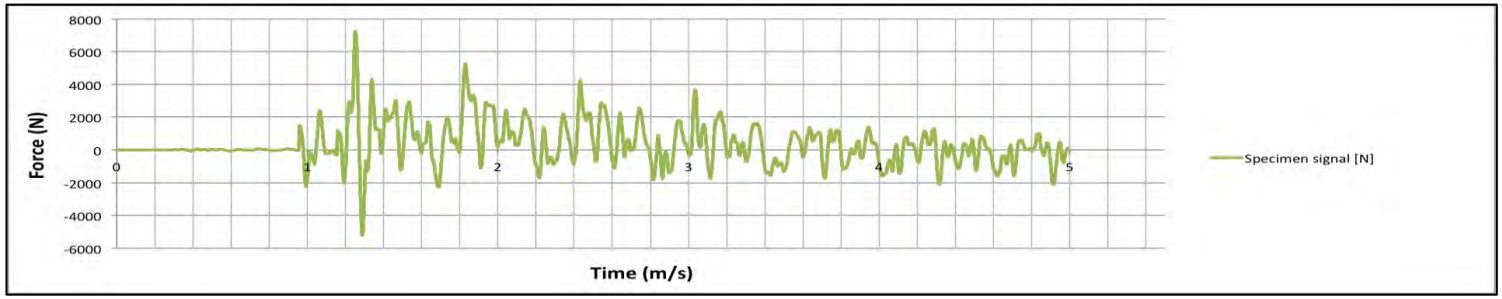

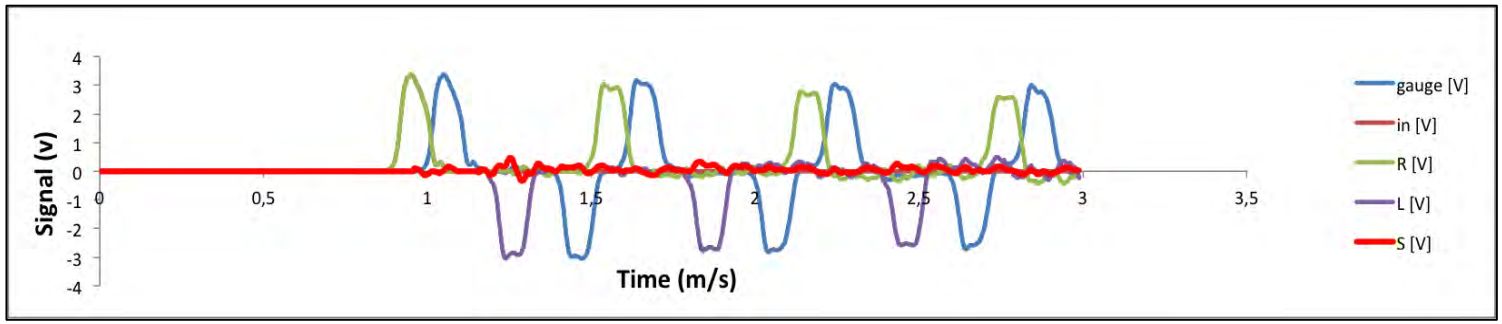

Specimen ID	Gas gun pressure (KPa)	Impact velocity (m/s)	Impact energy (J)	Peak impact force (N)	Hard tissue damage
B8-14 (scalped)	340	12.24	7.79	7480.98	 Depressed comminuted fracture and concentric fracture (18.93 mm x 13.83 mm)

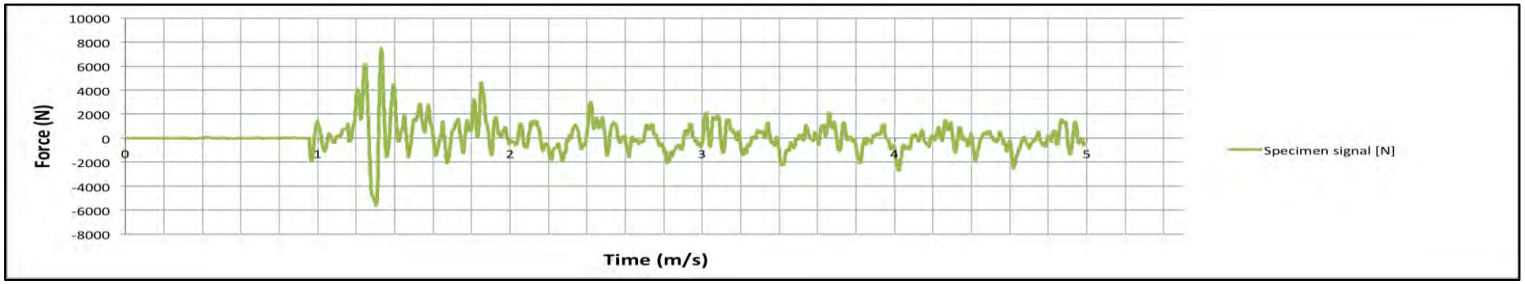

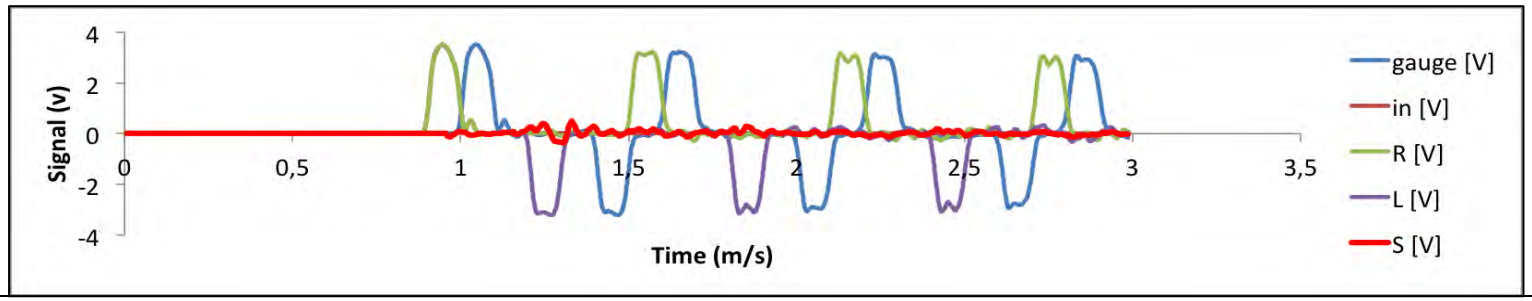

Specimen ID	Gas gun pressure (KPa)	Impact velocity (m/s)	Impact energy (J)	Peak impact force (N)	Hard tissue damage
B35-14 (scalped)	300	11.78	9.81	10159,12	 Comminuted depressed fracture (20.19 mm x 18.71 mm)

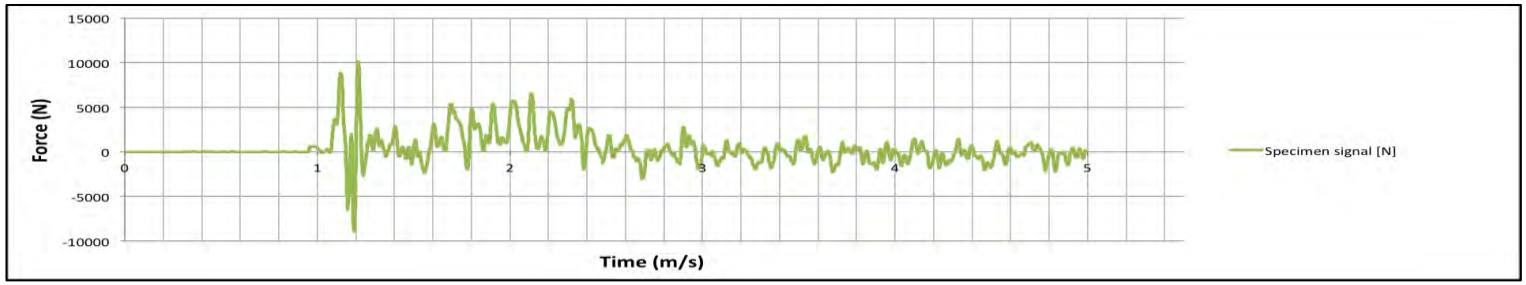

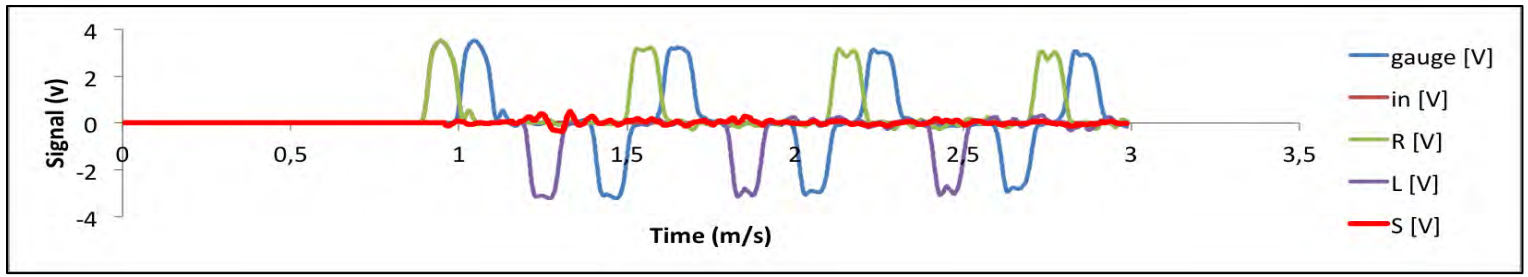

Appendix F:
Author guidelines-Legal Medicine

LEGAL MEDICINE

Official Journal of the Japanese Society of Legal Medicine.

TABLE OF CONTENTS

DESCRIPTION

AUTHOR INFORMATION PACK

ISSN: 1344-6223

Legal Medicine provides an international forum for the publication of original articles, reviews and correspondence on subjects that cover practical and theoretical areas of interest relating to the wide range of legal medicine. Subjects covered include forensic pathology, toxicology, odontology, anthropology, criminalistics, immunochemistry, hemogenetics and forensic aspects of biological science with emphasis on DNA analysis and molecular biology. Submissions dealing with medicolegal problems such as malpractice, insurance, child abuse or ethics in medical practice are also acceptable.

AUDIENCE

Scientists in legal medicine, forensic pathologists, anthropologists, molecular biologists,

serologists, odontologists, toxicologists, psychiatrists, lawyers dealing with medicolegal problems, insurance companies

IMPACT FACTOR

2013: 1.441 © Thomson Reuters Journal Citation Reports 2014

ABSTRACTING AND INDEXING

Chemical Abstracts MEDLINE® EMBASE PubMed

CSA Database Scopus

EDITORIAL BOARD

GUIDE FOR AUTHORS

INTRODUCTION

Types of paper

Original Research Article (full-paper): full-length research report.

Short Communication: description of a technical aspect of a field or issue, report on a procedure or method, or work on validation of techniques or methods. Usually a brief description or analysis of an unusual case or a small series of cases. Case reports are acceptable only if the contribution to the better understanding in forensic pathology, forensic toxicology, or medical law is clearly described.

Review Article: full-length paper reviewing the state of the art or the published literature in a particular area of general interest to the readership.

Announcement of population data: authors are invited to submit population data to the journal in table format: as an example, please refer to Legal Medicine Volume 11 (2009), pages 302-304. Click here:

http://cdn.elsevier.com/promis_misc/LEGMED%2011%202009%20302%20304.pdf

Letter to the Editor: usually a discussion of a previously published item or commentary on the Journal. Publication of letters is solely at the discretion of the Editor. Letters commenting on previously published items are ordinarily shared with the original authors to afford them an opportunity to respond to the commentary.

Papers submitted are subject to peer review. Papers will be evaluated by at least two anonymous persons, either members of the Editorial Board or qualified invited referees. Authors may expect to hear a decision -- acceptance, revision, or rejection -- from the Editor-in-Chief within 6 to 8 weeks after the paper has been received. Papers requiring revision and/or shortening will be returned to the authors by the Editor-in-Chief specifying the requested alterations and including the (anonymous) referee reports. Authors are requested to submit the revised paper within 3 months to the Editor-in- Chief; if submitted at a later date, it will be treated as a new paper and the date of receipt will be altered to the date of submission of the revised paper.

Papers should be concise, but with sufficient experimental detail to permit a critical appraisal of the work. Unnecessary repetition should be avoided. Responsibility for the accuracy of materials in the manuscripts, including appropriate references to related work, lies entirely with the authors.

Contact details for submission

Authors should send queries concerning the submission process or journal procedures to AuthorSupport@elsevier.com. Authors can check the status of their manuscript within the review procedure using Elsevier Editorial System.

BEFORE YOU BEGIN

Ethics in publishing

For information on Ethics in publishing and Ethical guidelines for journal publication see:

http://www.elsevier.com/publishingethics

and

http://www.elsevier.com/journal-authors/ethics.

Human and animal rights

If the work involves the use of animal or human subjects, the author should ensure that the work described has been carried out in accordance with The Code of Ethics of the World Medical Association (Declaration of Helsinki) for experiments involving humans

http://www.wma.net/en/30publications/10policies/b3/index.html;

EU Directive 2010/63/EU for animal experiments

http://ec.europa.eu/environment/chemicals/lab_animals/legislation_en.htm;

Uniform Requirements for manuscripts submitted to Biomedical journals http://www.icmje.org.

Authors should include a statement in the manuscript that informed consent was obtained for experimentation with human subjects. The privacy rights of human subjects must always be observed.

Conflict of interest

All authors are requested to disclose any actual or potential conflict of interest including any financial, personal or other relationships with other people or organizations within three years of beginning the submitted work that could inappropriately influence, or be perceived to influence, their work. See also: http://www.elsevier.com/conflictsofinterest.

Further information and an example of a Conflict of Interest form can be found at: http://help.elsevier.com/app/answers/detail/a_id/286/p/7923.

Submission declaration

Submission of an article implies that the work described has not been published previously (except in the form of an abstract or as part of a published lecture or academic thesis or as an electronic preprint, see:

http://www.elsevier.com/postingpolicy)

that it is not under consideration for publication elsewhere, that its publication is approved by all authors and tacitly or explicitly by the responsible authorities where the work was carried out, and that, if accepted, it will not be published elsewhere including electronically in the same form, in English or in any other language, without the written consent of the copyright-holder.

Authorship

All authors should have made substantial contributions to all of the following: (1) the conception and design of the study, or acquisition of data, or analysis and interpretation of data, (2) drafting the article or revising it critically for important intellectual content, (3) final approval of the version to be submitted.

Changes to authorship

This policy concerns the addition, deletion, or rearrangement of author names in the authorship of accepted manuscripts: *Before the accepted manuscript is published in an online issue*: Requests to add or remove an author, or to rearrange the author names, must be sent to the Journal Manager from the corresponding author of the accepted manuscript and must include: (a) the reason the name should be added or removed, or the author names rearranged and (b) written confirmation (e-mail, fax, letter) from all authors that they agree with the addition, removal or rearrangement. In the case of addition or removal of authors, this includes confirmation from the author being added or removed. Requests that are not sent by the corresponding author will be forwarded by the Journal Manager to the corresponding author, who must follow the procedure as described above. Note that: (1) Journal Managers will inform the Journal Editors of any such requests and (2) publication of the accepted manuscript in an online issue is suspended until authorship has been agreed.

After the accepted manuscript is published in an online issue: Any requests to add, delete, or rearrange author names in an article published in an online issue will follow the same policies as noted above and result in a corrigendum.

Article transfer service

This journal is part of our Article Transfer Service. This means that if the Editor feels your article is more suitable in one of our other participating journals, then you may be asked to consider transferring the article to one of those. If you agree, your article will be transferred automatically on your behalf with no need to reformat. More information about this can be found here:

http://www.elsevier.com/authors/article-transfer-service.

Copyright

This journal offers authors a choice in publishing their research: Open access and Subscription.

For subscription articles

Upon acceptance of an article, authors will be asked to complete a 'Journal Publishing Agreement' (for more information on this and copyright, see http://www.elsevier.com/copyright). An e-mail will be sent to the corresponding author confirming receipt of the manuscript together with a 'Journal Publishing Agreement' form or a link to the online version of this agreement.

Subscribers may reproduce tables of contents or prepare lists of articles including abstracts for internal circulation within their institutions. Permission of the Publisher is required for resale or distribution outside the institution and for all other derivative works, including compilations and translations (please consult http://www.elsevier.com/permissions). If excerpts from other copyrighted works are included, the author(s) must obtain written permission from the copyright owners and credit the source(s) in the article. Elsevier has preprinted forms for use by authors in these cases: please consult http://www.elsevier.com/permissions.

For open access articles

Upon acceptance of an article, authors will be asked to complete an 'Exclusive License Agreement'

(for more information see http://www.elsevier.com/OAauthoragreement). Permitted reuse of open access articles is determined by the author's choice of user license (see http://www.elsevier.com/openaccesslicenses).

Retained author rights

As an author you (or your employer or institution) retain certain rights. For more information on author rights for: Subscription articles please see http://www.elsevier.com/journal-authors/author-rights-and-responsibilities.

Open access articles please see http://www.elsevier.com/OAauthoragreement.

Role of the funding source

You are requested to identify who provided financial support for the conduct of the research and/or preparation of the article and to briefly describe the role of the sponsor(s), if any, in study design; in the collection, analysis and interpretation of data; in the writing of the report; and in the decision to submit the article for publication. If the funding source(s) had no such involvement then this should be stated.

Funding body agreements and policies

Elsevier has established agreements and developed policies to allow authors whose articles appear in journals published by Elsevier, to comply with potential manuscript archiving requirements as specified as conditions of their grant awards. To learn more about existing agreements and policies please visit http://www.elsevier.com/fundingbodies.

Open access

This journal offers authors a choice in publishing their research:

Open access

• Articles are freely available to both subscribers and the wider public with permitted reuse.

• An open access publication fee is payable by authors or their research funder.

Subscription

• Articles are made available to subscribers as well as developing countries and patient groups through our access programs (http://www.elsevier.com/access)

• No open access publication fee

All articles published open access will be immediately and permanently free for everyone to read and download. Permitted reuse is defined by your choice of one of the following Creative Commons user licenses: **Creative Commons Attribution-NonCommercial-ShareAlike (CC BY-NC-SA)**: for non- commercial purposes, lets others distribute and copy the article, to create extracts, abstracts and other revised versions, adaptations or derivative works of or from an article (such as a translation), to include in a collective work (such as an anthology), to text and data mine the article, as long as they credit the author(s), do not represent the author as endorsing their adaptation of the article, do not modify the article in such a way as to damage the author's honor or reputation, and license their new adaptations or creations under identical terms (CC BY-NC-SA).

Creative Commons Attribution-NonCommercial-NoDerivs (CC BY-NC-ND): for non-commercial purposes, lets others distribute and copy the article, and to include in a collective work (such as an anthology), as long as they credit the author(s) and provided they do not alter or modify the article.

Elsevier has established agreements with funding bodies

http://www.elsevier.com/fundingbodies.

This ensures authors can comply with funding body open access requirements, including specific user licenses, such as CC BY. Some authors may also be reimbursed for associated publication fees. If you need to comply with your funding body policy, you can apply for the CC BY license after your manuscript is accepted for publication.

To provide open access, this journal has a publication fee which needs to be met by the authors or their research funders for each article published open access.

Your publication choice will have no effect on the peer review process or acceptance of submitted articles.

The open access publication fee for this journal is **$2,500**, excluding taxes. Learn more about Elsevier's pricing policy: http://www.elsevier.com/openaccesspricing.

Language (usage and editing services)

Please write your text in good English (American or British usage is accepted, but not a mixture of these). Authors who feel their English language manuscript may require editing to eliminate possible grammatical or spelling errors and to conform to correct scientific English may wish to use the English Language Editing service available from Elsevier's WebShop

(http://webshop.elsevier.com/languageediting/)

or visit our customer support site (http://support.elsevier.com) for more information.

Submission

Submission to this journal proceeds totally online and you will be guided stepwise through the creation and uploading of your files. The system automatically converts source files to a single PDF file of the article, which is used in the peer-review process. Please note that even though manuscript source files are converted to PDF files at submission for the review process, these source files are needed for further processing after acceptance. All correspondence, including notification of the Editor's decision and requests for revision, takes place by e-mail removing the need for a paper trail.

Submit your article

Please submit your article via http://ees.elsevier.com/legmed.

Additional information

Manuscripts that are not properly prepared will be returned to the authors without review, since it is not feasible for the Editors to undertake extensive revision or rewriting of manuscripts submitted.

PREPARATION

Article structure

Original Articles and Brief Communications should be organized as follows:

1. Abstract and Keywords 2. Introduction 3. Materials and Methods 4. Results

5. Discussion 6. Acknowledgements 7. References 8. Tables 9. Legends to Figures

Subdivision - numbered sections

Divide your article into clearly defined and numbered sections. Subsections should be numbered 1.1 (then 1.1.1, 1.1.2, ...), 1.2, etc. (the abstract is not included in section numbering). Use this numbering also for internal cross-referencing: do not just refer to 'the text'. Any subsection may be given a brief heading. Each heading should appear on its own separate line.

Introduction

State the objectives of the work and provide an adequate background, avoiding a detailed literature survey or a summary of the results.

Materials and Methods

Material and Methods should be as brief as possible, but sufficiently descriptive to permit a qualified reader to repeat the experiments reported. Only truly new procedures should be described in detail; previously published procedures should be cited as references. Modifications of previously published procedures need be given in detail only when this is necessary to repeat the work. In a case report, the case history should be presented in this section. Describe statistical methods in sufficient detail to enable a knowledgeable reader with access to the original data to verify the reported results. When possible, quantify findings and present them with appropriate indicators of measurement error or uncertainty (such as confidence intervals).

Results

The Results of experiments should be presented in figures and tables, although some results that do not require documentation may be given solely in the text. Discussion in this section should not be extensive.

Discussion

The Discussion should be concise (usually less than four typed pages) and should focus on the interpretation of the results, rather than a repetition of the Results section. In some shorter papers, combining the Results and Discussion into one section entitled Results and Discussion

may provide a clearer presentation.

Essential title page information

• ***Title.*** Concise and informative. Titles are often used in information-retrieval systems. Avoid abbreviations and formulae where possible. • ***Author names and affiliations.*** Where the family name may be ambiguous (e.g., a double name), please indicate this clearly. Present the authors' affiliation addresses (where the actual work was done) below the names. Indicate all affiliations with a lower-case superscript letter immediately after the author's name and in front of the appropriate address. Provide the full postal address of each affiliation, including the country name and, if available, the e-mail address of each author.

• ***Corresponding author.*** Clearly indicate who will handle correspondence at all stages of refereeing and publication, also post-publication. **Ensure that phone numbers (with country and area code) are provided in addition to the e-mail address and the complete postal address. Contact details must be kept up to date by the corresponding author.**

• ***Present/permanent address.*** If an author has moved since the work described in the article was done, or was visiting at the time, a 'Present address' (or 'Permanent address') may be indicated as a footnote to that author's name. The address at which the author actually did the work must be retained as the main, affiliation address. Superscript Arabic numerals are used for such footnotes.

Abstract

A concise and factual abstract is required. The abstract should state briefly the purpose of the research, the principal results and major conclusions. An abstract is often presented separately from the article, so it must be able to stand alone. For this reason, References should be avoided, but if essential, then cite the author(s) and year(s). Also, non-standard or uncommon abbreviations should be avoided, but if essential they must be defined at their first mention in the abstract itself.

Graphical abstract

Although a graphical abstract is optional, its use is encouraged as it draws more attention to the online article. The graphical abstract should summarize the contents of the article in a concise,

pictorial form designed to capture the attention of a wide readership. Graphical abstracts should be submitted as a separate file in the online submission system. Image size: Please provide an image with a minimum of 531 × 1328 pixels (h × w) or proportionally more. The image should be readable at a size of 5 × 13 cm using a regular screen resolution of 96 dpi. Preferred file types: TIFF, EPS, PDF or MS Office files. See http://www.elsevier.com/graphicalabstracts for examples.

Authors can make use of Elsevier's Illustration and Enhancement service to ensure the best presentation of their images and in accordance with all technical requirements: Illustration Service.

Highlights

Highlights are mandatory for this journal. They consist of a short collection of bullet points that convey the core findings of the article and should be submitted in a separate file in the online submission system. Please use 'Highlights' in the file name and include 3 to 5 bullet points (maximum 85 characters, including spaces, per bullet point).

See http://www.elsevier.com/highlights for examples.

Keywords

Immediately after the abstract, provide a maximum of 6 keywords, using American spelling and avoiding general and plural terms and multiple concepts (avoid, for example, 'and', 'of'). Be sparing with abbreviations: only abbreviations firmly established in the field may be eligible. These keywords will be used for indexing purposes.

Abbreviations

Define abbreviations that are not standard in this field in a footnote to be placed on the first page of the article. Such abbreviations that are unavoidable in the abstract must be defined at their first mention there, as well as in the footnote. Ensure consistency of abbreviations throughout the article.

Acknowledgements

Collate acknowledgements in a separate section at the end of the article before the references and

do not, therefore, include them on the title page, as a footnote to the title or otherwise. List here those individuals who provided help during the research (e.g., providing language help, writing assistance or proof reading the article, etc.).

Footnotes

Footnotes should be used sparingly. Number them consecutively throughout the article, using superscript Arabic numbers. Many word processors build footnotes into the text, and this feature may be used. Should this not be the case, indicate the position of footnotes in the text and present the footnotes themselves separately at the end of the article. Do not include footnotes in the Reference list.

Table footnotes

Indicate each footnote in a table with a superscript lowercase letter.

Artwork

Electronic artwork General points • Make sure you use uniform lettering and sizing of your original artwork. • Embed the used fonts if the application provides that option. • Aim to use the following fonts in your illustrations: Arial, Courier, Times New Roman, Symbol, or use fonts that look similar. • Number the illustrations according to their sequence in the text. • Use a logical naming convention for your artwork files. • Provide captions to illustrations separately. • Size the illustrations close to the desired dimensions of the printed version. • Submit each illustration as a separate file. A detailed guide on electronic artwork is available on our website: http://www.elsevier.com/artworkinstructions. **You are urged to visit this site; some excerpts from the detailed information are given here.** *Formats* If your electronic artwork is created in a Microsoft Office application (Word, PowerPoint, Excel) then please supply 'as is' in the native document format. Regardless of the application used other than Microsoft Office, when your electronic artwork is finalized, please 'Save as' or convert the images to one of the following formats (note the resolution requirements for line drawings, halftones, and line/halftone combinations given below): EPS (or PDF): Vector drawings, embed all used fonts.TIFF (or JPEG): Color or grayscale photographs (halftones), keep to a minimum of 300 dpi. TIFF (or JPEG): Bitmapped (pure black & white pixels) line drawings, keep to a minimum of 1000 dpi. TIFF (or

JPEG): Combinations bitmapped line/half-tone (color or grayscale), keep to a minimum of 500 dpi. **Please do not:** • Supply files that are optimized for screen use (e.g., GIF, BMP, PICT, WPG); these typically have a low number of pixels and limited set of colors; • Supply files that are too low in resolution; • Submit graphics that are disproportionately large for the content.

Color artwork

Please make sure that artwork files are in an acceptable format (TIFF (or JPEG), EPS (or PDF), or MS Office files) and with the correct resolution. If, together with your accepted article, you submit usable color figures then Elsevier will ensure, at no additional charge, that these figures will appear in color on the Web (e.g., ScienceDirect and other sites) regardless of whether or not these illustrations are reproduced in color in the printed version. **For color reproduction in print, you will receive information regarding the costs from Elsevier after receipt of your accepted article**. Please indicate your preference for color: in print or on the Web only. For further information on the preparation of electronic artwork,

please see http://www.elsevier.com/artworkinstructions.

Please note: Because of technical complications that can arise by converting color figures to 'gray scale' (for the printed version should you not opt for color in print) please submit in addition usable black and white versions of all the color illustrations.

Figure captions

Ensure that each illustration has a caption. Supply captions separately, not attached to the figure. A caption should comprise a brief title (**not** on the figure itself) and a description of the illustration. Keep text in the illustrations themselves to a minimum but explain all symbols and abbreviations used.

Tables

Number tables consecutively in accordance with their appearance in the text. Place footnotes to tables below the table body and indicate them with superscript lowercase letters. Avoid vertical rules. Be sparing in the use of tables and ensure that the data presented in tables do not duplicate results described elsewhere in the article.

References

Citation in text

Please ensure that every reference cited in the text is also present in the reference list (and vice versa). Any references cited in the abstract must be given in full. Unpublished results and personal communications are not recommended in the reference list, but may be mentioned in the text. If these references are included in the reference list they should follow the standard reference style of the journal and should include a substitution of the publication date with either 'Unpublished results' or 'Personal communication'. Citation of a reference as 'in press' implies that the item has been accepted for publication.

Reference links

Increased discoverability of research and high quality peer review are ensured by online links to the sources cited. In order to allow us to create links to abstracting and indexing services, such as Scopus, CrossRef and PubMed, please ensure that data provided in the references are correct. Please note that incorrect surnames, journal/book titles, publication year and pagination may prevent link creation. When copying references, please be careful as they may already contain errors. Use of the DOI is encouraged.

Reference formatting

There are no strict requirements on reference formatting at submission. References can be in any style or format as long as the style is consistent. Where applicable, author(s) name(s), journal title/book title, chapter title/article title, year of publication, volume number/book chapter and the pagination must be present. Use of DOI is highly encouraged. The reference style used by the journal will be applied to the accepted article by Elsevier at the proof stage. Note that missing data will be highlighted at proof stage for the author to correct. If you do wish to format the references yourself they should be arranged according to the following examples:

Reference style Text: Indicate references by number(s) in square brackets in line with the text. The actual authors can be referred to, but the reference number(s) must always be given. *List:* Number the references (numbers in square brackets) in the list in the order in which they appear in the text. *Examples:* Reference to a journal publication: [1] Van der Geer J, Hanraads JAJ, Lupton

RA. The art of writing a scientific article. J Sci Commun 2010;163:51–9. Reference to a book: [2] Strunk Jr W, White EB. The elements of style. 4th ed. New York: Longman; 2000. Reference to a chapter in an edited book: [3] Mettam GR, Adams LB. How to prepare an electronic version of your article. In: Jones BS, Smith RZ, editors. Introduction to the electronic age, New York: E-Publishing Inc; 2009, p. 281–304. Note shortened form for last page number. e.g., 51–9, and that for more than 6 authors the first 6 should be listed followed by 'et al.' For further details you are referred to 'Uniform Requirements for Manuscripts submitted to Biomedical Journals' (J Am Med Assoc 1997;277:927–34).

(see also http://www.nlm.nih.gov/bsd/uniform_requirements.html).

AudioSlides

The journal encourages authors to create an AudioSlides presentation with their published article. AudioSlides are brief, webinar-style presentations that are shown next to the online article on ScienceDirect. This gives authors the opportunity to summarize their research in their own words and to help readers understand what the paper is about. More information and examples are available at http://www.elsevier.com/audioslides. Authors of this journal will automatically receive an invitation e-mail to create an AudioSlides presentation after acceptance of their paper.

Supplementary data

Elsevier accepts electronic supplementary material to support and enhance your scientific research. Supplementary files offer the author additional possibilities to publish supporting applications, high- resolution images, background datasets, sound clips and more. Supplementary files supplied will be published online alongside the electronic version of your article in Elsevier Web products, including ScienceDirect: http://www.sciencedirect.com. In order to ensure that your submitted material is directly usable, please provide the data in one of our recommended file formats. Authors should submit the material in electronic format together with the article and supply a concise and descriptive caption for each file. For more detailed instructions please visit our artwork instruction pages at http://www.elsevier.com/artworkinstructions.

Submission checklist

The following list will be useful during the final checking of an article prior to sending it to the journal for review. Please consult this Guide for Authors for further details of any item. **Ensure**

that the following items are present: One author has been designated as the corresponding author with contact details:

• E-mail address • Full postal address • Phone numbers. All necessary files have been uploaded, and contain: • Keywords • All figure captions • All tables (including title, description, footnotes) Further considerations • Manuscript has been 'spell-checked' and 'grammar-checked' • References are in the correct format for this journal • All references mentioned in the Reference list are cited in the text, and vice versa • Permission has been obtained for use of copyrighted material from other sources (including the Web) • Color figures are clearly marked as being intended for color reproduction on the Web (free of charge) and in print, or to be reproduced in color on the Web (free of charge) and in black-and-white in print • If only color on the Web is required, black-and-white versions of the figures are also supplied for printing purposes. For any further information please visit our customer support site at http://support.elsevier.com.

AFTER ACCEPTANCE

Availability of accepted article

This journal makes articles available online as soon as possible after acceptance. This concerns the accepted article (both in HTML and PDF format), which has not yet been copyedited, typeset or proofread. A Digital Object Identifier (DOI) is allocated, thereby making it fully citable and searchable by title, author name(s) and the full text. The article's PDF also carries a disclaimer stating that it is an unedited article. Subsequent production stages will simply replace this version.

Use of the Digital Object Identifier

The Digital Object Identifier (DOI) may be used to cite and link to electronic documents. The DOI consists of a unique alpha-numeric character string which is assigned to a document by the publisher upon the initial electronic publication. The assigned DOI never changes. Therefore, it is an ideal medium for citing a document, particularly 'Articles in press' because they have not yet received their full bibliographic information. Example of a correctly given DOI (in URL format; here an article in the journal *Physics Letters B*):

http://dx.doi.org/10.1016/j.physletb.2010.09.059

When you use a DOI to create links to documents on the web, the DOIs are guaranteed never to change.

Proofs

One set of page proofs (as PDF files) will be sent by e-mail to the corresponding author (if we do not have an e-mail address then paper proofs will be sent by post) or, a link will be provided in the e-mail so that authors can download the files themselves. Elsevier now provides authors with PDF proofs which can be annotated; for this you will need to download Adobe Reader version 9 (or higher) available free from:

http://get.adobe.com/reader. Instructions on how to annotate PDF files will accompany the proofs (also given online). The exact system requirements are given at the Adobe site: http://www.adobe.com/products/reader/tech-specs.html. If you do not wish to use the PDF annotations function, you may list the corrections (including replies to the Query Form) and return them to Elsevier in an e-mail. Please list your corrections quoting line number. If, for any reason, this is not possible, then mark the corrections and any other comments (including replies to the Query Form) on a printout of your proof and return by fax, or scan the pages and e-mail, or by post. Please use this proof only for checking the typesetting, editing, completeness and correctness of the text, tables and figures. Significant changes to the article as accepted for publication will only be considered at this stage with permission from the Editor. We will do everything possible to get your article published quickly and accurately – please let us have all your corrections within 48 hours. It is important to ensure that all corrections are sent back to us in one communication: please check carefully before replying, as inclusion of any subsequent corrections cannot be guaranteed. Proofreading is solely your responsibility. Note that Elsevier may proceed with the publication of your article if no response is received.

Author orders

When your article is published, you can commemorate your publication with printed author copies of the journal issue, customized full-color posters, extra offprints, and more. Please visit http://webshop.elsevier.com to learn more.

Offprints

The corresponding author, at no cost, will be provided with a personalized link providing 50 days

free access to the final published version of the article on ScienceDirect. This link can also be used for sharing via email and social networks. For an extra charge, paper offprints can be ordered via the offprint order form which is sent once the article is accepted for publication. Both corresponding and co-authors may order offprints at any time via Elsevier's WebShop (http://webshop.elsevier.com/myarticleservices/offprints). Authors requiring printed copies of multiple articles may use Elsevier WebShop's 'Create Your Own Book' service to collate multiple articles within a single cover (http://webshop.elsevier.com/myarticleservices/booklets).

AUTHOR INQUIRIES

You can track your submitted article at:

http://help.elsevier.com/app/answers/detail/a_id/89/p/8045/. You can track your accepted article at http://www.elsevier.com/trackarticle. You are also welcome to contact Customer Support via http://support.elsevier.com.

Appendix G:

Acknowledgements

"If we knew what we were doing, it would not be called research, would it?" – Albert Einstein

I would like to express my gratitude to the following people who made my project possible:

- **Dr Marise Heyns:** for supervising me throughout my research project. I would also like to recognise her role in assisting me in obtaining a research permit from Cape Nature, as well as the collection of baboon specimens. Dr. Marise Heyns is also acknowledged for her intellectual help, more specifically in shaping my ideas and always having an educated answer to all of my uncertainties, in addition to reviewing the drafts of my minor dissertation.

- **Mr. Calvin Gerald Mole:** for taking on the role of my personal tutor. You have not only shaped my ideas, but also provided me with insight into literature. You have spent many hours attending to my queries, assisting me in specimen collection, and supporting me during my time spent in the lab. You have further challenged and enriched my ideas and have always given me professional suggestions when reviewing the drafts of my minor dissertation. I thank you for your positive attitude even when things went wrong.

- **Mr. Trevor Cloete:** from the Blast and Impact Survivability Research Unit in the Department of Mechanical Engineering. Thank you for providing me with the apparatus necessary to conduct my research and also assisting me with troubleshooting.

- **National Research Foundation (NRF):** for granting me the NRF Freestanding Master's Scholarship that was received for the degree MPhil Biomedical Forensic Sciences for the period 01/01/2014 – 31/12/2014.

- **Mrs. Esmé Beamish:** from the Cape Peninsula Baboon Research Unit for supplying me with Cape (Chacma) Baboon specimens.

- **Mr. Justin O'Riain:** from the Cape Peninsula Baboon Research Unit for supplying me with Cape (Chacma) Baboon specimens.

- **Cape Nature:** for their donation of Cape (Chacma) Baboon specimens.

- **University of Cape Town Writing Centre:** not only did this organization encourage me through the entire journey of my minor dissertation; they further helped me to bring my writing together. They also assisted in giving it shape and helping me to reach a point of satisfaction in my own work.

Appendix G:
Ethics

UNIVERSITY OF CAPE TOWN

Health Sciences Faculty
Research Ethics Committee
Room E53-24 Groote Schuur Hospital Old Main Building
Observatory 7925
Telephone [021] 406 6338 • **Facsimile** [021] 406 6411
e-mail: nosi.tsama@uct.ac.za

07 April 2014

AEC REF NO: 014/008

Ms Lisa Jane Coetzé
IIDMM

Dear Ms Coetzé

PROJECT TITLE: INVESTIGATION OF BLUNT INJURIES AND THE FORCE ASSOCIATED WITH A SKULL FRACTURE DUE TO IMPACT WITH A HOPKINSON PRESSURE BAR: AN ANIMAL MODEL

Thank you for submitting your study to the Faculty of Health Sciences Animal Ethics Committee for review.

The FHS AEC appreciates the notification about the study; however, the ethics approval is not required in this instance.

Please quote the REC REF in all your correspondence

Yours sincerely

PROF PJ COMMERFORD
CHAIR, HSF AEC

lemjedi

CapeNature

HEAD OFFICE

postal	Private Bag x29 Gatesville 7766
physical	PGWC Shared Services Center cnr Bosduif & Volstruis Streets Bridgetown 7764
website	www.capenature.co.za
enquiries	Lee-Anne Benjamin
telephone	+27 21 483 0120
fax	086 556 7734
email	lbenjamin@capenature.co.za
reference	1/2/1/6/5/F6
date	28 August 2014

Dr M Heyns
University of Cape Town
Department of Clinical Laboratory Sciences
Private Bag X3
RONDEBOSCH
7701

Dear Dr Heyns

APPLICATION TO COLLECT FAUNA SPECIMENS FOR SCIENTIFIC RESEARCH

I refer to your application to collect specimens in the Western Cape Province.

Attached are permit No.'s: **AAA007-00131-0056** dated **28 August 2014** to collect specimens in the Western Cape Province. Please take special note of the standard conditions attached to the permits. I specifically draw your attention to permit condition (i). **It is imperative that you make contact with the Reserve Manager BEFORE you intend collecting on any nature reserve, conservation area, wilderness area and / or state forest**. No deviation is allowed from the fore-mentioned conditions without the prior written approval of the Chief Executive Officer: Western Cape Nature Conservation Board.

Please also take note of the *pro forma* (copy attached), which must please be used when submitting your collection / distribution records to CapeNature as per the conditions to your permit. Please feel free to add columns for extra data to the *pro forma* but no columns should be deleted. This pro forma is also available electronically from CapeNature.

Should you have any queries please do not hesitate to contact this office.

Yours faithfully,

CHIEF EXECUTIVE OFFICER

Appendix I:
Budget

Research Budget 2014

Student

Lisa Jane Coetzé (CTZLIS001)

Degree

MPhil Biomedical Forensic Science

Project

Investigation of blunt injuries and the force associated with a skull fracture due to impact with a Hopkinson pressure bar: an animal model.

Budget

Item:	Cost:
• Latex free gloves 5 boxes	R750
• Masking Tape	R25
• Cleaning Material (Ethanol)	R160
• Anatomical waste disposal	R3157.83
• Specimen collection	R7187.30
• **Total**	R11 280.13

Note

This budget does not include the price for the animal heads as the Peninsula Baboon research Unit and Cape Nature donated specimens.